AN ABSTRACT OF THE DISSERTATION OF

John Francis Morrow IV for the degree of Doctor of Philosophy in Robotics presented on November 30, 2022.

Title: A Novel Method for the Quantitative Assessment of Fingered Robot Hand Designs for In-Hand Manipulation using Human Studies and Object-Centric Benchmarks

Abstract approved: _____

Cindy Grimm Ravi Balasubramanian

Fingered robot hands are complicated systems made of three essential system components: its morphology, its actuation, and its software control. These system components are tightly coupled to each other. Due to this, it is hard to benchmark robot hand performance in a way to understand the contributions of the individual system components. This defense introduces a new approach to characterizing a robot hand's system components using human subjects and novel object-centric benchmarks to study the contributions of the morphology and actuation system components at in-hand manipulation tasks. What is demonstrated are two studies using this method to study a hand's actuation and morphological system components. In the first, a hand's actuation component is studied at how well it can utilize tools (pen, spray bottle). In the second, a hand's morphological component is studied at how well it can perform fundamental in-hand manipulation tasks. Hand performance is compared between designs in order to build a quantitative understanding of how a robot hand's design affects its performance. Other roboticists can use this method on their own hands and on their own tasks to improve the systemic understanding of their own hands.

A Novel Method for the Quantitative Assessment of Fingered Robot Hand Designs for In-Hand Manipulation using Human Studies and Object-Centric Benchmarks

by

John Francis Morrow IV

A DISSERTATION

submitted to

Oregon State University

in partial fulfillment of
the requirements for the
degree of

Doctor of Philosophy

Presented November 30, 2022
Commencement June 2023

Doctor of Philosophy dissertation of John Francis Morrow IV presented on November 30, 2022.

APPROVED:

Co-Major Professor, representing Robotics

Co-Major Professor, representing Robotics

Associate Dean of Graduate Studies for the College of Engineering

---

Dean of the Graduate School

I understand that my dissertation will become part of the permanent collection of Oregon State University libraries. My signature below authorizes release of my dissertation to any reader upon request.

John Francis Morrow IV, Author

TABLE OF CONTENTS

Page

TABLE OF CONTENTS (Continued)

Page

LIST OF FIGURES

LIST OF FIGURES (Continued)

Figure Page

LIST OF TABLES

Table Page

LIST OF APPENDIX FIGURES

Figure Page

LIST OF APPENDIX FIGURES (Continued)

Figure Page

Chapter 1: Robot Hand Design for Manipulation

Robots interact with the world using robot end effectors. End effectors are built according to a robot's specifications, and therefore can greatly vary in design and function. So far, many end effectors focus on grasping objects effectively. However, roboticists are beginning to explore end effectors for manipulation tasks. Many robot end effectors designed for object grasping and manipulation use fingers. In this work, we focus on end effectors which utilize fingers. To differentiate them from other end effectors, we will refer to these as *robot hands*.

Robot hands are complicated systems built of many components. A robot hand is guaranteed to have three essential system components: 1) its morphology (the body), 2) some sort of actuation scheme that moves the morphology, and 3) the software controllers (low level and high level) to drive actuators with purpose. This is visualized in Figure 1.1. Due to their complicated nature, robot hand systems are difficult to characterize and compare to one another. To understand why this is, it is necessary to understand more about robot hand systems.

The **morphology component** is all about the body of the robot hand. For a typical robot hand this pertains to the structure of the palm, the structure and placement of the fingers, and any extra structures needed to accommodate other system components. Figure 1.1 contains a more detailed list of attributes in the morphology component at the bottom of the figure.

The **actuation component** is built into the morphology component. Actuation pertains to how the fingers will move, including the motors, transmission (tendons, gearing, etc), and low-level feedback (encoders, torque at joints).

The **software control component** directs the actuation component and receives the low-level feedback. Directing the actuation requires low-level and high-level software controllers. The low-level layer consists of drivers and basic code to make the motors work. The high-level layer uses the low-level layer to make the hand move towards the completion of some task.

The high-level layer could also connect to non-essential high-level feedback components (e.g. cameras, fingertip force sensors). We excluded a high-level sensing component as an essential component because it is still an active research field and many hands in research do not use one.

It is important to understand that the three essential components are tightly coupled to each other — for example, the morphology can't move without actuators, nor can the actuators do anything without some sort of software. Figure 1.2 relates these system components at a high level, located in the top-right of the figure.

When characterizing and comparing robot hands this creates problems because there are too many variables to consider. When characterizing hand performance, this means that it is difficult to understand how each system component contributes individually to system performance. When comparing robot hands, this is problematic because its difficult to isolate system components for direct component to component comparisons.

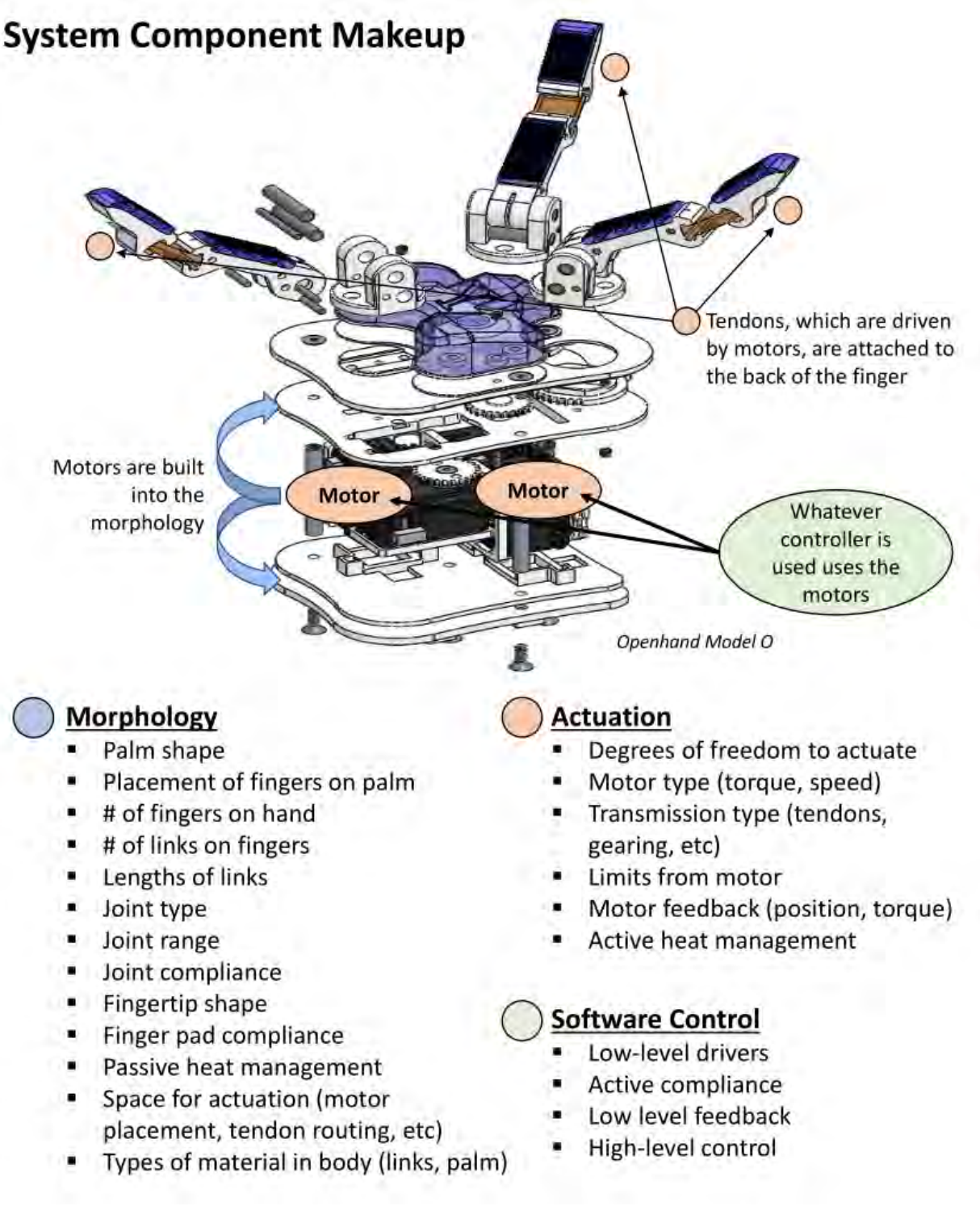

Figure 1.1: Robot hands are made of three essential system components: its morphology (body), its actuation, and its software control.

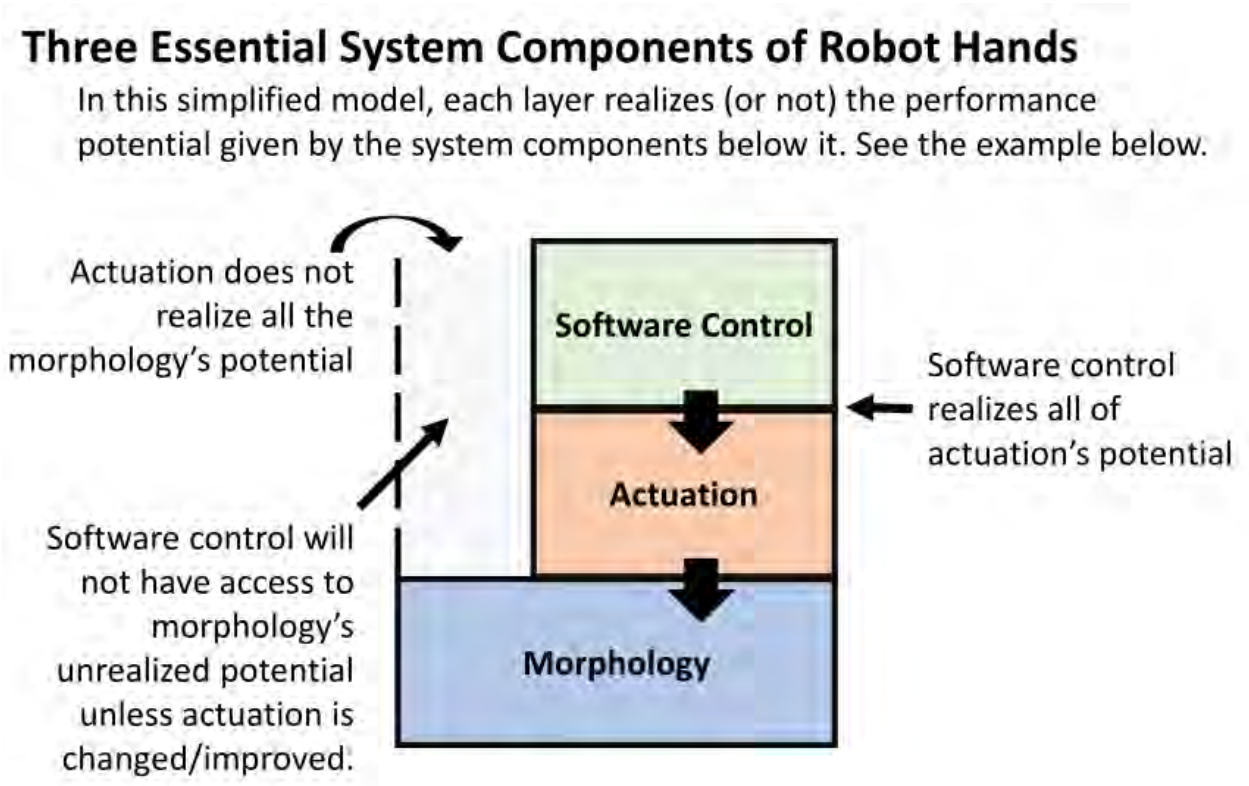

Figure 1.2: A basic system model of the three essential system components in every robot hand (morphology, actuation, and software control). Each system component builds off of the potential the component below it.

This is not a problem that we can ignore; it is necessary to understand system component performance due to the fact that system components build off of each other. The morphology component is foundational; therefore it provides the max potential of a hand. This is because the actuation component builds off of the morphology's potential — it can realize the entirety of the potential or a small portion of it depending on how the actuation is designed. The software control component, in turn, builds off of the actuation component.

Understanding the max performance that the morphology brings to a robot hand can enable better perspectives for characterizing and communicating hand performance, such as characterizing actuation systems by how well they realize the potential provided by the morphology.

The coupling of system components leads to problems when trying to dissect issues with robot hands — anecdotally, many roboticists dread debugging these complicated systems. This is partly due to complications when trying to understand component contributions separately from others.

This only becomes more complicated when one tries to compare robot hands to each other. This is because now there are two systems to unravel and compare. However, even small changes in a single hand's component can have profound effects up the chain — for example, changing an actuation scheme, even just adding or subtracting an actuator, can profoundly change how software control is manifested. The sheer number of variables at play that make it difficult to characterize and build an understanding of the contributions of each system component.

Improving our understanding of robot hands relies on unravelling the system components and enabling effective comparisons to be made about robot hands. To that end, my work here intends to mitigate these two problems by designing new benchmarks and methodologies to enable the characterization of components and the comparison of robot hand designs at manipulation tasks.

1.1 Important Vocabulary and Context

Research into robot hands and in-hand manipulation is built on years of robot and human grasping research. This section provides a basic guide to the terminology and context of robot hand research for readers who need it. The terminology and concepts provided in this section will not be defined later, so please refer back to this section as needed.

Structurally, a robot hand consists of fingers and a palm. The segments in a finger are called **links**. The closest link to the palm is called the **proximal link**. The furthest link, which is the last link in the chain, is called the **distal link**. Links between the proximal and the distal link are called **intermediate links**. Intermediate links are often numbered if there is more than one. This naming convention also applies to joint names, with some minor variations. Figure 1.3 shows these concepts in the top left of the figure.

An effective exercise is to consider the structure of the human hand, which is also referred to as an anthropomorphic hand design. The human hand contains four fingers, each with three links — therefore there is one proximal (closest to palm), one intermediate, and one distal link (furthest). There is also a two-linked thumb with one proximal and one distal link.

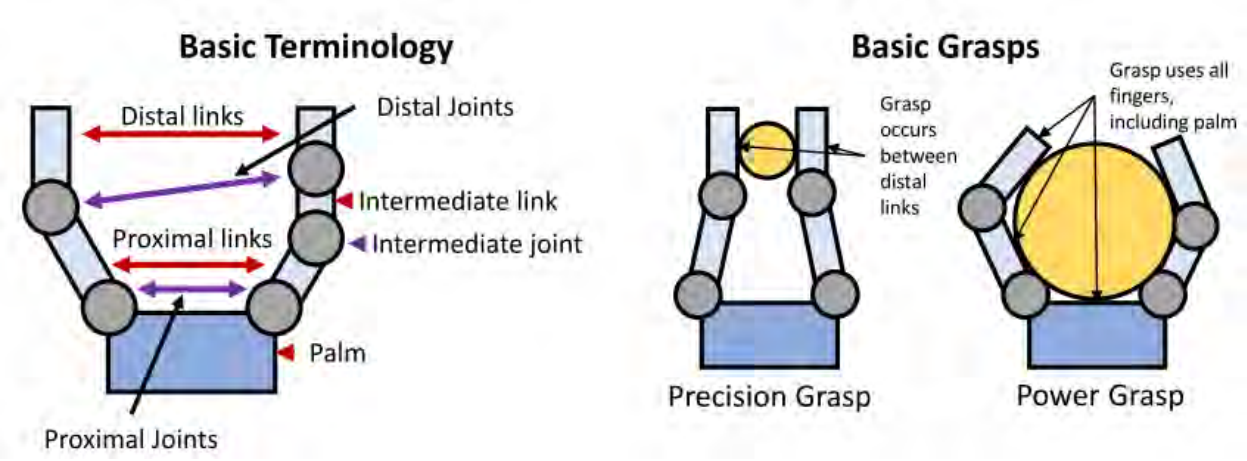

Figure 1.3: Basic terminology and concepts about robot hands. (left) Structural terminology. (right) Basic grasp types.

When using a robot hand, there are two ubiquitous grasps to know: the precision and power grasps (1). These two grasps form the foundation of modern grasping taxonomies — a type of grasp is either one of or a combination of these grasps.

Precision grasps, shown in the top right of Figure 1.3 utilize the distal links to grasp an object. Precision grasps are known for enabling greater dexterity and sensitivity. It is generally called a precision grasp because of the relatively higher precision required to make this grasp (2; 3).

Power grasps, also shown in the top right of Figure 1.3 utilize the whole hand to grasp an object, usually including the palm. Power grasps are known for stability. It is generally called a power grasp because of the extra stabilizing power that comes from grasping with the whole hand (2; 3).

Roboticists often choose to simplify contact points on multi-finger scenarios within grasps by consolidating similar contact points based on contact position and force. Consolidated points are known as *virtual fingers*.

Roboticists use many actuation schemes to make a hand perform these grasps. An actuation scheme is the setup used to make the fingers move for a particular hand design. When a finger curls, it *flexes*. When a finger straightens, it *extends*.

Degrees of freedom (DOF) is a measure of how many variables are required to define the state of a mechanical system. For robot hand morphologies, one could simply count the number of joints.

We label actuation schemes by how many degrees of freedom are controlled. For a **fully-actuated hand**, all of the degrees of freedom are under control. Therefore, the hand's behavior — every single degree of freedom — is under the control of the software. Figure 1.4 shows an example of a fully-actuated scheme using tendons on the left. Note how there is a tendon on each side of each link. In this scheme, a roboticist is able to control each link separately and in each direction using the corresponding tendon for the motion they desire.

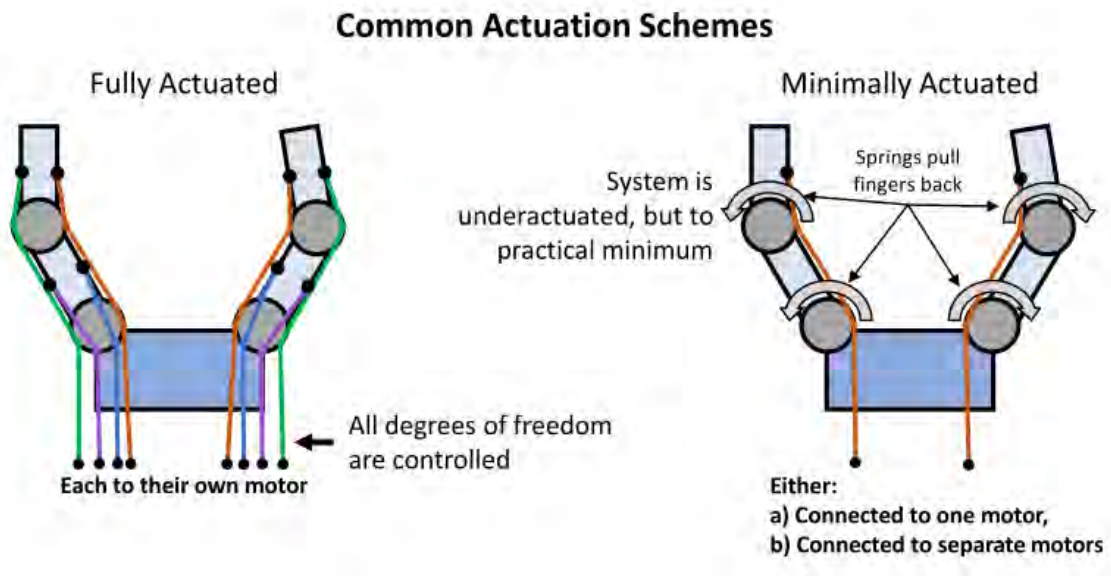

Figure 1.4: Two fundamental actuation schemes. (Left) Fully-actuated schemes control every degree of freedom. (Right) Minimally actuated schemes are underactuated schemes that minimize control.

A hand which does not have all degrees of freedom under control is called an **under-actuated hand**. These hands are advantageous because of the reduced control complexity — there are simply fewer tendons to pull to make this kind of hand work. Of course, the tradeoff is that there is a reduction in performance.

Considering the human hand, it is also underactuated. It controls our 22 joints with 38 tendons (4), which is not enough to drive every joint in two directions.

In this work, we discuss a new label for a common under-actuated design schemes called **minimal actuation** to differentiate them from more complex, but underactuated schemes. When a hand is minimally actuated, the *minimum* number of degrees of freedom are actuated to get the hand working. Such an actuation scheme is shown in the right of Figure 1.4. Note how there is only one tendon on the distal link of each finger, however the tendon is also connected to the proximal link. Therefore, both links will move when the tendon is actuated. Also note how there is no tendon to extend the finger. Therefore, such a design scheme requires some mechanism to extend the finger when it is not being actuated. This is typically accomplished using springs.

Cleverly, depending on which link makes contact first also dictates which kind of grasp is made. If the proximal link makes contact first, then a power grasp is made. First contact with the distal link will make a precision grasp. This is shown in Figure 1.6.

Due to the variety of hand designs, it is sometimes difficult to fit these concepts to every hand design. For instance, soft pneumatic actuators have been used as fingers, however, they are continuous and therefore it is difficult to fit the concept of links to those fingers (5). There are also hands where the concept of a palm is difficult to place. A novice reader should not despair, however, because it is also equally difficult for expert roboticists to fit these concepts onto some of

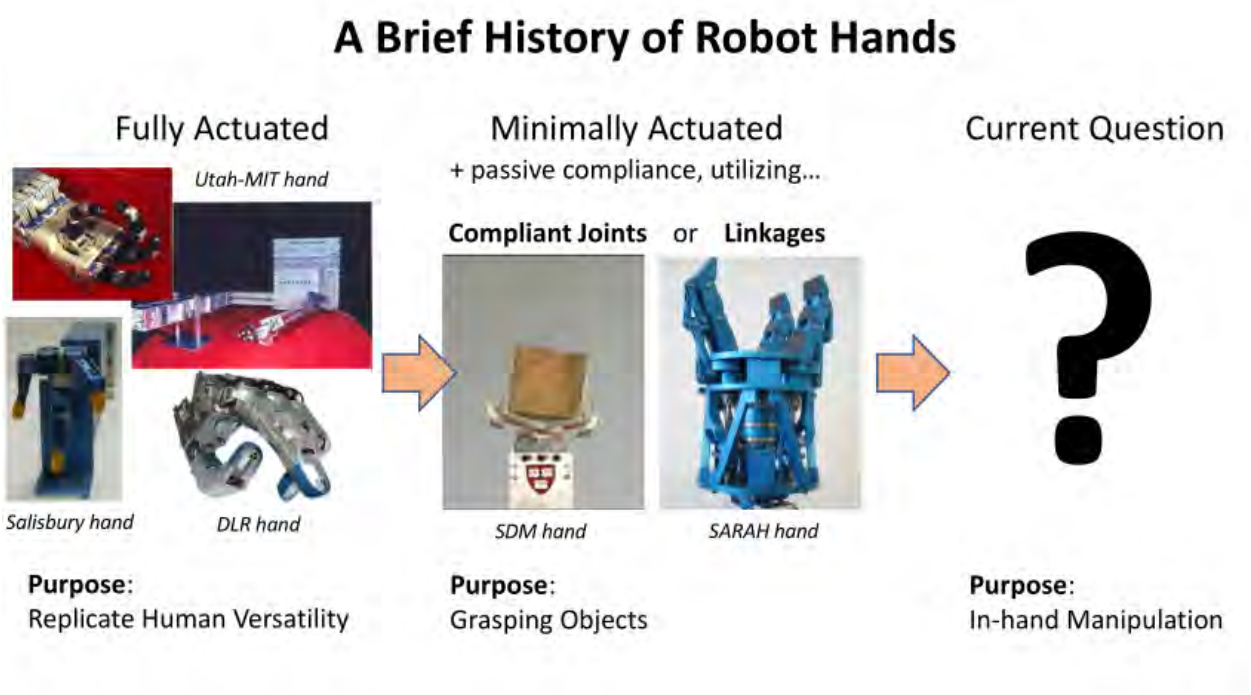

Figure 1.5: Robot hand research began with great scope, however difficulties to control such systems in real time resulted in researchers refining their scope and greatly simplifying hand designs. Looking ahead for manipulation tasks, it is unclear what the next iteration of hand designs will be.

these more exotic hand designs.

1.2 A brief history of robot hands

The entire history of fingered robot hands can be simplified into a story of the attempts robot hand designers have made to create a hand that is highly capable but also practical to control. The first robot hands were inspired from, and aimed at surpassing, the human hand. Examples include the Utah-MIT hand (1986, (6)), the Salisbury hand (1987, (7)), and the DLR hand (1998, (8)).

These hands were fully-actuated systems. Theoretically, these hand's were highly capable, however, their control complexity was too high for real-time control. Figure 1.5 shows these hands on the left. Even with current techniques, it is difficult for roboticists to effectively use all of the degrees of freedom for real-time, dynamic tasks.

Roboticists were aware that the high control complexity needed to be lowered in order to make hands more practical. To that end, researchers simplified their scope to focus on grasping and then significantly reduced the control complexity to match that scope. This resulted in the widespread adoption of underactuated hands.

However, although referred to as under-actuated hands, the under-actuated hands at the time are better understood to be *minimally-actuated* robot hand designs. This is because only one actuator was used to control a finger, or even an entire hand (refer to bottom of Figure 1.3). Re-

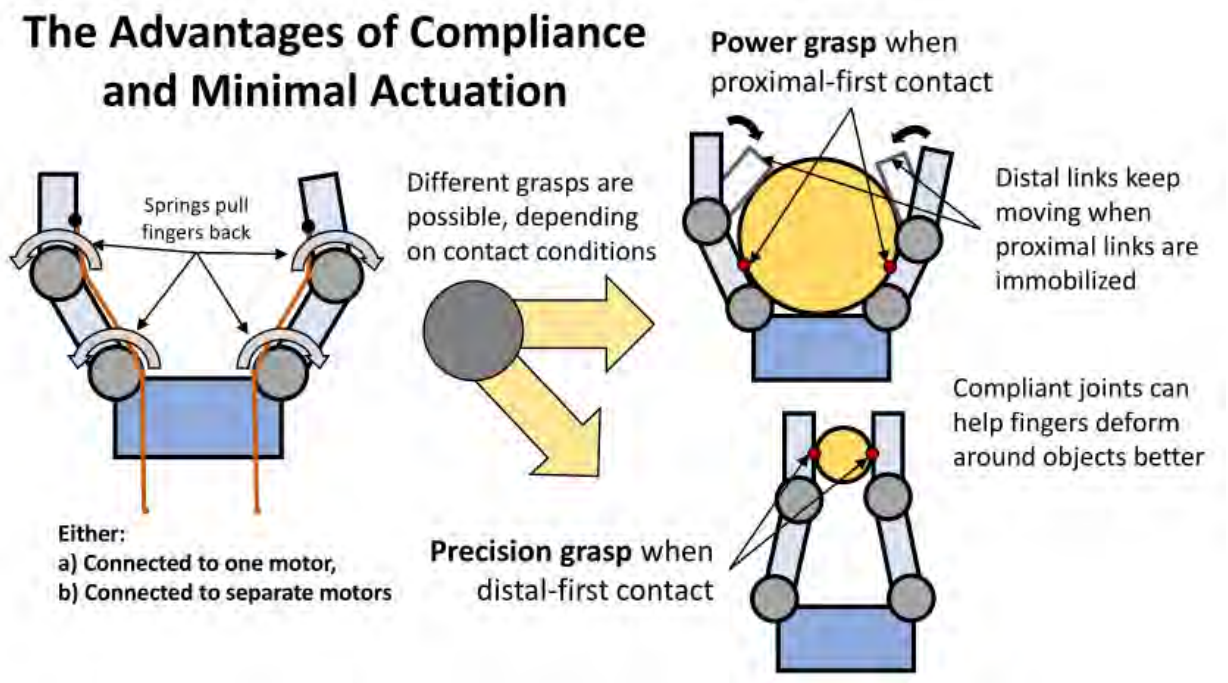

Figure 1.6: Robot hand research mitigated performance losses when simplifying robot hands by utilizing passively compliant joints and clever design of actuation schemes.

searchers mitigated the loss in performance, despite the significant reduction of control complexity, using *passive compliance* and *actuation synergies*.

Passive compliance is a hardware modification where compliance is built into a hand's design (see it listed under 'Morphology' in Figure 1.1). This typically occurs using rubber joints (such as the SDM hand, ihy, openhand) or mechanical linkages (gosselin, sarah hand, robotiq). The difference between the two techniques is that rubber joints can comply in 6 DoF, whereas linkages limit compliance to the direction of actuation.

Passive compliance harmonizes with minimal-actuation to give fingers the ability to wrap around objects as they flex. This occurs because all the links in a finger are coupled in minimally-actuated systems. Therefore, as links come into contact with an object, other links can continue to flex. This means that a passively-compliant, minimally-actuated hand can perform both precision and power grasps, depending on which links contact the object first, as shown in Figure 1.6. The added advantage that this brings is that this happens dynamically with no extra code — all the fingers have to do is close — reducing software complexity and processing requirements for realtime control.

Synergies specialize actuation schemes to make specific, coordinated finger flexing patterns. A synergy is a foundational movement which significantly contributes to many different movement patterns or tasks. The idea behind synergies is that because a synergy contributes to many tasks, one could make a hand more versatile by having it only do that synergy. Roboticists use passive compliance and under-actuation to cover the rest needed to complete a task.

When a synergy is built into a hand this movement is connected to one tendon. Pulling this tendon makes the hand perform the synergy movement. Most commonly, roboticists utilize a two step process to implement synergies. First, they need to identify synergies present when grasping sets of objects, typically using human study or modelling approaches. Then, they build actuation schemes which are designed to reproduce those synergies.

1.2.1 Manipulation and Minimally-Actuated Hands

Minimally-actuated hands are also being used for manipulation tasks, despite their original intention as solutions to simplify and improve grasping. However, manipulation tasks are more complex than grasping and therefore will require more from these minimally-actuated systems.

Roboticists have applied minimally-actuated hands (without modification) to manipulation tasks with some success. Odner et al (9) and Calli et al (10) characterize the manipulation ability of their compliant robot hand. Ma et al developed algorithms for manipulation using caging grasps (11). Calli & Dollar demonstrate in-hand manipulation with a UAH utilizing computer vision and model predictive control (12; 13). Odner & Dollar demonstrate a precise grasping movement with a manipulation component (grasping a coin from a table surface) by implementing a ridged surface on the fingers (14).

One should note, however, that some of the advantages of minimal-actuation and compliance for grasping, are now liabilities for manipulation. For example, the compliance in a finger makes it difficult to apply precise forces, which are typically needed for manipulation tasks. Further, roboticists need to get creative to make the most of these limited systems, since they have so little control over the hand as a whole.

Others have begun adding complexity back into the minimally-actuated paradigm to complete more complex manipulation tasks. It should be noted, however, that these modifications treat the original, minimally-actuated design as a foundation rather than coming up with new, radically different designs. The first modifications added the ability for fingers to rotate at their base (15). Aukes et al implemented the ability to lock joints on a UAH, which allowed their hand to exhibit under-actuated and fully-actuated behaviors (16). Yang et al replicated joint locking on a hand with soft actuators for fingers (17). Tincani et al implemented a UAH with active surfaces called the Velvet hand (18; 19). Spiers et al demonstrated a hand with fingers that have two friction modes for sliding movements (20). Ma et al replaced a finger with an active tank tread mechanism for in-hand manipulation, and the other finger on this hand used two tendons instead of one (21). McCann & Dollar demonstrated a unique hand design for manipulation that uses planar manipulation which is fundamentally based on a stewart platform (22). Bircher et al redesigned their UAH with custom linkages that support in-hand reorientation (23). Some robot hand designers added a higher complexity thumb to their design to improve manipulation.

There are few radically different robot hand designs for manipulation which increase control complexity. Ma & Dollar proposed a concept hand design for precision manipulation with custom

fingertips that have compliant joints. The distal joints, which are custom spiked balls, are fully-actuated (6 DOF, (24)). Others have investigated the role of redundant actuators for manipulation tasks (25).

It is also important to consider how a hand interacts with the arm that it is attached to. Many robot arms have sufficiently high degrees of freedom to do many complex tasks with simple hands. However, increasing complexity on a robot hand is often justified as a supplement to the high-dof robot arm (26). In the real world, robots will likely work in closed and cluttered environments – not conducive for robot arms with simple grippers. Dexterous hands can cover for constraints placed on a robot arm in such environments by reducing the need for arm movement, such as for re-grasping objects in complex manipulations.

It is difficult to navigate the space of modifications out there for manipulation because it is unclear what each modification brings to the table. Researchers are currently realizing the need for better benchmarks for evaluating robot hand performance to clarify how well these new hands work. This is evidenced by multiple workshops and special issues in journals on this very topic (27; 28; 29; 30).

Fundamentally, in order to understand what the advantages and disadvantages of a design are, we need to be able to comprehensively compare hands to each other as a whole system, and at the system component level (Fig. 1.2). Currently, we lack a method to do this. This is due to the intricasies of the coupled system components in a robot hand — as a consequence, most robot hand design is done intuitively and it is difficult to build a quantitative understanding based on that.

1.3 Research Objectives and Contributions

The insufficiencies of existing benchmarks to effectively characterize the lower level manipulation capabilities of robot hands makes it difficult to build a quantitative understanding of robot hand design performance. The lack of a quantitative understanding about hand design forces roboticists to rely on intuition and empirical methods of hand design - which makes it difficult to share knowledge.

Our research goal is to build new processes to unravel robot hand systems necessary to start that understanding at its foundation — which is building a quantitative understanding of the contributions that a hand's morphology (alone) brings to robot hand performance. To get past this, we need to design new benchmarks and methodologies that can study system components. These benchmarks must be able to enable the study of the contributions of each system component that a robot hand has towards manipulation performance.

We demonstrate that by using a human study methodology and benchmarks which characterize how objects are moved, we can effectively circumvent the coupling that a hand's morphology has with the actuation and software control components. We then apply our novel benchmark and human studies to study the potential that a hand's morphology provides to the robot hand's manipulation performance.

We list our contributions as:

1. a new approach for characterizing the maximum capabilities of a robot hand's actuation and morphology components.
2. with regards to actuation, using the human as an ideal controller, we analyzed human-desired actuation strategies with a fully-posable version (puppeted as if fully-actuated) of the Barrett hand using a pen and spray bottle.
    - we accomplish this using a novel human-study design called Physical Human Interactive Guidance for manipulation (mPHIG)
3. with regards to morphology, using novel benchmarks with mPHIG, we analyzed human-actuation strategies on fully-posable versions of basic, two-fingered robot hands for fundamental, in-hand manipulation tasks
    - we accomplish this using a novel testing suite for in-hand manipulation, called the Asterisk Test
    - We also develop a novel, visual geometric representation of the space between a hand's fingers, which we call the potential hand-object contact region. We use this characterization to normalize results between robot hands for more effective comparisons of manipulation performance.
4. finally, we find...
    (a) insights into how human-preferred actuation strategies differ from current underactuated hand designs
    (b) that the 2v2 hand, as controlled by humans, represents a baseline in versatile in-hand manipulation performance.
    (c) that additional degrees of freedom do not contribute much to improve manipulation performance
    (d) Identify assymetries of performance in a hand's workspace
    (e) fingerpad compliance is critical to human-performed manipulations

1.4 Structure of Dissertation

In this work, we isolate and study a hand's morphology to characterize its potential at fundamental in-hand manipulation tasks. In this work, first we systematically go through the two core building blocks of our method in Chapters 2 and 3. Then we use our method, described in Chapter 4, to characterize and compare robot hand designs for manipulation tasks in Chapter 5.

Chapter 2 introduces our method to isolate system components using human studies called Physical Human Interactive Guidance for manipulation (mPHIG). In mPHIG, humans puppet robot hands to complete tasks. Because the human subjects are manually moving the hand, they get unparalleled feedback and unrestricted freedom to move that our methods of human control cannot. This also mitigates the problems of transposing and controller transparency that all human data collection and control methods wrestle with.

We start Chapter 3 with a new hand measurement method for normalizing object translation within a hand by a hand's size. This new method is designed to enable fairer comparisons between robot hands. The rest of Chapter 3 details a novel benchmark made to characterize in-hand performance, called the asterisk test. This benchmark specifically links robot hand design to fundamental precision manipulation abilities. We also discuss the new perspectives that make up this benchmark.

Chapter 4 details how we use mPHIG and the Asterisk Test to study system components of robot hands. Inside we describe three studies. In the first, we use mPHIG to study and compare actuation strategies for tool-use scenarios (using a pen and a spray bottle) on three-fingered hands. The second study builds off of the first by characterizing distal link geometries to explain the first study's findings. Finally, in the third, we use mPHIG and the Asterisk Test to study hand morphology and the potential that it would bring to in-hand manipulation performance.

Chapter 5 presents the results of the three studies described in Chapter 4. Chapter 6 provides future work.

Chapter 2: Using a Human as an ideal controller and sensor for manipulation

Humans exhibit extraordinary manipulation abilities that serve as a continual inspiration for robot systems. Many roboticists have studied human strategies and applied them to robot systems with great effect. However, it is also difficult to use human data because of mismatches between human and robot hand designs and capabilities. Mismatches requires transposing data from a human hand perspective to a robot hand perspective in a way that preserves the utility of the human data. This mismatch also can make it difficult for humans to transfer their skills to robot hands, known as low controller transparency.

In this chapter we survey the literature for how humans are used already in robot hand research: namely, taxonomies and other in-depth studies, demonstrations for learning, and human-in-the-loop implementations. Within this survey, we also discuss the current problems in the field, particularly that of transposing human data to robot hands and controller transparency. Finally, we introduce our novel human-study design, which we call Physical Human Interactive Guidance for manipulation (mPHIG).

2.1 Background

The study of human manipulation capabilities is necessary because manipulation is mainly a subconscious activity in the human brain. Humans can also train new skills — as they are trained, these skills become more and more subconscious. (have thinking fast and slow in here?) By storing them in the subconscious a human is able to recall skills almost immediately, in many environments, and without much thought.

Four ways that humans are used in manipulation are through taxonomies, in-depth study into human approaches to grasping and manipulations, as expert demonstrations for learning techniques, and as controllers in human-in-the-loop systems.

2.1.1 Taxonomies and other In-depth Studies

From the beginning we have used the human hand to characterize grasp types through taxonomies of human grasps. The current state-of-the-art taxonomy is the GRASP Taxonomy, which itself is the reconciliation of 22 human grasping taxonomies that came before it (1). This taxonomy lists 33 grasps that come from 17 basic grasp prototypes. The GRASP taxonomy organizes these grasps based on three attributes: 1) the focus of the grasp (power vs. precision), 2) the direction of the grasp forces relative to the palm (opposition types), and 3) the number of virtual fingers used for the grasp.

Bullock & Dollar observed human in-hand manipulation behaviors and organized them into a taxonomy (31). This taxonomy evaluates manipulations based on the presence of contact, the type of contact (prehensile contact), and the nature of the motion of the manipulation. Manipulations are first organized by two criteria: whether motion occurs at contact, and how the object moves (rotation vs. translation). Unfortunately, this taxonomy is hand-centric — therefore work must be done to adapt this taxonomy onto other kinds of hand designs.

Others have studied other aspects of human grasping and manipulation behavior. For example, identifying how often items in taxonomies are used, how people approach grasping and manipulation, and the specifications and limits of the strategies humans employ. Such in-depth studies typically feature humans 'in their natural habitat', aka using their own hands. With this in mind, it can be difficult to transfer these findings directly onto robot hands.

Examples of in-depth studies are how humans choose grasps (32; 33; 34; 35; 36; 37; 38), grasp with uncertainty (39), couple grasping with their vision (40; 41), rate robot grasps (42; 43; 44), use their fingers for precision manipulation (45; 46; 47; 48; 49), among other topics (31; 50; 51; 52; 53; 54).

This research has occurred in parallel with grasping research in Human Factors, which is primarily focused on applying and accomodating the human grasping system (not understanding it). Research topics include for example the relationship between hand physiology and grasping (especially for force output) (55; 56; 57; 58; 59; 60; 61; 62) , on studying tool use and accommodating tool design (63; 64; 65; 66; 67) , and on modelling a grasp (68; 69; 70).

2.1.2 Robots Learning Manipulation from Human Demonstrations

Humans have not always been studied by fellow humans. Learning from Demonstration (LfD) techniques have used human demonstrations for years (71). Further, machine Learning techniques, such as Reinforcement Learning (RL), have also begun to use humans. In this section, we describe these problems in greater detail with examples from LfD implementations, due to the maturity of the research.

In general, the quality and structure of any learning algorithm is dependent on the data fed into it. Researchers must make many decisions when using human data - for example, what hand should the human use (their own or a robot) and how to record that data. Each decision needs to keep in mind two problems: 1) how easily it can incorporate human data onto a robot hand (called transposing) and 2) the quality of feedback and control that a human receives, called controller transparency.

In LfD, human demonstrations fall into one of two categories: record mapping and embodiment. The key difference between the demonstration categories is the frame of references that the data is recorded in.

Record mapping techniques record the demonstration from an external frame of reference to the robot learner. This can manifest itself in many ways.

Miyata et al. (72) and Liarokapis et al. (73) measured the hand pose of a human demonstrator with a motion capture system. Hand pose and orientation, as well as the pose of the thumb, index, and pinky fingers, have also been recorded with a data glove (74). Huang et al. (75) recorded a bottle opening task demonstration using a combination of a motion capture system, force torque sensor, and wearable haptic device.

Computer vision techniques have also been used for record mapping. Kang and Ikeuchi (76) used a four camera setup with a cybergove to record their demonstrations. Heuser et al. (77) used only a stereoscopic vision system for their demonstrations. In doing so, the hand was tracked with color-histogram based tracking and hand posture was recorded with PCA.

Record mapping has also been demonstrated with a focus only on the object being grasped. Liarokapis et al. (73) attached motion tracking markers on a valve for a valve turning task.

Record mapping is easy to implement and imposes little restriction on the demonstrator. The main disadvantage to record mapping is that the demonstration data must be converted to the robot's hand before it can learn (transposing). This can produce a serious challenge to those trying to implement LfD or reinforcement learning.

Mapping a human hand grasping demonstration to a robot learner depends heavily on the robot's hardware: specifically, its hand. Robot hands vary widely between anthropomorphic and non-anthropomorphic designs. Both types introduce mapping challenges depending on the hand's capabilities; for example, their drive mechanisms and physical constraints.

Oztop et al. (78) describes two of the simplest mapping techniques: joint space and cartesian fingertip mapping. Joint space mapping is most suitable for power grasps, and cartesion fingertip mapping for precision grasps. Interpolation between the joint space and cartesian fingertip space in a single mapping is also a viable solution.

Liarokapis et al. (73) provide a good example for cartesian fingertip mapping. Since the three-fingered Barrett hand does not match to the human hand, the actions of several human fingers had to be interpolated into the three-finger Barrett configuration. For this implementation, the thumb directly corresponded to one fingertip position, and the other human fingers were interpolated between for the remaining two fingers on the Barrett hand.

The dimensionality of the mapping can provide further challenges. PCA, Nonlinear PCA (NLPCA), and Sequential NLPCA (SNLPCA) have been used to reduce the dimensionality of high-dimensional human demonstration data (79). PCA is regarded as the default method (80; 79). NLPCA and SNLPCA are typically used for complex tasks.

Ciocarlie and Allen (81) defined low-dimensional regions inside the grasp space with PCA, which they termed grasp space (or grasp synergies). They used simulated annealing to fit grasps to objects using those synergies.

Ekvall and Kragic (74) used an artificial neural network (ANN) to lower the dimensionality of the control data to fit a data glove implemention to two robot hands: the barrett and robonaut hand. The ANN was trained by sampling a number of common human grasp poses and matching those to robot hand poses. Finger locking issues occurred when fingers were wrapped over each

other and were not unwrapped in a specific order known only to the ANN.

The second demonstration category is **Embodiment mapping**. Embodiment use the robot's hand to record the demonstration. This means that the mapping between the demonstration and the robot learner is not needed since the demonstration is already in the robot learner's frame. This is an advantage that embodiment mapping techniques hold over record mapping.

However, controller transparency becomes a bigger problem because the demonstrator must control the robot for the demonstration. Deficiencies in feedback and control can severely limit the quality of the demonstration.

Sauser et al. (82) used an instrumented glove for human demonstrators to control a robot hand for demonstration. This work also utilized a secondary learning phase — which they called the self demonstration phase. In this second learning phase the demonstrator corrected robot grasps by disturbing the held object.

Oztop et al. (78) used a motion capture system to track a human hand for robot hand teleoperation. Human subjects had to train for a week to prepare for an in-hand ball-swapping task demonstration.

There is another encoding step between the learning and demonstration phases in an LfD scenario. There are three methods to encode demonstrations to develop policies from: (1) mapping function, (2) system model, and (3) the plan (83). The mapping function directly approximates the policy from the demonstration data. The system model is a model of the world's dynamics built from the demonstration data. This is typically represented as a transition matrix for a Markov decision process. Markov decision processes also use reward functions. The reward functions could be generated from the demonstration or by hand. A plan is an association of actions taken from the demonstration. The conditions before and after the action occurs are also associated with the action. The plan would be directly generated from the demonstration. Policies are then derived from the encoded demonstration, using the learning algorithms described at the beginning of this section.

2.1.3 Human in the Loop Implementations

There are three general strategies that describe all methods humans can use to control robots (in order of increasing autonomy): direct, shared, and supervisory (84). Direct techniques use minimal robot autonomy and rely on total human control. Shared techniques use a combination of human and autonomous control. With supervisory techniques, the system is mainly autonomous and human input is in the form of a supervisory or commanding role. These methods are used to synergize human and autonomous system proficiencies. What humans typically contribute are their judgement, adaptability, high-level understanding of the world, and their understanding of abstract or high level commands.

How well human-in-the-loop systems enable human proficiences through their interfaces and through feedback is called *controller transparency*. Leeper et al. (84) studied the effectiveness of

these three human-in-the-loop (HitL) strategies for grasping an object in a cluttered environment with a PR2 robot. Each Graphical User Interface (GUI) studied will be described. (1) The direct strategy interface utilized a GUI using a set of arrows and rings around a virtual PR2 gripper enabling the operator to change the pose of the gripper in real time. (2) Two shared strategy interfaces were implemented: a) In the first, human operators indicated waypoints that the robot autonomously planned between, and b) in the second, human operators specified the final hand pose of the robot. (3) For the supervisory strategy, operators selected a grasp to implement from a set of pre-computed grasps planned by the robot's grasp planner. Of the four interfaces tested, the supervisory strategy was found to be the most successful and most preferred between the human subject operators.

The nature of supervisory techniques makes it easy to implement them. GUIs have been used to provide a point-and-click interface for robots both in simulation and in real life (84). In another application, a gesture drawing interface on a tablet was implemented to control robots vacuuming in a house (85).

Human gestures, such as pointing, are another well-implemented supervisory control method (86). Quintero et al. (87) developed a pointing-aware system that used the first-generation Kinect sensor, having an average error of 9.6cm when determining where a human is pointing. This work was further implemented on the Kinect 2 with improved results (88). Such GUIs are common in situations where the robot and human are in the same environment (89; 90)

Direct strategy systems are more complicated to implement, but this is necessary to give humans adequate control and context. Robotic surgery systems provide arguably the most intuitive interfaces for HitL control because of their high sensitivity and ergonomic design. While grasping could be a required part of surgery, these interfaces are highly specialized for movements necessary in surgery, though not grasping (91). Currently, the da Vinci surgical robot by Intuitive Surgical Inc. is the most commonly used surgical robot (92). A human surgeon would utilize hand and foot controls with a camera feed interface shown through a binocular viewer. The thumb and index fingers on the hands of each operator are placed in adjustable loops which are connected to a haptic device. The fingers are used to open and close jawed instruments for surgery. A modified Phantom Omni haptic interface was also used as a da Vinci simulator training device (93). In another application, NASA's Robonaut 2 is GUI controlled with sliders for direct motor control (94).

2.2 Physical Human Interactive Guidance for Manipulation

In the embodiment mapping techniques and human in the loop implementations described already, there is still some sort of fundamental disconnect between the human and the context of the task. This makes it difficult to use these techniques for our focus on in-hand manipulation because these techniques are not transparent enough to make use of humans nuances of control and perception in manipulation. This is ultimately an issue of haptics — currently, humans aren't able to receive the information needed to manipulate objects to their fullest. A different Embodiment Mapping

technique, called Physical Human Interactive Guidance, is a technique which has the ability to fill this gap.

In this technique, human subjects manually move robots through the motions of a task. This technique empowers human subjects to move the robots in the ways that they prefer because they have full control. In addition to that, because they are right in the context of he task with the robot, the human subjects can make use of their senses directly — which enables them to make

In previous work, human subjects positioned a robot arm and hand system to study and compare human grasps to state of the art robot grasps (95). The objects to be grasped also were to be grasped with a functional intent, such as grasping a wine glass to lift and pour liquid. Researchers observed a new feature of human grasps that was not present in autonomous grasps, called skewness. Skewness represents how aligned the wrist is with the object's prinicpal axis before grasping. In this work, humans consistently utilized grasps with low skewness, whereas robot generated grasps varied. When robot planners were adjusted to consider skewness, grasp success improved from 77-93%.

Other work has used PHIG to study how humans coordinate degrees of freedom that are intrinsic to the robot hand (e.g. how the fingers flex) and extrinsic (e.g. global pose of hand) (96). Human subjects directed a soft robotic hand (RBO v2 (97)) attached to a Barrett WAM arm to grasp six objects with various constraints on how the subject could coordinate degrees of freedom. In the experimental condition with the fewest constraints, human subjects puppeted the hand with a stick attached to the wrist of the arm.

Adapting PHIG for manipulation would involve human subjects controlling fingers on a hand. This can be advantageous to robotics research because of how well humans can adapt to tools. In a way, robot hands can be another tool which humans adapt to. With this in mind, using human subjects can effectively normalize control strategies across hands (see Fig. 2.1) — human subjects will use the same strategies between hands (but these strategies are tailored to each specific hand design) to complete a task. These strategies employed in common across hand designs become the common thread to normalize (as best as possible) system components across hands. This ultimately simplifies data collection because no transposing is required if the human is using the robot hand you wish to study.

Further, by puppeting fingers human subjects can also utilize their own senses in the task by feeling through the robot hand fingers.

This provides a high degree of sensing which should provide almost perfect controller transparency.

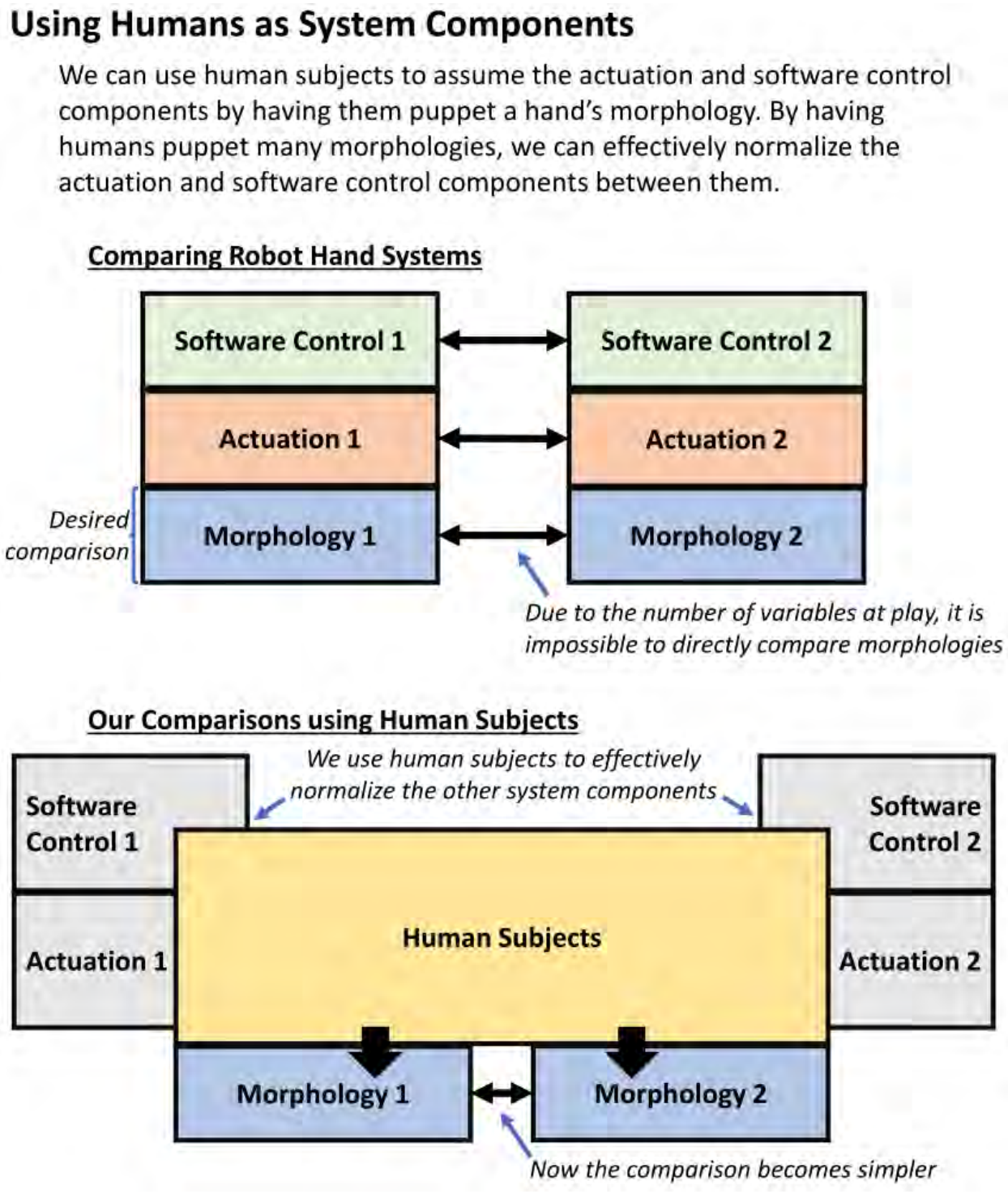

Figure 2.1: Human subjects can be used to stand in for system components on a robot hand. We use this to make comparisons of system components that would not be possible otherwise.

Chapter 3: The Asterisk Test: Measuring In-Hand Manipulation Performance

For manipulation tasks roboticists have recently realized the need for better benchmarks to improve existing design processes. However, the types of benchmarks being considered for manipulation are too high-level to provide links between a robot hand's design and its ability to do manipulation tasks.

We present a novel benchmark for characterizing fundamental, in-hand manipulations. This benchmark avoid the pitfalls of current benchmarks by using an object-centric methodology to characterize low level performance: how well the hand can maneuver an object through its space.

The benchmark contains three test sets which characterize different aspects of manipulation space. In the first, robot hands must translate an object in eight cardinal directions (the asterisk) as far as possible to characterize translation ability. In the second, robot hands must rotate an object in place as much as possible to characterize rotation ability. In the third, translation and rotation is combined; robot hands must translate an object in the asterisk directions after rotating the object a set amount. This third test characterizes how robust translation performance is with suboptimal contacts which were brought about by the rotation.

In Section 3.1, we discuss the task-specific benchmarks currently used in robot manipulation and contrast them with object-centric benchmarks, which enable lower-level investigations into hand design performance. Next we present a novel representation of a hand's region of potential contact, in Section 3.2, which we use to normalize results. Finally, we present our new benchmark for fundamental manipulation tasks, called the Asterisk Test, in Section 3.3.

3.1 A Change in Perspective: Task-specific vs. Object-centric metrics

To date, researchers have most commonly used a combination of time-based, task-specific, and binary measures for quantifying robot hand capability (e.g. time to complete tasks, counting successful grasps, etc). Task-specific metrics characterize performance on high-level aspects of a task, which focus solely on the task and not the hand.

Such metrics have been used to study manipulations to characterize a wide range of hands and controllers (98; 9; 99; 10; 100; 13). Other metrics have been used to characterize elements of the robot hand subsystem; for example characterizing a hand's strength and speed (101), characterizing a finger's kinematic workspace and how they overlap on a hand design (102), characterizing how well a hand rotates an object in hand (103), and optimizing finger placement and link length on a hand design for both grasping and manipulation (104; 105).

Task-specific metrics are important for understanding overall performance on a task and their main advantage is that they are agnostic to hand design. However, they are insufficient because

they are high-level. Currently, roboticists use task-specific metrics as a tool direct their focus in what is largely an intuitive investigation into a robot hand's performance. Lower-level metrics would allow roboticists to focus directly on what they want to know, while still being agnostic to hand design, which would improve scientific communication and simplify design processes.

For example, rotation is fundamental to manipulation, but most methods indirectly measure a hand's rotational ability by necessitating rotation in the tasks they are measuring (106; 10). For example, the box and block (107), rubik's cube (100), and NIST peg in hole (108) tests require robot hands to rotate objects, however rotational movement is not directly benchmarked. Another benchmark considers rotation capabilities as part of a larger objective, such as characterizing a robot's ability to change an object's orientation (103). Other work has characterized rotational ability using characterizations unique to the robot hand design being characterized. For example, the Model GR2 (109), Model Q (110; 111), and Model W (112) Yale OpenHand designs are each characterized at their designed method of rotation manipulation.

Object-centric metrics, in contrast, solely focus on the what the object is doing in a task. Objects used in manipulations are tracked throughout the task — effectively capturing how the hand is moving (read: manipulating) the object without requiring any specific information about the hand design.

There already exist object-centric benchmarks, such as grasping force vector fields (113; 114), and Manipulability (115). There are also other manipulation metrics designed from an object-centric perspective that are still task-specific, such as trajectory tracking (104; 105).

An object-centric benchmark for in-hand manipulation would need to characterize how well a hand can move an object through the space inside its fingers. This space is more than just a hand's kinematics because of the dynamics present in a manipulation task (the dynamics: contacts, forces that a finger can do, compliance, inertia, energy in system).

For the Asterisk Test, we take inspiration from the manipulability metric (115) which considers an arm's dexterity and how it can flow through the workspace. However, we apply this idea of flow to the object being manipulated and how it is maneuvered through the workspace using the fingers. We call this concept *maneuverability*.

To keep the benchmark simple, we can make generalizations across the space given performance at discrete directions (the asterisk, see Fig 3.1) rather than sampling the whole space of manipulations. We adapt the manipulation taxonomy constructed by Bullock and Dollar (45) for this purpose, which defined the asterisk shape. We can then generalized performance with a quantitative assessment of how symmetrical the robot's performance is across the x and y axes.

We incorporate maneuverability into the Asterisk Test with how it judges performance. We do this by judging the *quality* of a hand's ability to manipulate in discrete directions by comparing the object's path to the ideal path using nine metrics.

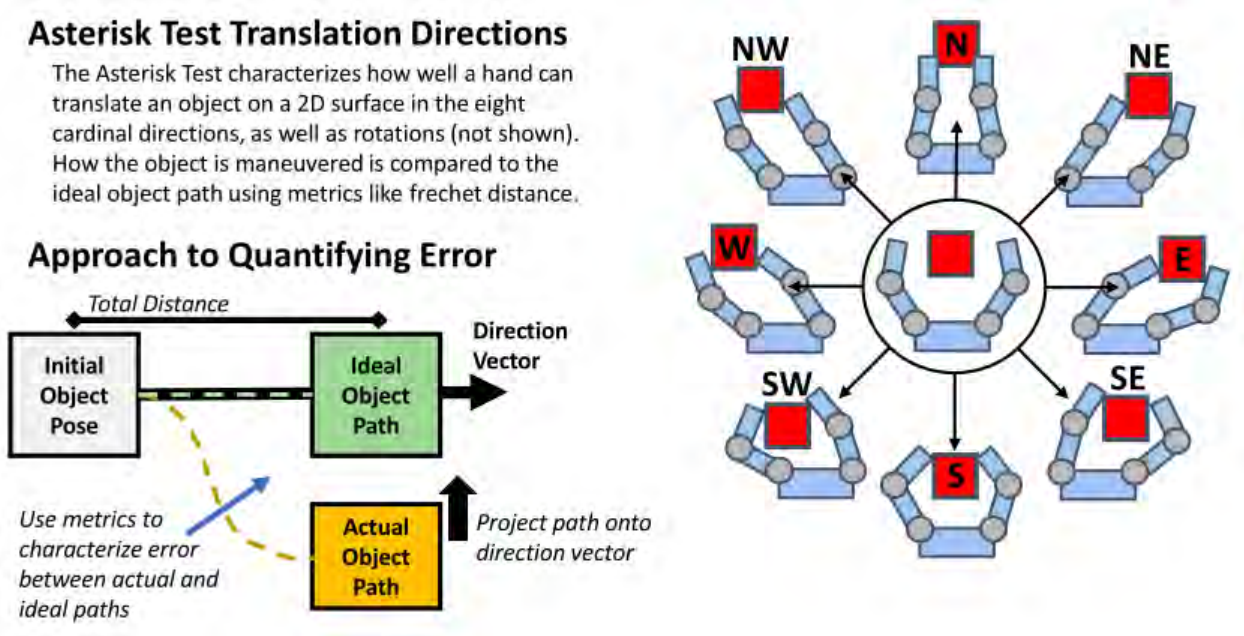

Figure 3.1: The Asterisk which the Asterisk Test is named after. One component of the Asterisk Test is to translate an object in eight cardinal directions on a tabletop. Object pose is collected throughout the trial and benchmarked using benchmarks like frechet distance.

3.2 A Measurement Method for Normalizing a Hand's Space

It is difficult to compare robot hands to each other because of the number of variables present when making a comparison. One major variable is that of hand size; the space within a hand's fingers can vary immensely given different capabilities in the fingers (due to different joints, link lengths, materials, etc.). For example, when comparing how hands might grasp an object, this object might have a different relative size between each hand which would not be a fair comparison.

Previous studies have used finger length to normalize the space (116). This is problematic however, because it only incorporates one aspect of a hand's space and not others (such as how far apart the fingers are, how do the fingers close, etc). The issue of a hand's space has a greater impact when comparing manipulation performance, compared to grasping. This is because manipulation tasks involve an object moving inside the space of the fingers. This requires a new method of normalization to normalize translations within the entire space.

We developed our own method of measurement to represent a hand's space in order to more effectively normalize hand performance for in-hand manipulation tasks. We do this by first defining a novel coordinate system (span, depth, width) and then measuring the space between the fingers at different levels of actuation. Using these measurements we can normalize how the object moves within the hand's space for fairer comparisons between hands.

We pair this measurement method with the Asterisk Test to normalize translations by a hand's size for easier comparisons between hands. We also use these measurements to normalize object size and the initial distance that objects are placed.

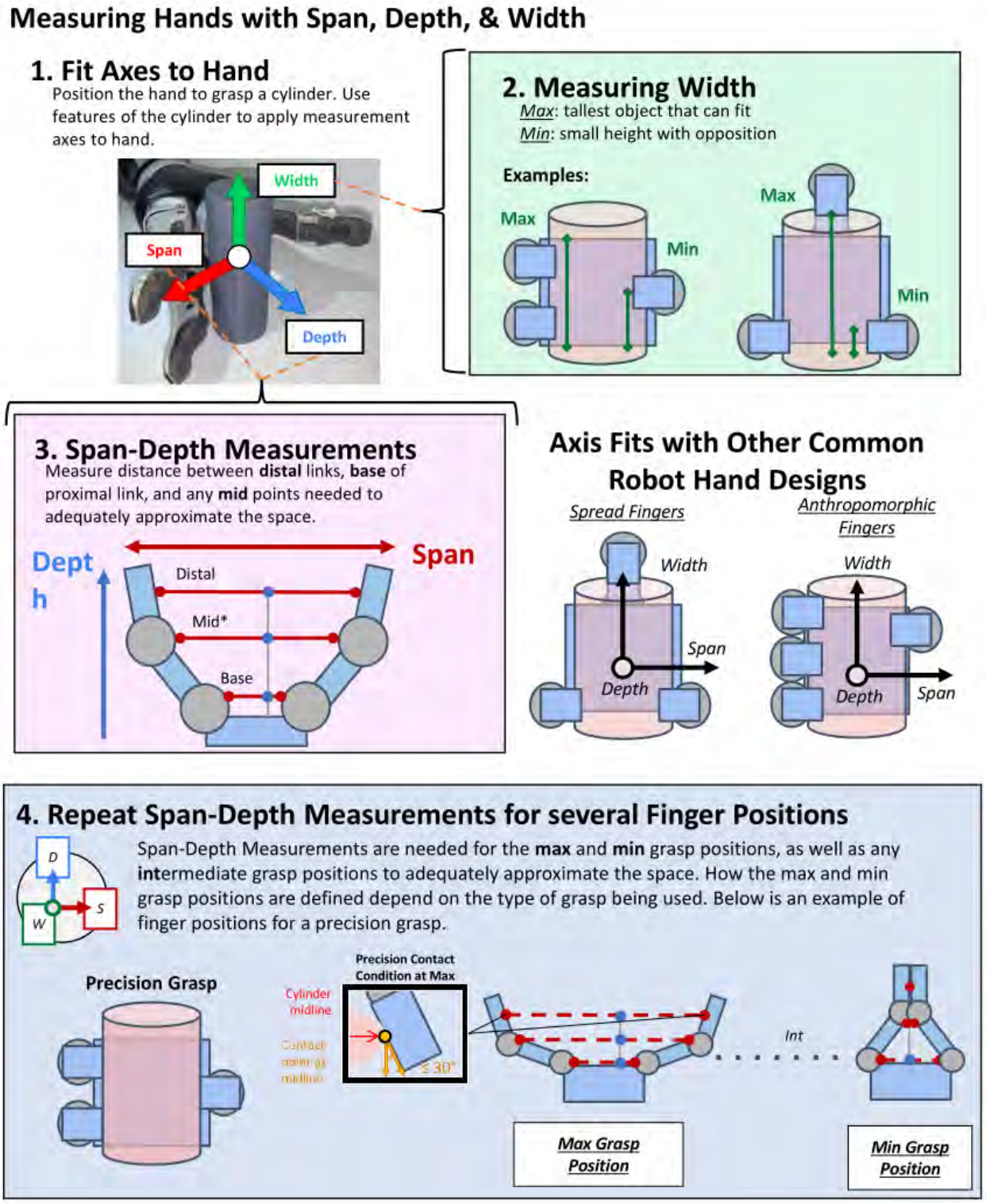

Figure 3.2: Our measurement method is a four step process, which involves: fitting measurement axes to a hand (1), and making various sets of measurements to represent the entire hand's space and how it changes as the fingers close (2-4).

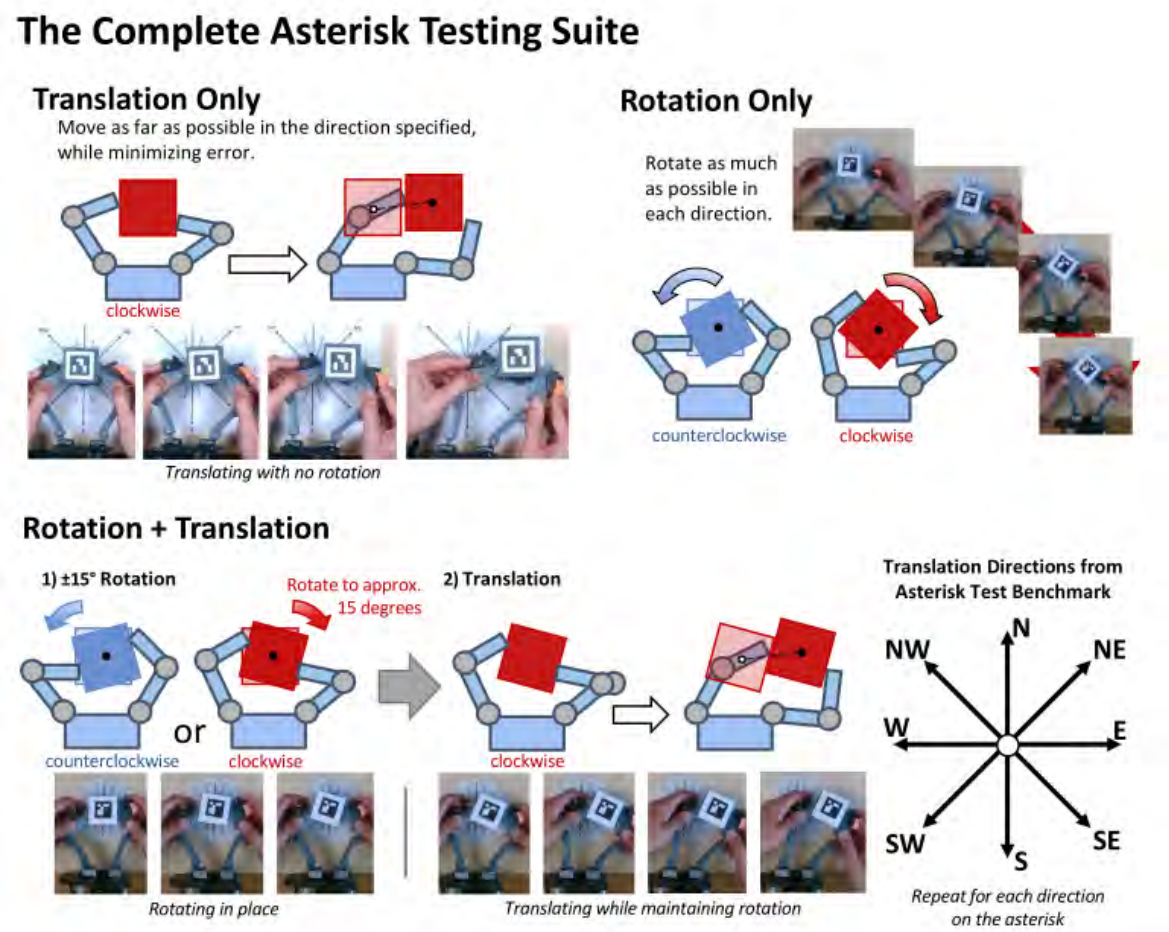

Figure 3.3: The Asterisk Testing suite consists of three sets of tests: Translation-Only (top left), Rotation-Only (top right), and Rotation+Translation (bottom).

Detailed instructions for our measurement method are provided in Appendix A. We also provide a concise visual guide in Figure 3.2 as a reference.

3.3 Benchmarking Fundamental, Distal Manipulations: The Asterisk Test

Considering the current capabilities of most robot hands right now, we designed the Asterisk Test to focus on 2D manipulations, as if performed on a table top. Considering Bullock and Dollar's manipulation taxonomy (117), we chose eight cardinal directions (see Fig 3.1) and two rotations (clockwise and counterclockwise) to characterize the manipulation space of a hand.

Due to the object-centric nature of this test, the Asterisk Test can be easily adapted for most objects, hands, and controllers. This makes it well suited for an investigation into the contributions of the system components.

3.3.1 Protocol

The Asterisk Test focuses on how a hand maneuvers an object in eight cardinal directions. The objective of the Asterisk Test is to move an object as far as possible in a specified direction and while minimizing error.

We divide the characterization into three test sets: translation-only tests, rotation-only tests, and combination tests (see Fig 3.3).

The translation-only tests are the eight cardinal directions. Translations start equidistant from each finger. In these tests, a hand must translation an object as far as possible and as close to the ideal as possible. Rotation is not desired.

Rotation-only tests are the opposite. In these tests, a hand must rotation an object clockwise and counterclockwise as far as possible, with as little translation as possible.

Combination tests (also called R+T tasks) discretely combine rotation and translation tasks to test for how robust object maneuverability is on a hand. The R+T task is as follows: 1) first the hand must rotate the object to $\pm 15^\circ$ in the center of the asterisk, then 2) the hand must translate the object in the direction of the trial, while maintaining the 15° rotation as best as possible. During the translation, we require the object to maintain that rotation to the end of the translation, $\pm 10^\circ$. The contact conditions are the same as in the rotation-only trials.

We chose the +/-15 degree rotation empirically to allow as many hands as possible to be able to complete the test while still having a discernible rotation.

The translation component of the R+T task is the same as a normal translation Asterisk Test — moving the object in each direction of a 2d asterisk on a surface as far as possible and as close to the desired direction as possible with no re-grasping.

A trial ends when the hand can no longer move the object in the testing direction. We calculate error based on how far a trial deviates from its ideal — namely a straight vector in the desired direction.

All that the Asterisk Test requires is a way to track the x, y, and θ coordinates of the object throughout each trial. Two simple solutions to this are to use ARuCo tags with a camera (118) or a motion capture system.

We require contact to stay on the side that the fingers originally contacted. Re-grasping an object is not allowed, however the *position* of the contact can still be changed (i.e. sliding or rolling) as long as it does not round a corner to another side (if there are defined sides on the object; ex: a cube).

When reporting Asterisk Test data we strongly recommend reporting *all* testing variables (the hand design, controller, object size and shape, and initial object positioning) used in testing, as well as any other changes to the standard protocol, to enable comparison with other Asterisk Test studies.

3.3.2 Performance Metrics

Our data gathering step generates an object path for each trial. Each path was normalized by the hand's dimensions. Specifically, the x translations were normalized with a hand's maximum span; the y translations were normalized with a hand's maximum depth (119).

We compare each object path to the desired straight-line path and to the limit of the hand's dimensions. We call this path the *target line*. In general, the magnitude of the target line is based on the distance between the object's initial position and the hand's span and depth. Each target line has a magnitude of half the normalized distance (normalized by either hand span and/or depth, depending on the direction) because the object was placed centered to the hand's palm (see Figure 3.3).

We use the following nine metrics for evaluating the difference between the target line and the object path (using the "similaritymeasures" python library (120)):

Trial Distance: The distance that a trial went in the target line direction. We calculate this as the magnitude of the object path projected onto the target line.

Arc Length: The length traveled on the object path.

Movement Efficiency: The total distance divided by arc length.

Max Error: The distance of the furthest point on the object path to the target line. This metric is normalized by the trial's arc length.

Frechet Distance: The minimum of the maximum pairwise point distances between two discrete curves without respect to time. This metric enables comparison of the entire object path to the target line. A lower value indicates lines are more similar to each other. See (121) for a description using the analogy of a dog on a leash.

Total Area Between Curves: The area between the object path and the target line.

Region of Max Error: The largest area between the two curves within a sliding window of width 20% of the total distance. We also record the window's center location at the point of max area, called the **Location of Max Error**, represented as a percentage along the full target line.

Max Rotation Error: The largest object rotational deviation from the starting orientation along the object path. In this work, the benchmark prefers no rotation.

When analyzing the data, these metric values were aggregated by direction and compared to other directions as a set. When comparing each object path to its target line, we scale the target line to the *Trial Distance* for a fair comparison.

3.3.3 Data Processing: Handling Multiple Trials

We display asterisk test results by representing the average path of each direction. We averaged each trial by sampling 20 points along the target line and averaging all points on all valid object paths within a certain bound around each sample point. We also calculated the error of each point

in the average from the average point. We represent the magnitude of the average error at each averaged point and represented this on the asterisk plot as a shaded region.

3.3.4 Calculating Symmetries

We define a symmetry as a direction pair that is similar to another. We determine symmetries by calculating the p value between each direction's set of metric values for each metric separately using the Welch (Unequal Variance) T test. If less than 1/3 of the metrics indicated a statistical significance, we considered the direction pair symmetrical.

For the 2D asterisk test there are 28 (8*7/2) possible direction pairs. We focused on assessing symmetries across the x ($\overline{CG}$) and y ($\overline{AE}$) axes of the asterisk. We used these two groups of symmetries (six direction pairs total) to represent the symmetry of the entire hand.

Chapter 4: Methodologies to study the actuation and morphological component contributions of robot hands at in-hand manipulations

We use our approach to investigate how the actuation and morphological components contribute to overall robot hand performance at manipulation tasks. In this chapter, we detail the methodologies of both studies. Results are provided in the next chapter.

For the actuation component study, we use mPHIG to study how four three-fingered robot hands, based on the Barrett hand and Model O hand, can use a pen and spray a spray bottle. The primary difference between these hands is what is available to the human subject to control. For the Barrett hand, one hand uses a minimally underactuated scheme and is controlled via sliders, and another is puppeted with no limits to how fingers are moved. For the Model O, one version uses rubber joints and the other uses pin joints. The rubber joints are provided to give human subjects additional degrees of freedom at the distal link.

We then follow-up on this study by investigating how fingerpads were used in the previous study. We do this with two straightforward characterizations: the flick test and the pull test. The flick test characterizes how well a hand can resist a sudden, strong impulse. The pull test characterizes fingerpad surface area by how well it can resist an object being pulled out of its grasp.

Finally, we detail our study into a hand's morphology, which uses mPHIG and the Asterisk test to characterize how well a hand can translate and rotate an object using the distal links. This study is divided into two parts: an exploratory study and a validation study. The exploratory study uses human subjects to explore the maneuverable space of 10 hand designs. In the validation study, we take the best trials for each hand-direction-rotation set and use additional human subjects to validate the repeatability of the best trials.

4.1 Studying human actuation strategies for tool-use

We chose two highly-dexterous tasks that would be difficult to automate with existing technology. Our tasks were selected from Bullock and Dollar's (117) hand-centric manipulation taxonomy, with a focus on tasks that were sufficiently difficult for a human puppeteering a robot end effector to complete. The tasks are: drawing on a bowl with a sharpie (in taxonomy: C P M W NA (14)) and using a spray bottle (in taxonomy: C P M W N (15)). Both tasks take place on a flat table.

We analyze the data using both qualitative (descriptive analysis of the manipulation from a video recording, questionnaire asking for subjective feedback) and quantitative (joint angles, time and success rates on task) data. Our results show that there are demonstrable differences between hand types in both efficacy and control strategies.

Contribution: Our contribution is a physical study design that enables side-by-side comparison of the capabilities (and limitations) of different robotic hand designs. This design lets us use the

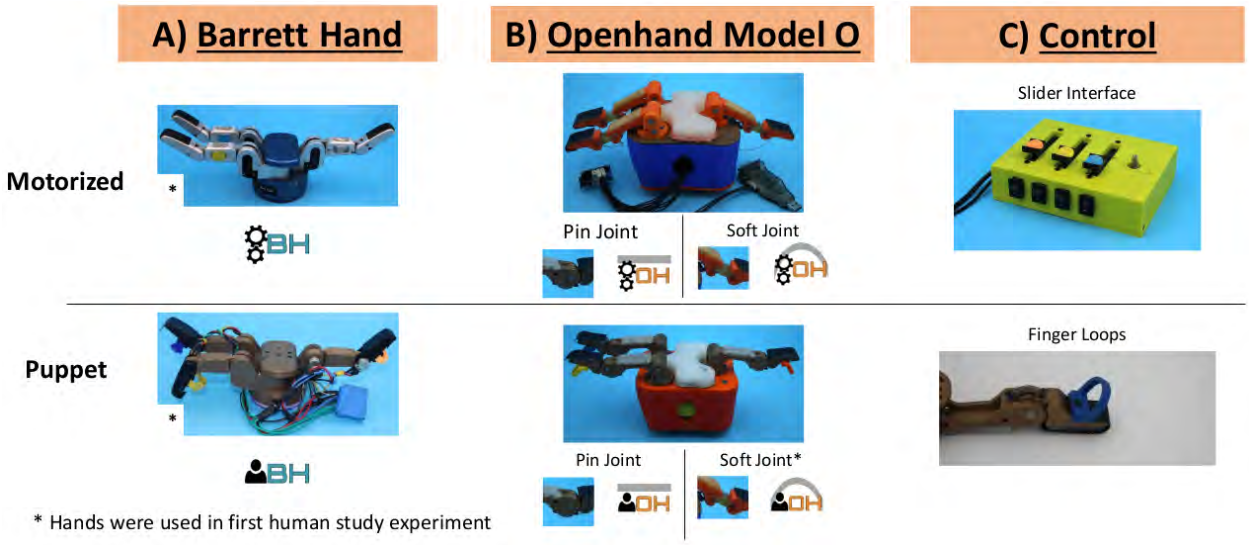

Figure 4.1: The hands which we used for the study (2 left columns) and the control interfaces used for each hand (far-right column). The motorized hands used the slider interface and the puppet hands used the fingerloops. The Openhand model had two designs, one with a pin joint and the other a soft joint.

"Human Grasp Planner" with nearly complete capabilities, but without the problem of having to map from the human hand back to a robotic one. We use this data to draw conclusions on effective strategies for hand design and control for manipulation tasks.

4.1.1 Robot Hands Studied

We used three robot hand setups which had different kinematic constraints: 1) a commercial Barrett hand, 2) a puppet hand version of the Barrett Hand, and 3) a puppet hand version of the Openhand Model O. Each hand is shown in Figure 4.1 and is described below.

The commercial Barrett hand used an underactuated strategy. This underactuated design supports only closing or opening the finger in a set relationship between the proximal and distal joints. The Barrett hand employs a patented slip-gearing system to implement compliance. Because of an inability to move the fingers directly, this robot hand was technically not a puppet hand. Participants controlled the end effector using a custom control box with three linear sliders (one for each finger, color coded for ease of use) and a rotating knob to control finger spread.

The puppet hand version of the Barrett hand is identical in morphology to the original end effector. A key difference, however, is that the puppet Barrett hand does not have any joint constraints. Each joint can freely rotate, including past 180 degrees on the distal joint. Participants manually moved the fingers on the puppet Barrett hand. For ease of use, we added plastic loops on the back of the distal links for participants to rest their fingers. These were color coded and matched the color scheme for the underactuated hand. We also instrumented the puppet Barrett hand with rotary potentiometers at each joint to collect joint angle measurements.

The Openhand Model O was also used in puppet hand form. We used the Model O variant with compliant distal links. We replaced the silicone in the joints with Dragonskin 10 rubber (Smooth-On) to make it easier for participants to manipulate the distal link. We implemented plastic loops for participants in a similar manner to the puppet Barrett hand. We used Dragonskin 10 in the fingerpads for consistency. We also modified the palm rubber to be thicker so that the palm-finger depth would match the Barrett hand more closely. We were unable to instrument the Model O as we did the Barrett hand because of the compliant distal joints. Therefore, this end effector does not appear in the quantitative analysis of the joint angles for the human study.

Across all hands, we normalized the finger pad friction by using standard electrical tape across the finger pad.

After initial data collection, we ran a less rigourous follow-up study of the posable Barrett hand modified to have compliant fingerpads and added an Openhand with rotary joints. We also added actuated versions of the Openhand, which used the slider controller for a fairer comparison between hand designs. Then we studied these new hands amongst ourselves.

4.1.2 Protocol

First, participants completed a short warmup to become familiar with the end effector setup used for the rest of the trial. After the warmup, participants completed the pen-drawing task followed by the spray task. Participants were given 15 minutes to complete each task. We recorded a video of each trial for analysis, as well as joint angle data for two of the three hands (see subsection on Robot hands below for more details).

After both tasks were completed, participants were given a survey to collect qualitative data regarding task performance and ease-of-use for that hand. At the completion of both end effector setups, participants were given extra survey questions comparing the two setups. We provide the survey questions in Appendix 4.1.3, for reference.

4.1.2.1 Warmup Tasks

For the warmup the subjects had to complete two subtasks: a grasping and writing task. The grasping subtask asked subjects to lift three objects of increasing difficulty: a Pringles can (YCB set), a toy plane (YCB set), and a thin plastic vacuum nozzle. The writing subtask consisted of writing 'OK' on a flat sheet of paper with the same King-Sized sharpie used in the bowl task (pen placed in the hand, rather than grasped). 'OK' was chosen because it was short and contained both curved and straight features for the subjects to practice on.

The subjects were not given a time limit for the grasping task and had 10 minutes to complete the writing task. All subjects successfully completed the warmup tasks within the time constraints.

4.1.2.2 Pen Task

In the pen drawing task, we asked participants to draw a pattern on a bowl. The pattern consisted of a zig-zag line which was printed on paper that we taped to the side of the bowl. As an extra challenge, we asked our participants to follow the pattern at a 1cm offset from the line printed on the paper. We chose to use the surface of a bowl instead of a flat surface because it required a larger range of surface contacts and stabilizing forces than a flat one.

The pen used was a King-Sized Sharpie, which was an adequate size for the larger robot hands. The bowl was taken from the YCB object set (122). We taped a piece of paper with a zig-zag pattern to the top of the bowl, as shown in Figure 4.2. We filled the bowl with a high friction putty that kept the bowl in the same place during the task, but made the bowl easy to move when cleaning up after the task.

In addition to the 15 minute time constraint, we limited participants to three tries during drawing — whichever came first. Participants would use up a try when a pen grasp failed at the time of contact with the bowl. If a participant's grasp failed before making contact with the bowl it did not use up a try. If the pen grasp failed at contact and before drawing, the pen was reset to its starting position and the participant would have to try the task from scratch again. If a participant had drawn some of the line before grasp failure, the participant was allowed to continue the line from where it ended.

The subjects were allowed to move or rotate the pen before picking it up. The pen had to stay on its side and subjects were not allowed to move the pen off of its side. Also, subjects were not allowed to move the pen when it was in contact with the robot hand or use the edge of the table to grasp the object.

4.1.2.3 Spray Task

In the spray task, participants had to pick up a janitorial spray bottle (946 mL size), angle it to approximately 45 degrees, and spray the bottle three times. The bottle had a freely rotating nozzle and was filled with 200-300 mL of water.

We were generous when considering which sprays from the spray bottles would count — as long as some water shot out of the spray bottle (instead of dripping out), we counted it as a spray.

The same procedures in the pen task applied to the spray task with one exception: we did not apply the concept of tries to the spray task.

4.1.3 Survey on Hand Ease-of-Use

After completing the tasks for a given hand design, subjects were given a five question survey to rate their performance and the hand design. After completing both hands, the subjects were given an additional three follow-up eight question to compare the two hands they used. Participants were allowed to ask clarification questions if they were confused about a question. The survey is

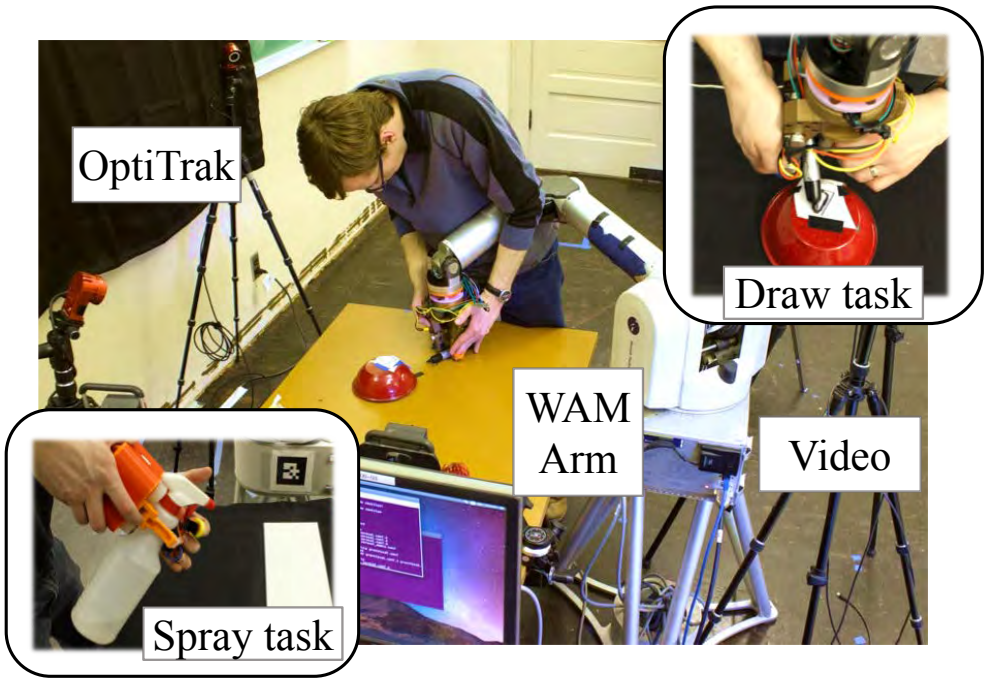

Figure 4.2: The setup of the PHIG study. Humans puppet the fingers of a robot hand directly for two tasks: drawing with a pen on a bowl (bowl task) and spraying a spray bottle (spray task). Author is featured in photograph — consent was provided.

provided in Appendix 4.1.3.

4.1.3.1 Participant Demographics

We recruited 18 participants through word of mouth. Each participant used two hand types for this study, meaning that a total of 12 subjects used each hand type (6 as first hand, 6 as second). All participants had normal (or corrected to normal) vision and physical capabilities. We chose two groups of participants: 1) two-thirds of the participants were engineering undergraduate students and 2) the remaining one-third of participants had little or no experience with robotic hands. We found no difference in the ability to perform the task based on engineering background.

4.1.3.2 Task and Data Analysis

We analyzed task performance using three metrics: 1) the time it took participants to complete the task, 2) the number of re-grasps or attempts made, and 3) survey responses. We determined these metrics by analyzing video of each trial.

During video analysis we segmented each video into grasping and manipulation phases. We defined the start of the grasping phase as the time the participant began manipulating the wrist/fingers of the end effector into a pre-grasp shape. We defined the end of the grasping phase as the time

when all of the fingers on the hand had reached stable contact. On average, successful grasping phases lasted 23 (standard deviation: 24) and 18 (standard deviation: 16) seconds for the pen drawing and spray bottle tasks, respectively.

We defined the start of the manipulation phase as the time when the participant started to perform the task. For the pen drawing task, this was when the pen first contacted the bowl. For the spray bottle task, this was when the spray bottle was lifted off the table. We defined the end of the manipulation phase as the time when the participant dropped the object or completed the task. If in the pen task a participant dropped the pen and re-grasped it using the same grasp, we cut out the grasp (recording it as a grasp phase) and joined the individual manipulation phases which bookend the grasp together.

We analyzed the joint angle data (Barrett hands only) by phase. Since each data segment has a unique duration we normalized these sequences by resampling each phase to 1000 samples. This enabled us to compare joint angle data between participants regardless of temporal length.

4.2 Characterizing the Dynamic Response of Robot Hand Designs

In the previous study, we observed that grasps using the entire fingerpad were clearly superior to grasps using the fingertips. This can potentially be explained by the following three observations: 1) the fingerpad grasp tends to have more surface area in contact with the object, increasing friction; 2) the fingertip grasp is only capable of applying restoring forces roughly perpendicular to the point of contact, while the finger pad has the ability to 'rock', applying a wider range of restoring forces in all directions; 3) the contacting surface shapes are different — the fingertip is more curved than the fingerpad.

Characterizing these directly is challenging because of the compliance in the contact surfaces and (for soft joints) the joint itself. It is also difficult to directly measure the perceived forces the participant is responding to, and how they respond to those forces. For this reason, we have designed our follow-up study to quantitatively measure robustness to disturbances.

4.2.1 Experimental Design

We describe the two characterization experiments we used to understand the benefits of the pad grasp over the tip one: the pull test and the flick test. In the pull test, we measured the force required to pull an object out of a grasp with normalized grasping force and normalized fingerpad friction. The flick test measures how well each grasp resists a large and sudden disturbance — a finger flick to the object it was holding.

For both tests, the objects were placed vertically in the grasp about 2cm from the table's surface; the operator was not required to pick the object up from the table. For both tests we used a 3d printed object with integrated force sensors (which we refer to as the instrumented object) to normalize the grasping force on the object for all trials.

We performed ten trials for each test, per hand. We did not recruit subjects for this test.

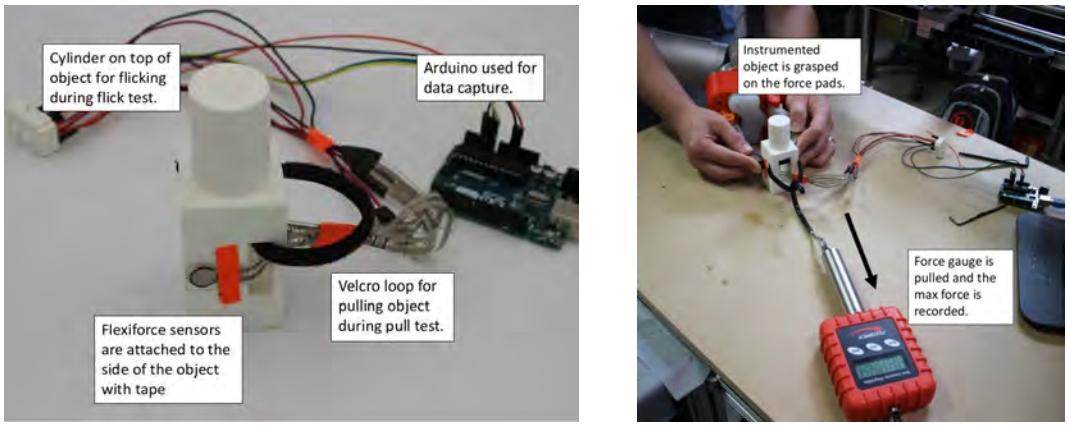

Figure 4.3: Flick and Pull Test. (Left) Instrumented object used in both pull and flick tests to normalize grasping force. (Right) Pull test setup. Flick test setup is identical, but without force gauge.

Below we describe various aspects of our follow-up study, including setup (Section 4.2.2), pull test protocol (Section 4.2.3), flick test protocol (Section 4.2.4).

4.2.2 Pull and Flick Test Setup

Both the pull and flick test used the same setup. For both tests we used a simple instrumented object, shown in Figure 4.3. This object had a rectangular base where we attached force sensors (Flexiforce). On top of the rectangular base was a cylinder for flicking. The total object dimensions are 4x4x7cm with a hollow inside for cable routing. We also route a thin velcro piece through the hollow inside for pulling the object.

The force sensors were taped onto the object so that the fingers would directly press on them when grasping the object. The force sensors were taped to make sensor placement easier between hands (Barrett vs Model O). We did not observe the tape to have any effect on any object grasps.

We set the normalized force for both tests to be 5N. Participants had access to real-time force data when grasping the object to help them normalize forces on the object.

4.2.3 Pull Test

This test measured the maximum force required to pull the instrumented object out of both the tip and pad grasps. We focused on the puppet Barrett and Model O hands because they were able to do both the tip and pad grasps. The testing setup is shown in Figure 4.3.

In the pull test, participants grasped the instrumented object with normalized force and held it about 2 cm off of the table. We used a force gauge with a large hook to pull the instrumented object out of the grasp. We pulled the instrumented object by hand, slowly increasing force as we pulled. The maximum force measured was recorded for each trial.

We analyzed results statistically using ANOVA between relevant hand pairings.

4.2.4 Flick Test

We performed the flick test with two objects: the instrumented object described above, and the pen used in the pen drawing task. Similarly for the pull test, we focused on the puppet Barrett and Model O hands because they were able to do both the tip and pad grasps.

In the flick test, participants grasped each object and held it about 2 cm off of the table. We were unable to attach force sensors to the pen, so only the instrumented object flick tests were guaranteed to be normalized. However, we attempted to normalize the pen grasp by having participants perform the flick test on the instrumented object first. Then we asked the participants to recreate the normalized force they felt with the instrumented object on the pen.

For each trial, the object is flicked perpendicular to the fingerpad/fingertip. We flicked the objects ourselves. We recognize that there is variation in the flicks between trials and attempted to normalize this variation between hands by using 10 trials.

We recorded results as one of three result conditions: 1) Fail, 2) Move, and 3) Stable. Fail is defined as instances when the grasp would fail when the object is flicked. We define the move condition as instances where the object moved more than five degrees in the grasp, but did not fall. We define a stable condition as instances where the object moved less than five degrees. We also attached a scoring system to each condition: Fail (0 points), Move (0.5 points), and Stable (1 point).

We analyzed results statistically using the Kruskal Wallis test between relevant hand pairings.

4.3 Exploring the Maneuverable Space

We study the morphological component's contribution to in-hand manipulation performance because it is the component which has received the least attention in robot manipulation. In this study, we use mPHIG and the asterisk test to characterize robot hands at fundamental in-hand translations and rotations using the distal links.

We use mPHIG to normalize the controller (a human subject) across hand designs. Using a human subject also allows us to study multiple robot hands while bypassing the need to develop an entire robot hand system.

The Asterisk Test characterizes how a hand maneuvers an object through its workspace. It compares the object's path to the desired path using a set of nine metrics. The test uses three sets of tasks to do this: translation-only, rotation-only, and rotation+translation tasks (see Fig 3.3). Please reference Chapter 3 for more details on the Asterisk Test.

This study is divided into two parts. The first uses human subjects to explore the maneuverable space of ten hand designs. In the second part, we best the best trials in each direction for each hand and used human subjects to validate how repeatable those trials were. We describe the protocols of each part separately because they differ slightly.

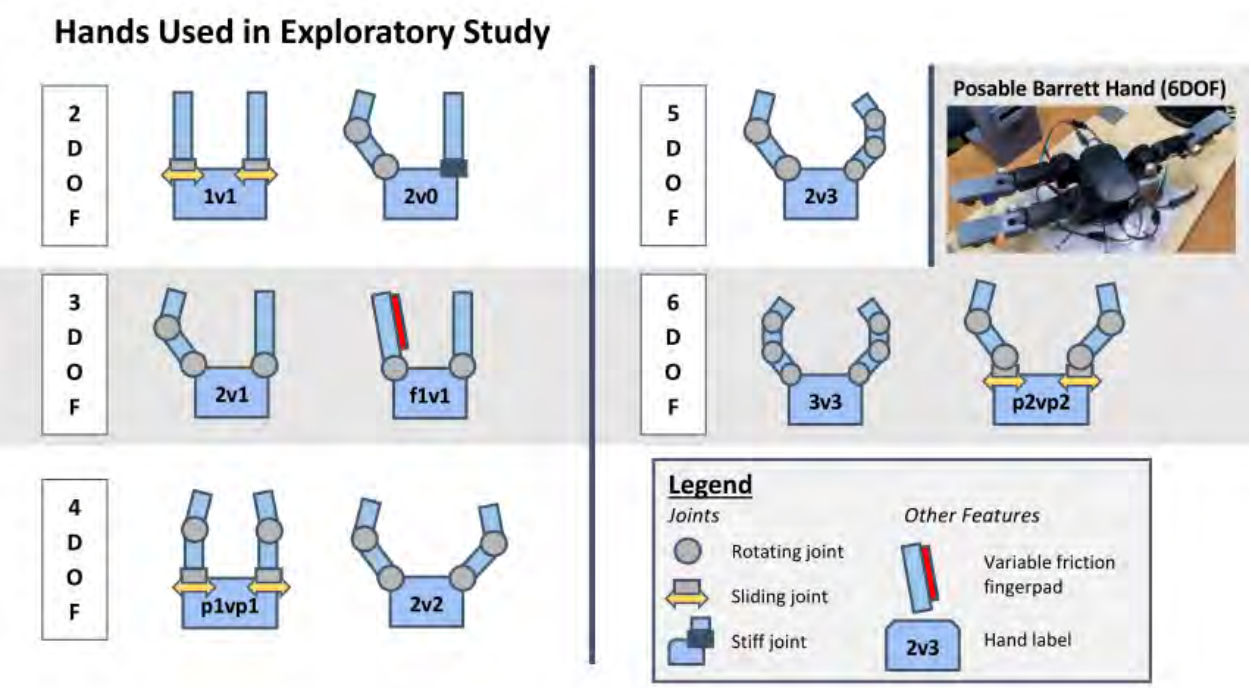

Figure 4.4: The ten hands studied in the exploration study utilized rotary joints and planar joints at the palm to cover a variety of degrees of freedom.

4.4 Exploration Study

In this study, three subjects performed the asterisk test for all ten hands over the course of a single day. Although undesirable, this was necessary due to COVID restrictions at the time. Subjects were placed in a testing room on their own, and the study was administered through zoom and controlled via remote desktop.

4.4.1 Hands Studied

Figure 4.4 shows the ten hands used in this study, which represent a wide variety of dof. At the low dof end is the 1v1 hand, 2 dof, which is a parallel jaw gripper with independently moving fingers. At the high dof end are the 3v3 and p2vp2 hands, each 6 dof, which utilize two three-linked fingers and two two-linked fingers on sliders, respectively.

The BH hand is the posable Barrett hand with compliant fingerpads used in the actuation study. The f1v1 hand utilizes a variable friction finger based on the model vf hand (20). The finger contained a low-friction pad which was moved out of the way when force was applied to it.

The rest of the hands are custom, modular designs based on the Yale Openhand. These hands utilize different combinations of rotary and planar joints. The planar joints only occur at the palm, meaning that the fingers can freely slide, changing the width of the palm.

Fingers on all hands were designed so that they were the same length, regardless of how many

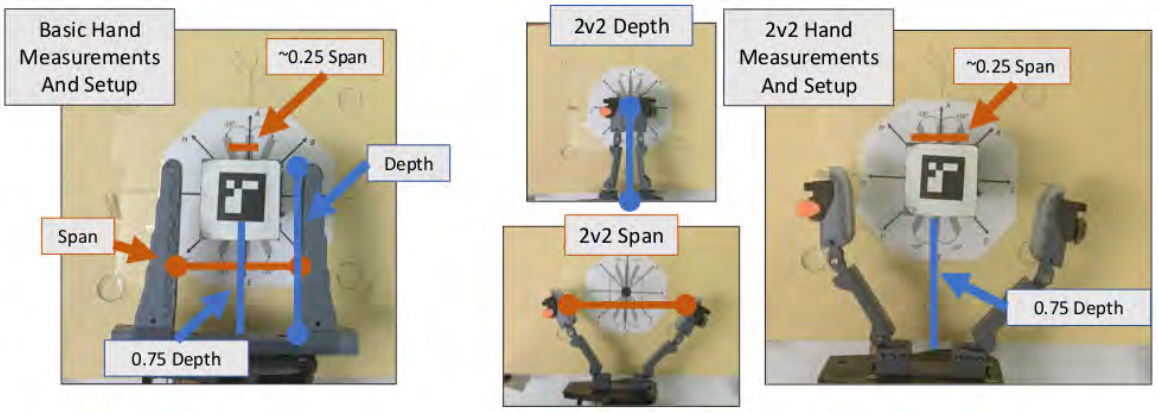

Figure 4.5: Hand Span and Depth measurements and asterisk test setup for both the 1v1 (left) and 2v2 hand (middle, right). Measurements for max span and max depth were used to set object size and initial position. Relevant dimensions and setup images were taken from top-down camera. Each object is sized smaller than the ARuCo code.

links there were. The hands were also designed to be modular to simplify assembly.

4.4.2 Protocol and Setup

In the Asterisk test, hands must translate an object in eight cardinal directions, repeated for three rotation conditions (x, p15, and m15), and rotate the object in place clockwise and counterclockwise.

The following additional constraints were placed on subjects during the asterisk test:

1. Once contact is established, contact cannot be broken until the end of the trial. No regrasping is allowed, however sliding and rolling contacts are. Fingers can pivot at object corners, however they cannot pivot onto a new surface.

2. Subjects had to let go at the end of the trial. This was meant to discourage leaning the object.

3. No time limit was place on each trial. Subjects were free to repeat trials until they were satisfied.

Directions were not repeated until the subject 'came around' the asterisk again. Directions were repeated five times. This was meant to help the subject explore the space and adapt new strategies to other directions. The order subjects completed directions was: [N, NE, E, SE, S, SW, W, NW, CW, CCW], repeated five times in order, and repeated for the three rotation conditions (no rotation, +15, -15). The rotation-only trials (CW and CCW) were not performed when the rotation conditions were +/-15.

We used an overhead camera to track an ARuCo marker on top of the testing object. The testing object was sized to be between 20-25% of a hand's max span. The center of the object, as well as two opposing walls, were hollowed out, to discourage pivoting on to a new side of the hand.

The object was placed equidistant between the fingers and about 75% the hand's max depth from the palm. The object was re-centered to this position after every trial.

See Figure 4.5 for example measurements, object size, and initial placements for the 1v1 and 2v2 hands.

4.4.3 Data Processing

After data was collected, we first normalized the data. The x component was normalized by the hand's max span. The y component was normalized by the hand's max depth. Then, the nine metrics were calculated.

Next was a garbage collection step; we checked to see whether the path had deviated too far from the target line. This was accomplished using a simple threshold of 0.2 normalized distance from the target line. If a path went outside the threshold, it would be labelled as a deviated path.

Finally, we collect non-deviated trials of corresponding hand, direction, and rotation type and then average their paths and metric values. We averaged each trial by sampling 20 points along the target line and averaging all points within a certain bound around each sample point. We also calculated the error of each point in the average from the averaged point.

We plot the averages paths on an asterisk. We represent the magnitude of the average error at each averaged point and represented this on the asterisk plot as a shaded region.

4.4.4 Hypotheses

Given prior experience with human subjects, we believe that our subjects will be able to adapt well to each hand design. We also hypothesize that they will utilize sliding and rolling contacts on each hand.

In terms of hand performance, we expect a improved performance with increased degrees of freedom. We expect that the sliders will have exceptional performance right and left. Considering asymmetrical hands, we hypothesize that they will have reduced performance due to whichever finger has fewer degrees of freedom.

4.5 Validating the best paths

The second part of the morphology study was used to validate how repeatable the best trials from the exploratory study were. The validation was performed on six of the original ten hands based on performance in the exploratory study. In addition, hands in the study were divided into two categories based on their exploratory results: high performing and low performing hands.

Six subjects were used, each doing the asterisk test on one low performing hand and two high performing hands, according to a latin squares design. Subjects were also given surveys after completing each hand, which asked about ease of use and desired changes to a hand's design (see B).

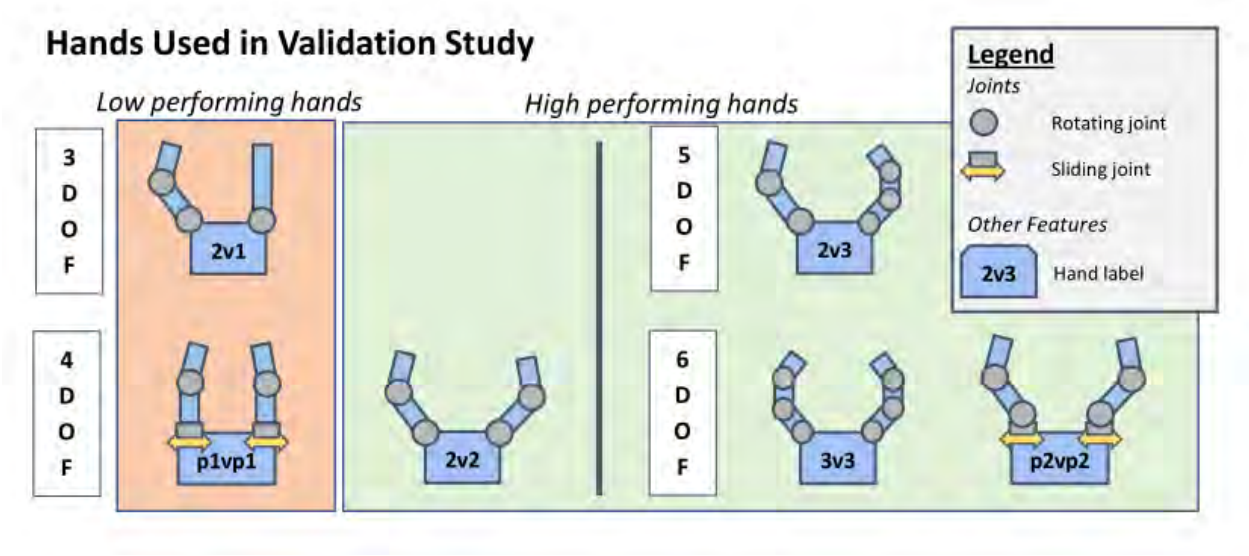

Figure 4.6: Six hands used in the validation study. Hands were divided into low performing and high performing categories according to their performance in the exploratory study.

4.5.1 Hands Studied

Figure 4.6 shows the six hands used in the study.

Two hands, the 2v1 and p1vp1 hands, were classified as low performing hands. The 2v2, 2v3, 3v3, and p2vp2 hands were classified as high performing hands.

The hands used were the same hands from the previous study. With that in mind, we observed that the fingerpads had lost some of their friction, which affected performance.

Four hands were not included due to time and performance concerns. The 1v1 hand was too basic to validate, however it was used as a warmup. The 2v0 hand was excluded due to poor performance. The f1v1 hand was excluded due to difficulties analyzing the data due to the strategies that the human subjects used. The BH was not included because of its tendency to tip objects in the exploratory study, due to its fingers not being directly opposite each other.

4.5.2 Protocol and Setup

We slightly modified the set of constraints placed on the human subjects. The main difference is that the new criteria for repeating trials and the trial end criteria were modified.

The constraints are as follows:

1. Once contact is established, contact cannot be broken until the end of the trial. No regrasping is allowed, however sliding and rolling contacts are. Fingers can pivot at object corners, however they cannot pivot onto a new surface.

2. The object was not let go at the end of the trial. Although the previous rule discouraged leaning, it would also cause the object to wobble at the end of a trial, which complicated data

analysis. Instead, subjects indicated verbally when they were done.

3. No time limit for trials.

4. Subjects had to move the object to within 75% of the total distance value of the best trial. If subjects had difficulties replicating the best trial, they were given three attempts before their performance would be saved, regardless of the total distance. Exceptions to this rule occurred when the third trial was not valid or was not consistent with their previous attempts. Three attempts would be repeated for each of the 3 trials recorded.

Subjects completed three trials for each direction before moving on to the next. The order of directions was also modified to accommodate symmetries. The updated order is: [N, NE, NW, E, W, S, SE, SW, CW, CCW].

Each hand was given its own custom tesitng object this time, sized to be exactly 25% of max hand span. This object was hollowed out more aggressively than the object used in the exploratory study.

Object initial distance was not changed in the validation study.

4.5.3 Best Trial Selection

We chose the trial with the highest total distance from a filtered set of trials with high quality. We filtered the trials to ensure that trials with high total distance, but poor metric performance were not considered for best trial.

We cut trials based on two metrics: movement efficiency (mvt_eff) and translational total distance (t_fd). Selected trials had to be within 30% of the best values attained for the metric on that hand in the specific direction.

We show the best trials selected for each hand for the 'x' rotation condition in Figure 4.7. We provide best trial plots for all hands in the validation study and the +/-15 R+T conditions in Appendix **??**.

4.5.4 Hypotheses

Given our experience with the exploratory study, we hypothesize that our next set of human subjects will be able to reproduce each best trial on every hand in the study.

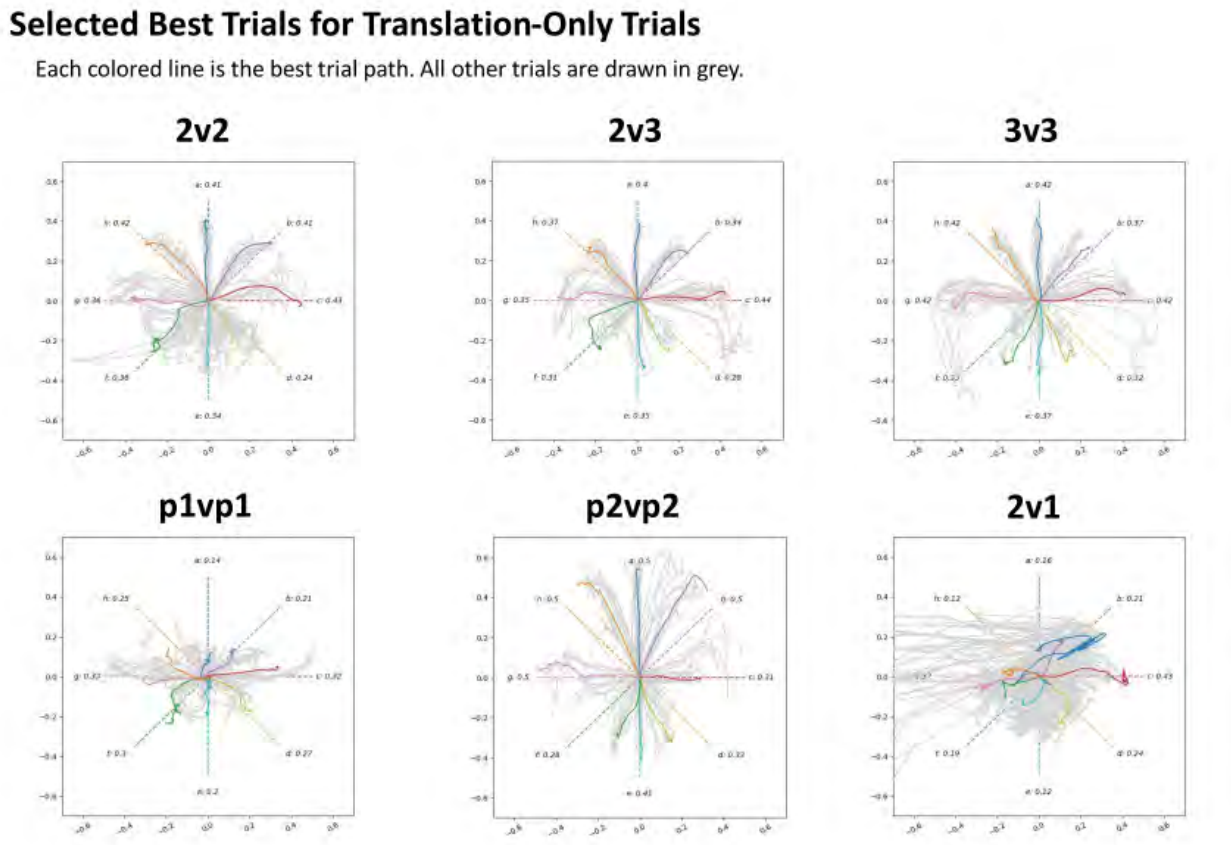

Figure 4.7: Selected best trials (colored) for each hand, for the x rotation condition. All of trials are drawn in grey.

Chapter 5: Results of actuation and morphological component studies

5.1 Tool-Use Study Results

We present qualitative and quantitative results on task performance, followed by a detailed comparison of the BH versus PH joint angles.

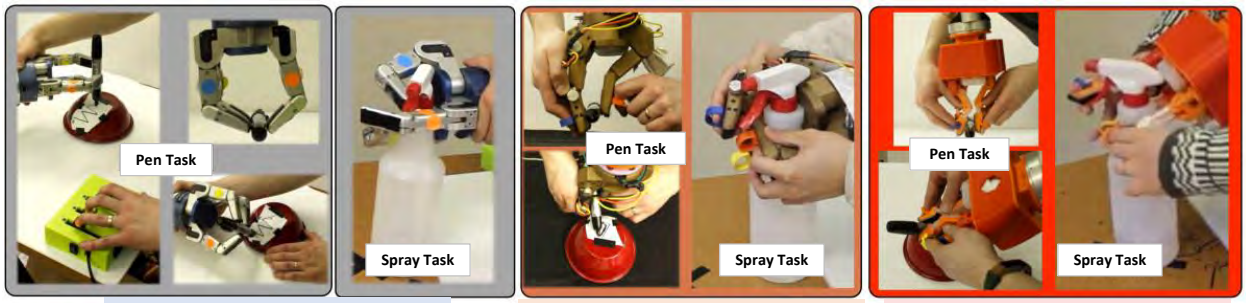

Figure 5.1: Qualitative results gathered from the PHIG study. (Top) Images gathered from trial video showing the types of grasps used for each task. (Bottom) Notable survey quotes, focused on the ease of use of each hand. With both the Posable and Open hand it was possible to bend the fingers backwards in order to grip the pen with the fingers flat instead of at the tips.

5.1.1 Human Task Performance

Task performance results are presented in Figure 5.2. The OH performed significantly better than the other hands in terms of average task completion time (paired t-test < 0.05 for the spray bottle, < 0.01 for the bowl). All hands performed similarly for the other metrics. There was no statistically significant difference in any metric based on hand order.

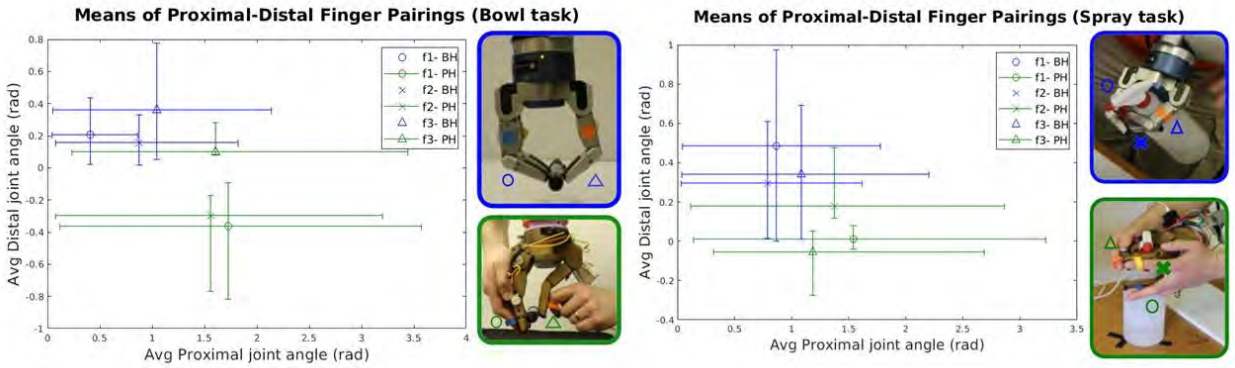

Task	Metric	Barrett Hand	Puppet Barrett	Puppet Model O
Bowl	Avg. Task Completion (sec)	190.58 sec	265.33 sec	**84.58 sec**
	Avg. Manip. Time (%)	**29.96%**	20.57%	22.27%
	Avg. Regrasps	3	6	**2**
Spray	Avg. Task Completion (sec)	383.33 sec	344.17 sec	**162.92 sec**
	Avg. Manip. Time (%)	**23.20%**	21.50%	20.89%
	Avg. Regrasps	4	5	**2**

Figure 5.2: Qualitative results gathered from the PHIG study. (Top) Images gathered from trial video showing the types of grasps used for each task. (Bottom) Notable survey quotes, focused on the ease of use of each hand.

Table 5.1: Percentage coverage of joint angle data for each added dimension, using pca.

PCA results, percentage coverage per dimension

	Bowl task			**Spray task**	
Dim	Barrett	Printed		Barrett	Printed
1	45.72991	50.40023		56.86313	47.05089
2	38.58421	27.53254		37.68461	28.6918
3	9.707124	13.04163		4.115794	13.6785
4	4.053381	4.859988		1.105763	8.449121
5	1.925369	4.165617		0.230695	2.129684

5.1.2 Survey Results

Participants rated the underactuated Barrett hand and the puppet Model O hand similarly. Both were consistently rated higher than the puppet Barrett hand. Participants commented that the underactuated Barrett hand was hard to control to get the grasp in the first place, but was better at holding a grasp. The comments were reversed for the puppet Model O hand: participants found the grasp easier to make (and reflected participant's desired grasps better), but maintaining the grasp was more difficult. We provide several representative quotes from survey responses in Figure 5.1.

Many participants rated the puppet Barrett hand poorly. The primary complaint made about this end effector was that a lack of fingertip compliance (the fingertip was 3d printed) made establishing grasps difficult.

Participants chose the proximal joint to be more important than the distal (9 versus 2). If only given the choice to make one finger fully actuated, the participants chose the thumb (2/16). The thumb was defined as the finger which did not move during finger spreading on both hands. Several participants also made comments about the general hand design: two suggested adding more joints on the thumb, two wanted to change the finger lengths, and another two wanted thinner fingers for easier manipulation.

5.1.3 Joint Angle Analysis

The mean proximal and distal joint angles for each task per hand are shown in Figure 5.2 for the bowl (left) and spray (right) tasks. Qualitatively, the OH joint angles closely mirrored the PH, as can be seen in Figure 5.1.

We provide further proximal and distal joint angle relationships with respect to time in Figure 5.3 (1000 time samples for each successful grasp analyzed). The underactuated nature of the BH is clear here, with participants primarily moving the proximal joint, or jamming the proximal joint which leads to only distal movement. Participants using the PH clearly did not employ monotonically decreasing angles, but often backtracked.

Running PCA on the joint angle data also showed that the BH and PH data could be described in 2 and 3 dimensions, respectively (Table 5.1).

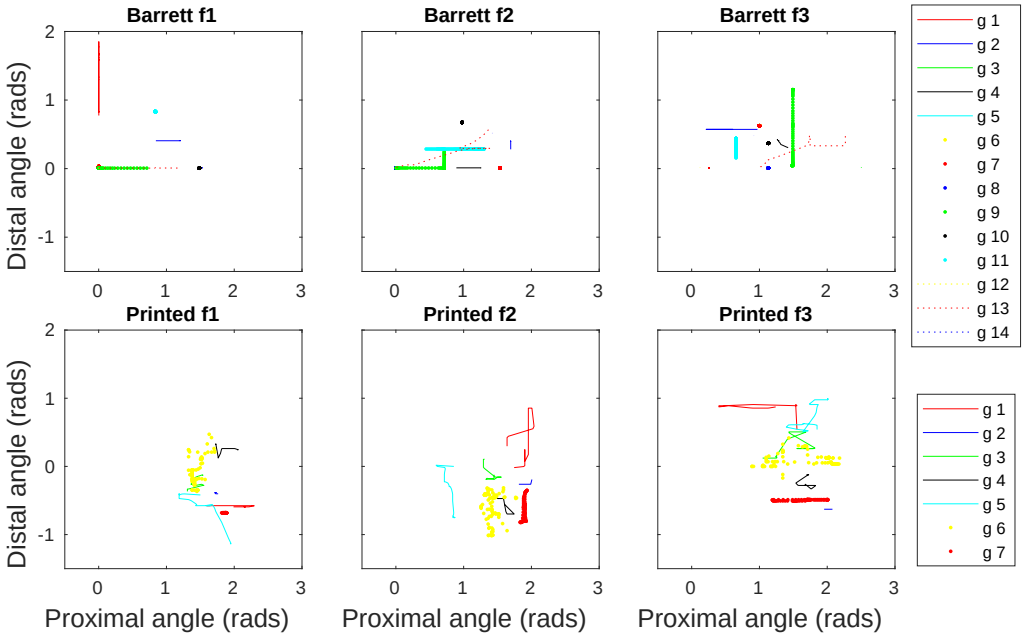

Figure 5.3: Finger joint angle relationships between BH and PH. 1000 time samples are plotted for each grasp to show how each was used.

5.1.4 Comparison of human controlled fully-actuated and underactuated grasps

First, we noticed that when given complete freedom over hand positioning, humans will depart from using underactuated control schemes. We show a general representation of these findings between the BH and PHs in Figure 5.2. The large standard deviations for PH show a lot of proximal joint variation between subjects. Interestingly, the distal joint has lower standard deviations and much tighter angle boundaries. Referencing the bowl results in Figure 5.2 specifically for its clarity, the averaged data shows fingers 1 and 2 bent backwards and finger 3 straight in opposition. This results in usage of the fingerpad (compliant) over the fingertip (less compliant).

Our hypothesis how humans approach these manipulation tasks (and their grasping subtasks) is with a combination of full and under actuation finger strategies (which we refer to as quasi-actuation). We believe that humans use the proximal joint in a fully actuated method to bring the distal link close to the object. Then the distal link governs actual contact with an underactuated scheme. We believe that humans use quasi-actuation to compensate for our lack of precision. We believe that these observations are support by the tendon routing in the bio-memetic robot-human hand by Xu & Todorov (123), as well as in part by the finger actuation scheme of the M2 hand (21). This leads us to conclude that underactuation alone cannot handle manipulation tasks - as a human approaches it, particularly with two joint fingers. We believe that when underactuation is utilized within a quasi-actuated control scheme, the real potency of underactuation will be realized.

However, the question remains about what the subjects optimize for when grasping without

hand constraints. We observed qualitatively that despite large proximal joint variance between subjects, the poses of the fingerpad relative to the objects between subjects are the same. This goes beyond pregrasp shapes - think instead of object centric finger positioning. Figure 5.3 supports these findings. In the figure, the BH joint angles move largely independent of each other (straight lines), contrary to the PH, where both proximal and distal joints are adjusted relative to each other (amidst lots of backtracking). On its own the PH joint angle data is difficult to analyze, however with the quasi-actuation scheme in mind as well as our own observations, we believe proximal (and by association, the distal) joint angles are more dependant on the hand position for stable grasps than considered with existing schemes, such as capture regions. We plan to follow up on these findings by analyzing joint angles in relation to the position of the object which will be grasped.

These findings are also echoed by Todorov & Ghahramani (124) in a dataglove experiment. They concluded from their findings that the synergies in a human hand for manipulation tasks (which also differed between tasks) arise from human closed-loop control and not by actuator design - again suggesting a human grasping perspective that is not hand-centric. Regarding grasp preshapes and their similarities to what we argue, we believe that grasp preshapes are only a symptom of a more generalizable object-centric human grasping system.

5.1.5 The Effect of Compliance

The PH and OH grasps were observed to be the same. If this is so, how can their performance metrics differ so much? We observed from the survey responses that the hard plastic of the hand did not comply well. In direct contrast to that, the OH used rubber on the finger pads which complied well to the objects. These findings suggest that compliance in the fingerpad is an important feature for a human on a hand.

On the same note, we are also unsure of any other study design choices that could have impacted the efficacy of certain actuation strategies, such as choice of normalized friction values, puppeteer system design choices, or slider box controller attributes.

5.1.6 Study Limitations

There are several limitations to this study, first and foremost being the sample size and the lack of quantitative data for the OH. Other observed disadvantages are the differences between the posable hand designs used. Several subjects noted that the thickness of the fingers was too big on the PH. The OH fingers are about 0.5 cm smaller in width than the BH/PH finger width. The OH finger span was also shorter than the Barrett, which made it easier to puppet.

5.2 Flick and Pull Test Results

In this section we present our results for both the pull (section 5.2.1) and flick (section 5.2.2) tests. We provide quantitative results in Table 5.2 for the puppet Barrett and Model O hands used in part

1 of the study. We provide extra quantitative results in Table 5.3 for the rest of the end effectors in this study.

5.2.1 Pull Test Results

The results for the pull test are given in the orange section of Table 5.2 and in Table 5.3.

There was significant difference between the tip and pad grasps for the Model O hand ($p < 0.0016$)and between tip grasp results between the Barrett hand and Model O tip grasps ($p < 0.00089$). All other relationships did not have significance between them (tip vs pad, Barrett hand ($p < 0.169$); pad vs pad, Barrett & Model O ($p < 0.624$)). We attribute the different effects of the pad grasp (being significant for the Model O, and not for the Barrett hand) to how force is transmitted at the distal link from our study participants.

For the Model O the distal joint is made of rubber, which can flex out of plane. We believe that our study participants could not transmit all of their force into the object because they were also trying to stabilize the finger in all directions. In contrast the Barrett hand, having a distal joint with a pin, naturally resists out of plane movements and therefore transmits all force into the object, no matter how the participant holds the grasp.

The puppet hand Model O with pin joints performed comparably to the fingertip grasp results for the Model O with rubber joints.

The actuated Model O hands performed relatively poorly. We believe that this is due to the human experimenter unconsciously maximizing finger surface area during grasps when using puppet hands. The actuated end effectors did not do that — instead a single tendon generated all of the finger's forces.

The actuated Barrett hand performed relatively well. However, we were unable to normalize the Barrett hand's grasping forces during the trials, however, we present these results because they reflect how the part 1 study participants used the hand.

5.2.2 Flick Test Results

The results for the flick test are given in the blue and green sections of Table 5.2 for the instrumented object and pen, respectively. Extra results are also given in Table 5.3.

There were significant differences between only a few hands in the flick test trials, and all significance occurred in trials with the pen object (Barrett tip vs Model O tip ($p < 0.0127$); Barrett tip vs Barrett pad ($p < 0.00045$). We attribute the size of the instrumented object to the complete lack of significance in those trials. Due to the size, we believe that the larger object maximized surface area and helped stabilize itself during a flick, regardless of the grasp used. This is also evident in the relatively decent scores for the instrumented object trials. The pen used in the other flick test trials did the opposite.

The pen object minimized surface area and its curved surface did not offer extra support during a flick. This meant that the design of the fingertip mattered much more than in the instrumented

Test	Barrett Tip	Barrett Pad	Openhand Tip	Openhand Pad
Pull Test Average	0.6720	0.7350	0.4810	0.7630
Pull Test Standard Deviation	0.1044	0.0917	0.1105	0.1517
Pull Test Standard Error	0.0330	0.0290	0.0349	0.0480
Flick Test Score (OBJ)	3	4.5	2	5.5
Flick Test Median Score (OBJ)	0	0.5	0	0.5
Flick Test Avg (OBJ)	0.3000	0.4500	0.2000	0.5500
Flick Test St.D. (OBJ)	0.4216	0.2838	0.2582	0.4378
Flick Test St.Err. (OBJ)	0.1333	0.0898	0.0816	0.1384
Flick Test Score (PEN)	0	4.5	3.5	4
Flick Test Median Score (PEN)	0	0.5	0.25	0.5
Flick Test Avg (PEN)	0	0.4500	0.3500	0.4000
Flick Test St.D. (PEN)	0	0.2838	0.4116	0.3944
Flick Test St.Err. (PEN)	0	0.0898	0.1302	0.1247

Table 5.2: Summary of pull and flick test results using puppet Barrett and Model O hands.

Tasks	Puppet Hands	Actuated Hands		
	Model O	Barrett*	Model O	
	Pin		Pin	Rubber
Pull	0.449 kg	0.932*	0.154 kg	0.201 kg
Flick (Obj)	2.5	7.5*	0	4
Flick (Pen)	5.5	5*	0	0

Table 5.3: Extra pull and flick test results using extra Model O variants and actuated Barrett hands. Each hand could only perform the fingertip grasp. **Note:* We were not able to normalize the Barrett hand's grasp forces. We present these results for completeness, but please acknowledge that these results are not normalized.

object tests. As evident in the data, the Barrett hand distal link geometry completely failed the flick test using the pen object. Only by changing the grasp to a pad grasp was it able to succeed.

Table 5.3 shows the results for the rest of the end effectors. The puppet Model O hand with pin joints performed the comparably to the puppet Model O with rubber joints. We believe that this is because the pin joints provided more stability for the experimenters to hold the objects.

The actuated Model O hands performed poorly for both objects. We believe that this poor performance is due to two factors: actuated end effectors grasped objects too statically, and the restoring forces available to the end effectors were too limited. When the human hands could puppet an end effector, often the grasp was very dynamic — especially when the experimenters responded to the flick. The actuated hands lacked that. Furthermore, the puppet hands had a wide range of restoring forces available to them because the human generating those forces. With the actuated hands there was only a single tendon in the finger — this limited the restoring forces available to the actuated end effectors.

5.2.3 On how the Fingerpad Grasp Improves over the Fingertip Grasp

We observed two overall tool grasping strategies in the human study, most noticeable for the pen-drawing task: the fingerpad and fingertip grasp. This is especially evident in Figure 5.2, where the averaged joint angle data shows fingers 1 and 2 bent backwards, and the thumb in a straight line. With current underactuated schemes, these finger positions are impossible to make. The human study ranked the fingerpad grasp as superior so long as the fingerpads were compliant.

In our data, we have observed that the fingerpad grasp acts as an equalizer between hand

designs. In the pull test, the Model O hand, which performed the test poorly with the fingertip grasp, improved with the fingerpad grasp to perform about the same as the Barrett hand. A similar observation is made in the flick test results. In the flick test the Barrett hand performed poorly using the fingertip grasp (using the pen), but with the fingerpad grasp it improved to perform at a similar level to the Model O hand in that test.

We also observed that in other situations the fingerpad grasp did not impact performance meaningfully. We observed this in the pull test results for the Barrett hand, for all of the flick test results with the Instrumented Object, and for the flick test results with the pen for the Model O. We believe in those situations that this is due to the design of the fingers.

To understand how the finger design could have impacted the design, we analyzed the fingertip and fingerpad grasp surface area. We analyzed the grasps by taking top-down images of grasping the instrumented object and the pen using both the Barrett and Model O hands. We found that the surface area increased on average approximately 2 times when switching to the pad grasp. This would explain the Model O's improvement in the pull test.

Although the pad grasp out-performs the tip grasp in general, the tip grasp was effective for two hands and two flick tests — the motorized Model O with soft joints (object) and the puppet Model O with pin joints (pen) — outperforming even the fingerpad grasps. This echoes statements by the participants that, once the tip grasp is established (motorized Barrett) it was easier to manipulate. Given that the pen is curved, and the test object is not, some of this might be attributed to the ability to hold and maintain a force perpendicular to the surface of the object (see Section below). The motorized hands make it easier to maintain the pressure (because of the under-actuation design) while manually holding the fingers in that position is challenging (maintaining pressure with the distal joint orthogonal to the point of contact with an unstable proximal joint). However, it should be noted that the tip grasp is extremely difficult to achieve with the mechanized hands.

This is further substantiated when considering which hands could complete the pen-drawing and spray tasks (see Table 5.4). Amongst the Model O variants tested, none could perform a fingerpad grasp — and those same hands were also unable to perform the pen-drawing task.

It is still unclear what our human subjects were optimizing for in the fingerpad grasp, although we hypothesize that the fingerpad grasp gives a human the ability to maneuver the object within the grasp better than the fingertip grasp. Qualitatively, we observed that the poses of the fingerpad relative to the objects between subjects was the same despite large proximal joint variations (see Figure 5.2). This suggests that the participants picked their finger positions based on the object's pose. We find support for these findings in a dataglove experiment by Todorov and Ghahramani (124). From their findings, they concluded that the synergies — which they measured for manipulation tasks (which were unique for each task) — arise from human closed-loop control and not by actuator design. This means that grasp preshapes are a symptom of a more generalizable object-centric human grasping system.

Interestingly, this is similar to how the human finger is controlled. We hypothesize that humans use a moderately-actuated control strategy (when we consider underactuation to be minimal actu-

Tasks	Puppet Hands			Actuated Hands		
	Barrett	Model O		Barrett	Model O	
		Pin	Rubber		Pin	Rubber
Pen-drawing	Pass	Fail	Pass	Pass	Fail	Fail
Spray	Pass	Pass	Pass	Pass	Fail	Fail

Table 5.4: Abilities of all robot hands tested to complete the pen-drawing and flick tests.

ation). This strategy is built into how the hands are actuated: the proximal link is fully actuated (this brings the fingertip close to the object) and the distal link is underactuated (it has the sole purpose of engaging with the object once it's near). This tendon routing is demonstrated by Xu and Todorov (123) as well as in part by the M2 hand tendon scheme by Ma et al. (125).

From this data we can conclude that underactuation may help with grip stability but is problematic for manipulation, in part because it prevents a fingerpad grasp.

5.2.4 On how well the Simpler Tasks Explain the Performance of the Complex Tasks

We hypothesized that the fingerpad grasp was better than the fingertip grasp because the fingerpad grasp had more surface area and could resist sudden disturbances easier. To test that hypothesis, we designed two characterization tests: the pull and flick tests.

With these tests, we also wanted to see how well these two aspects, more surface area and greater disturbance resistance, could explain each hand's performance at the pen-drawing and spray tasks.

We present our findings by task below. We show which end effectors could do each task in Table 5.4.

The end effectors which could do the pen-drawing task had at least a value of 0.45kg of force in the pull test and at least a score of 3.5 in the flick test.

For the spray task, we found that the end effectors needed to have at least 0.4 of force in the pull test and at least a score of 3.5 in the flick test. It should be noted that all of the puppet hands were able to complete the spray task.

These findings describe both the pen-drawing and spray task results well. However, from observation we believe that the spray task is still not represented well. Note how the Barrett hand grasps the spray bottle in Figure 5.2. Our study participants could perform the spray task with the Barrett hand by pulling the spray bottle trigger with the Barrett hand's intermediate joint.

This was also observed to be the way that our experimenter used the spray bottle with the puppet hand Model O with pin joints.

With this in mind, although more surface area and disturbance rejection is important to complete the spray task, we do not believe that they are the aspects which matters the most. We hypothesize that finger kinematics matter the most for the spray task. In this case, we further hypothesize that 3-link fingers would have an advantage in doing the spray task.

With this in mind, it is clear that more tasks are needed to characterize an end effector for generalized in-hand manipulation.

5.2.5 Study Limitations

In this section we describe the limitations of our study.

The Model O end effectors were designed without sensors incorporated into the hands. The soft distal joints used in with the Model O made the distal link's pose impossible to track without a motion capture system. However, a motion capture system is not viable for this test because of how often the human subject 'puppeteer' would occlude the motion tracking markers.

In our work it is difficult to compare the actuated hand's performance to the puppet hands. This is because of the of how different the methods are to each other. In the actuated versions, the end effector is driven by motors or tendons and and the human subject is removed a little from the context of the manipulation. In the puppet hand versions, the end effector is human-powered and the human subject is directly in the context of the manipulation. With the puppet hand versions, powering the end effector and manipulating objects could have presented a more difficult task to the participant than the actuated versions.

Another limitation is our usage of human-based measures in both the pull and flick test. In the pull test, a human tester regulated how the object was pulled by the force gauge. In this case, human variability would have caused variations in pulls between tests. In the flick test, a human tester flicked the objects with their finger. Flicking objects caused finger strain, which forced us to cycle through several testers during the flick test. In this case, flick strength and direction would vary as each tester grew more fatigued of flicking and between testers.

Our human study also had a low sample size, although this was somewhat offset by how consistent our participants were. Unfortunately, our in-person evaluation process is difficult to conduct on a large scale. We are currently considering other ways to utilize human control experience using, for example, on-line studies.

5.3 Results from Exploring the Maneuverable Space: Both Exploration and Validation

In this work we combined mPHIG and the asterisk test to study how well robot hand morphologies perform in-hand manipulation. We did this using two human studies. In the first, we used human subjects to explore the maneuverable space. In the second, we used human subjects to validate how consistent and do-able the best performances in the exploration study were.

We used the results we collected to make several comparisons:

1. How well the subjects validated the best trials,
2. How robust performance was between translation-only and rotation+translation trials,
3. Comparing translation-only results between hand designs.

In the following subsections, we offer a curated discussion of results for each of these comparisons. We provide the complete result figures in Appendix D for trial paths and statistical analyses. Hand setups and relative object sizes are also shown for each hand there.

5.3.1 Comparing Exploration and Validation Studies

We compared data between our first and second studies to understand how repeatable the best performance from the first studies were. We were surprised to observe that the human subjects in the validation study generally performed better than the best trials in the exploration study. Result plots can be found in Appendix D.1 and statistical results can be found in Appendix D.2.

Figure D.1 (page 87) shows the comparison between the exploration and validation for the 2v2 hand. The East, West, South, and South-West directions showed a significant difference between the exploration and validation data (see Figure D.6, page 93). However, as can be noted from the accompanying box-plot, we observe that the validation results (blue) were better than the exploration data with respect to total distance.

This can also be observed for the 2v3 hand (Figure D.7, page 94) in the East, West, South, South-East, and South-West; for the 3v3 hand (Figure D.8, page 95) in North, West, South, South-East, and South-West; for the p2vp2 hand (Figure D.9, page 96) in East, West, South, South-East, and South-West; and for the 2v1 hand (Figure D.10, page 97) in North, North-East, West, South, South-East, and South-West.

Overall, the significant improvements occur consistently in the South, South-East, and South-West. There can be many reasons for this. On reason is that between the exploration and validation study the fingerpads had a lower coefficient of friction. The lower coefficient of friction for subjects to slide the object along the single link finger, which is especially clear in the North direction.

In addition, it seems that the validation study had better training than the exploration study. In the exploration study, subjects were given a grasping task and practiced manipulating the object without a direct purpose. In the validation study, this was replaced with a directed object

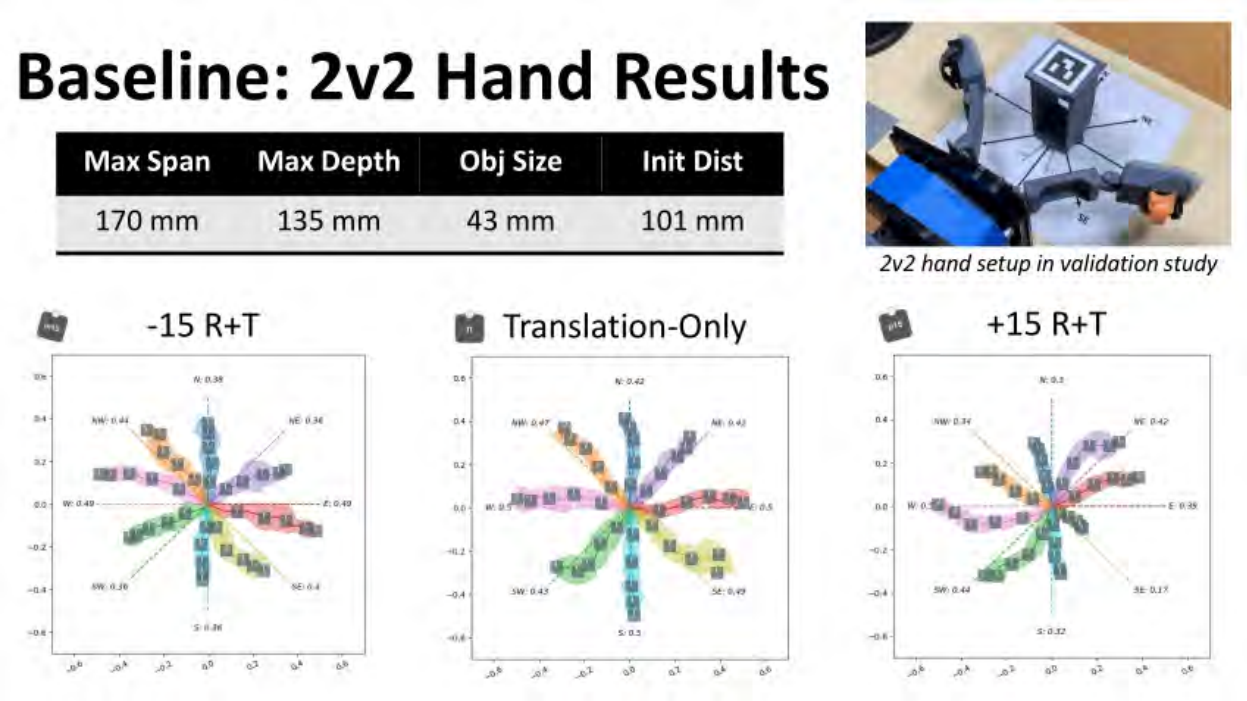

Figure 5.4: Validation study results for our baseline hand — the 2v2 hand. The 2v2 hand was chosen because it was the lowest degree of freedom hand that could perform all of the tests close to the edges of the normalized workspace (translation-only, rotation-only, and rotation+translation).

manipulation task. Further, before each trial, subjects were shown the recorded footage of the best trial from the exploration study. We observed that human subjects learned a trial quickly when shown a replay of the best trial.

For the p1vp1 (Figure D.10, page 97), we observed an overall lower level of performance. The exploration results had a significantly higher total distance than the validation results.

5.3.2 Translation+Rotation Results for each Hand

The Rotation+Translation tests were designed to test how well a hand could maneuver an objects in an in-hand manipulation task with more constraints. The +/-15 degree rotations before translation made the task more complicated because it forces subjects to use sub-optimal contacts for translating the object. We compared how well human subjects used the hands between translation-only and rotation+translation tasks to indicate how robust a hand design would be to small changes in contact position. Result plots can be found in Appendix D.1 and statistical results can be found in Appendix D.2.

However, in our results we found few patterns of statistical significance. What we did observe was a consistent visual skewing of the asterisk plots in the direction. It is important to note that this consistent visual skewing is due to the *averaged* line and might not be valid for the trial data. You can view this skewing in the 2v2 results shown in Figure 5.4.

We also list two more hand-specific observations that could bear more investigating. First, we noticed that depending on the direction of rotation with the 2v2 hand, one of the diagonals would not have a significant different from the translation-only results. For the -15 rotation, this diagonal is NE-SW. For the +15 rotation, this diagonal is NW-SE.

For the p2vp2 hand, there were some directions which deviated too much to count. In the -15 asterisk results, these directions were NW, W, and SE. In the +15 asterisk results, these directions were NE, E.

5.3.3 Between Hand Results

Due to the large amount of hands in our study we avoid making comparisons between each hands and instead opt for a more focused comparison. We used the 2v2 to focus our comparison — it was the perfect baseline because it was the lowest degree of freedom hand that could perform all of the tests (translation-only, rotation-only, and rotation+translation). As a result, all comparisons in this section are made to the 2v2 hand. These baseline results are shown in Figure 5.4.

Using the 2v2 as our baseline, we found that adding or subtracting degrees of freedom did not significantly affect performance, but instead added more nuance to a hand's capabilities. We provide a compilation of results in Figure 5.6.

Adding degrees of freedom to the 2v2: The 3v3 and p2vp2 hands each add different degrees of freedom onto the 2v2 hand. We found that each type of degree of freedom improves on the 2v2 in different ways. See Appendix D.2 for comprehensive figures and pvalues.

The 3v3 hand adds another link/joint to each finger of the 2v2 hand. Between the 2v2 and 3v3, the 3v3 hand significantly improves over the 2v2 in the S, SE, and SW directions with respect to total distance. Qualitatively, we observed that this improved performance is due to a higher degree of distal link control afforded by the extra joint/link.

The p2vp2 adds a slider at the base of each two link finger. Between the p2vp2 and the 2v2, the p2vp2 provides a significant improvement in N, NE, and S. It should be noted that when comparing NW the pvalue is close to significance, we attribute this to handedness in our subjects. Qualitatively, we observed that our subjects brought the fingers together when moving in the Northern hemisphere, and we hypothesize that this provided the boost in total distance.

It should be noted that both higher degree of freedom hands significantly improve the 2v2 results in S. This suggests that regardless of the added degrees of freedom, pulling objects towards the palm might require more degrees of freedom. Such design considerations might help with hands which try to transition from precision to power grasps might consider having larger degrees of freedom — which also explains

These patterns also exist when comparing the 3v3 hand to the p2vp2 hand, shown in Figure 5.5. Between these hands, the p2vp2 outperforms the 3v3 in the upper region and the 3 link fingers are better in SE and SW. However, there is no significant difference between these hands in S.

Subtracting Degrees of Freedom from the 2v2: The 2v1 hand is a hand with fewer

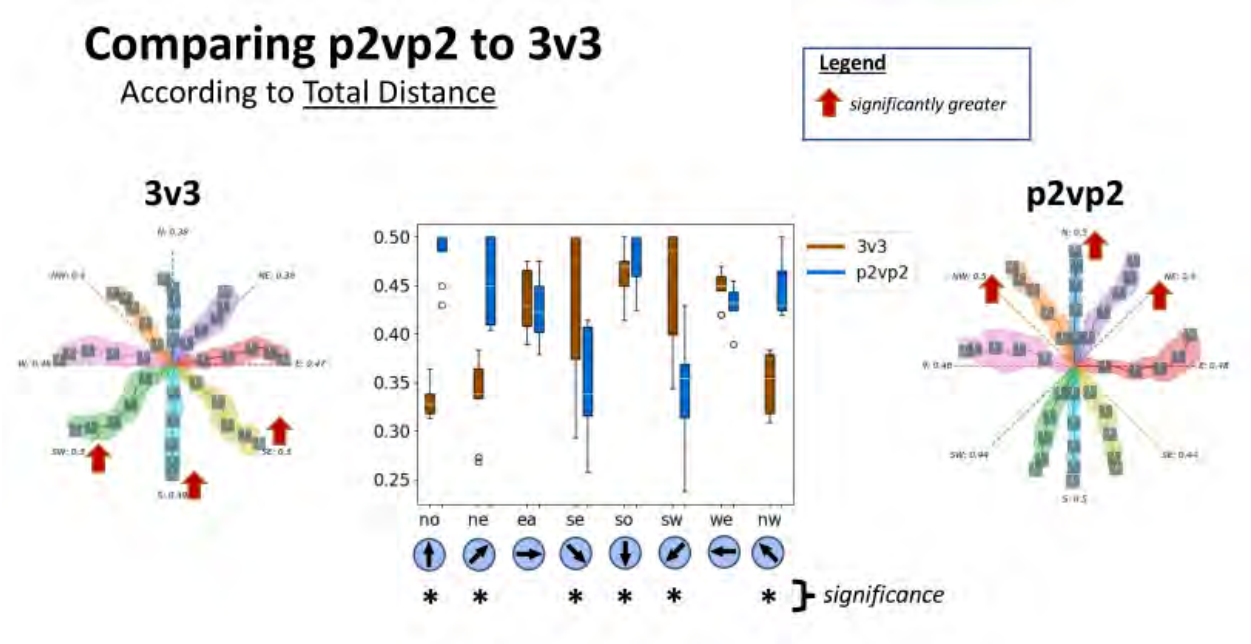

Figure 5.5: Statistical Comparison between 3v3 and p2vp2 hands, according to the Total Distance metric results. Both hands have the same number of degrees of freedom, but different joints, which provides nuanced advantages over the 2v2 hand. The same nuanced advantages are observable in this comparison between high DOF hands as well.

degrees of freedom. On this hand, one finger does not have a distal joint, and the finger link extends to approximately the same length as a double jointed finger. The 2v1 performs similarly to the 2v2 hand except in N and NE. Despite no significant difference, it should be noted that 2v1 hand has a much higher the high degree of variation for each direction. It should be noted that the reason why we make the 2v2 hand the baseline instead of the 2v1 is that the 2v2 hand could do rotation conditions.

2v2 vs p1vp1 - 4 DOF Hand Comparisons: We also compared how merely changing degrees of freedom would affect performance. For this comparison, we utilized the p1vp1 hand — this hand utilized sliders at the base of the finger and had no rotary proximal joint. The 2v2 significantly outperformed the p1vp1 in almost every direction, suggesting that a proximal rotary joint is key for in-hand manipulation.

Observations about Asymmetrical Hands: We observed that each side of the 2v3's asterisk results depended on the finger on that side. Therefore, the two link side performed similarly to the 2v2's asterisk and the three link side performed similarly to the 3v3's asterisk. This observation also holds for the 2v1 hand — the two finger side was not significantly different than the 2v2's left side.

What this suggests is that during object translation (especially in E and W), the finger on the outside of the object contributes the most to the translation. This suggests that the contribution of the other finger might be only to provide a stabilizing force.

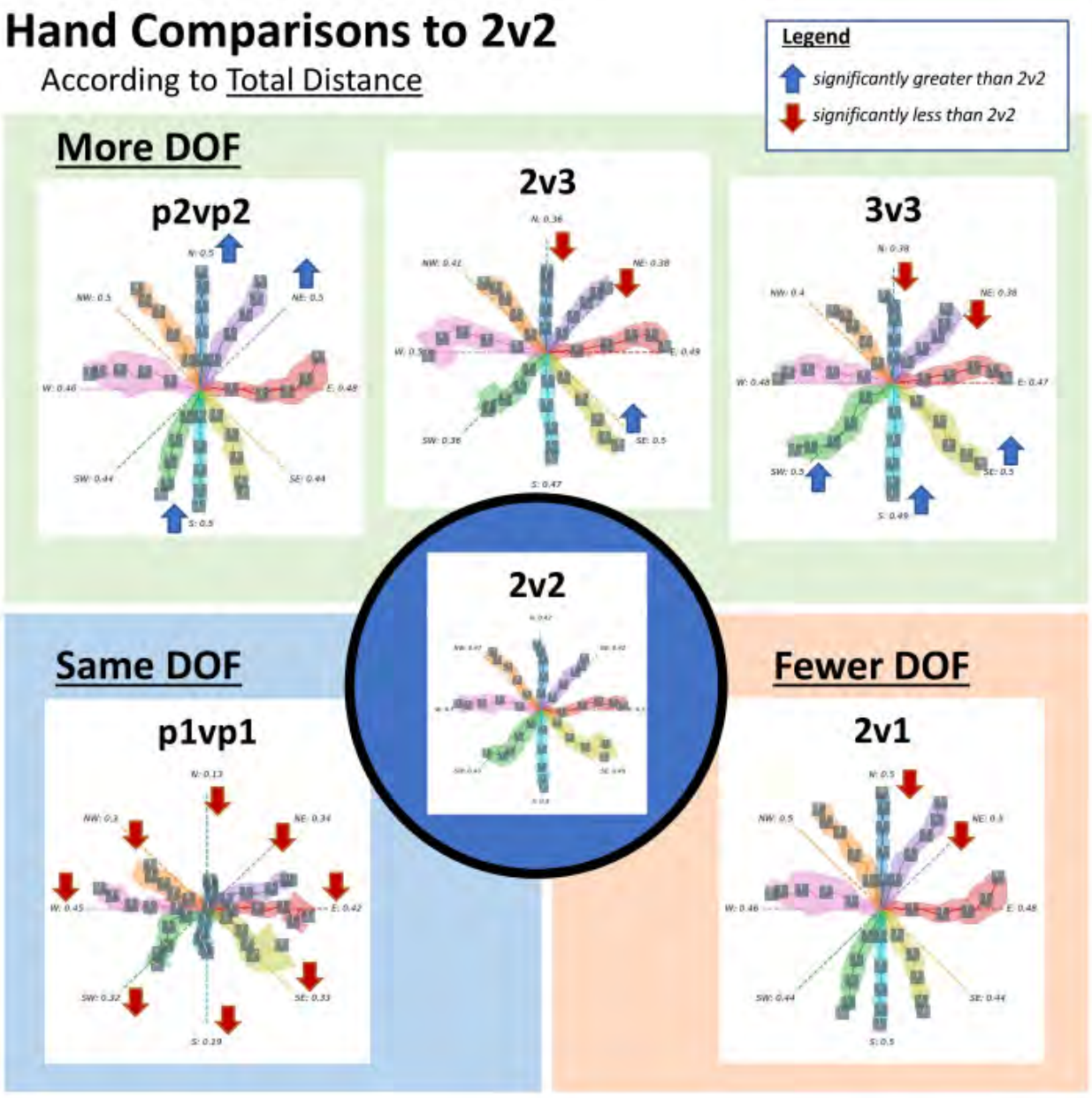

Figure 5.6: A visual compilation of statistical results when comparing the 2v2 to the other hands in the validation study. Statistical significance is shown as colored arrows — up and down indicate whether the 2v2 performed significantly worse or better than the compared hand, respectively. Complete results can be found in the Appendix D.

Chapter 6: Conclusions and Future Work

In this research we analyzed how a robot hand's morphology and actuation components contribute to in-hand manipulation performance. We do this by utilizing a new methodology for studying robot hand design, which is comprised of a human study design and object-centric benchmarks. Existing methods do not provide the right focus for analyzing system component task contributions, which leads to a lack of quantitative knowledge. Our research represents a new start for quantitative research into robot hand performance for in-hand manipulation.

We first adapted a human design design called Physical Human Interactive Guidance to study manipulation (which we call mPHIG). For that, our study design utilizes humans to manually puppet robot fingers (Chapter 2). This method mitigates two major problems in human studies with robot hands. The first problem involves transposing human data (typically the subject uses their own hand) to a robot hand design. Our method mitigates this problem because human subjects are given the freedom to move the robot hand however they like, thus making the human transpose to the robot hand in situ, which is an easy task when puppeting. The second problem involves controller transparency. Our method maximizes transparency by involving the human in the context of the task. Here human subjects use their own senses to puppet the hand, which is more natural than other forms of feedback utilized by other methods.

We also proposed a new object-centric benchmark for in-hand manipulation called the Asterisk Test (Chapter 3). This benchmarks characterizes performance by comparing it to an ideal performance using nine metrics. This method improves prior metrics because on low-level aspects of performance (the object path) rather than high-level task-specific aspects (time to complete a task, number of failures, etc). In addition, the low-level focus of this benchmark provides a way for separate analysis of system components.

We utilized mPHIG and the Asterisk Test to analyze the actuation and morphology components (Chapter 4). For the actuation component, we used mPHIG to study the minimally underactuated Barrett hand for tool-use tasks (using a pen and spray bottle) (4.1). We compared its performance to other versions of the Barrett hand or those with similar finger layouts (Model O hand). Study results (5.1) showed similar performance between hands, but also a human preference for using compliant fingerpads over fingertips and for different actuation schemes than the minimally underactuated scheme on the Barrett hand. We further investigated the fingerpad and fingertip contacts for their ability to resist dynamic perturbations (4.2, results: 5.2).

Finally, for the morphology component, we used mPHIG with the Asterisk Test to analyze robot hand design performance at in-hand manipulation tasks. We conducted this study in two parts: first, we explored what is possible in the maneuverable space (4.3) and then we validated the highest performing trials with additional subjects (4.5. Study results (5.3) showed that a two-linked two fingered design provided versatile in-hand performance with little value added with

additional degrees of freedom. Human subjects were able to validate a majority of the best trials, indicating consistency between human subject findings. We also discussed 'lessons learned' for future mPHIG studies.

Future Work: In the future, we can apply our study method to a wider range of robot hand designs, including those with planar links and variable friction components, as well as more relative object sizes and initial positions. In addition, we can put greater emphasis onto measuring how contact points vary throughout a manipulation task.

Another useful study would be to combine our actuation study with the morphology asterisk test study. With such a combination, which would require a method to track joint changes on our puppeted hands, we can study how humans *want* robot hands to move. This can improve teleoperation interfaces and contribute to the development of "moderately underactuated" actuation schemes (as opposed to minimally underactuated schemes) which are designed for manipulation.

There are also some general improvements needed for the measurement method and mPHIG. For the measurement method, we need to adapt the method to work with asymmetrical hands. For mPHIG, we need to explore other methods of puppeting fingers whcih would provide better control on high DOF hands but keep the low controller transparency and minimized transposing that mPHIG provides.

Finally, others can utilize the Asterisk Test with automatic methods to study optimal control performance on robot hand designs. With optimal control, we can determine quantitatively the "ground truth" manipulation performance of a robot hand design — that is, the performance potential which the morphology component provides for in-hand manipulation tasks.

APPENDICES

Appendix A: Instructions for Hand Measurements

We present the methodology of the most recently submitted manuscript for our measurement method.

Our goal is to provide an approximation of the space enclosed by the hand's palm and fingers. Unfortunately, this is not straightforward because some hands have a "natural" orientation whereas others do not. Therefore, we define our own coordinate system which can harmonize with a hand's natural orientation, if it exists, and impose order on a hand if there is not.

We accomplish this by defining our axes of measurement (span, depth, width) and fitting them to a hand using a grasping scenario (Sec A.0.1). This grasping scenario, grasping a cylinder, dictates the hand orientation that the axes are transfered onto. The grasping scenario is only used to select the hand orientation for measurement — the grasp does not have to be performed.

Using these axes, we prescribe sets of measurements to approximate the fingerspace at finger positions across actuation (Sec A.0.2, A.0.3, and A.0.4). Which finger positions to use depends no the type of grasp one is trying to characterize the fingerspace for — each type of grasp has unqiue specifications for what a valid grasp is, which need to be considers when measuring the fingerspace (Sec A.0.5 and A.0.6).

More instructions, supporting software, and example measurements are provided on github (126).

A.0.1 Functional Axes: Span, Depth, and Width

To define the coordinate system we use for measuring the hand we first attach the coordinate system to a cylinder (or sphere) resting on a table (see Fig. A.1). The measurer then places the hand and configures the fingers in order to grasp the cylinder from the side. The intention is to define a clear in-out from the palm (depth) and left-right finger closing direction (span). While no physical object is required it can be helpful to use one in order to set up this positioning. The functional definition of the axes is as follows:

Span — is the axis parallel to both the reference cylinder's top/bottom faces and the palm's normal — i.e., a line passing through the middle of the cylinder parallel to the table. Moving in the span axis is akin to moving the reference cylinder between the fingers across the table surface. This axis measures the largest object the fingers can span; the primary open/close motion of the fingers should be in this axis.

Depth — is the axis orthogonal to the plane of the palm. Moving in the depth axis is akin to moving the reference cylinder closer to, or farther from, the palm. Span and Depth are typically coupled under finger actuation; "opening" the fingers in the span direction will usually change the depth.

Width — is the axis normal to the table top. Moving in the width axis is akin to lifting the cylinder

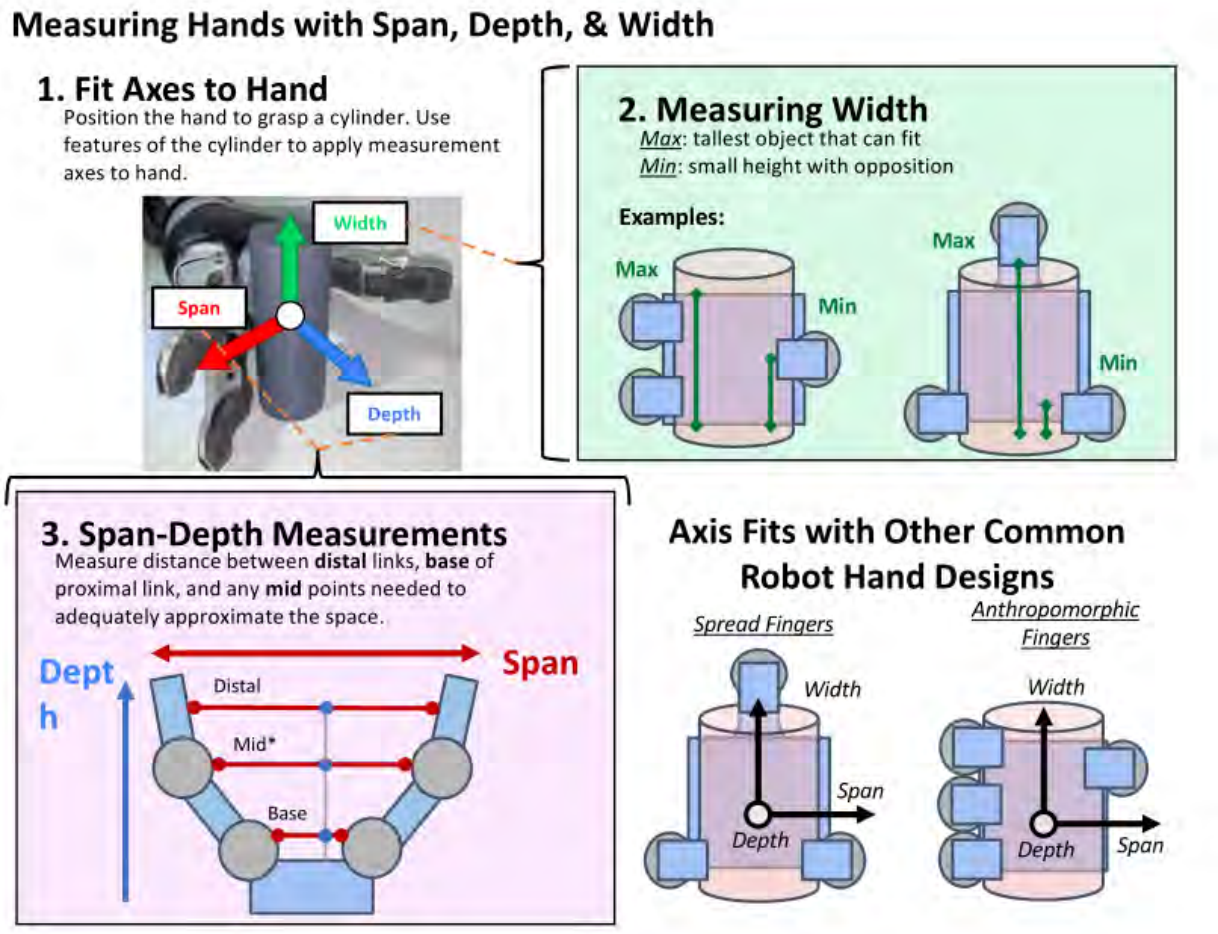

Figure A.1: Our measurement method: **1)** The three measurement axes are fit to the hand using a grasping scenario. Other axis fits are shown in the bottom-right. **2)** Measure the hand's max and min width. **3)** Make at least two span-depth measurements, one at the base and another at the distal links.

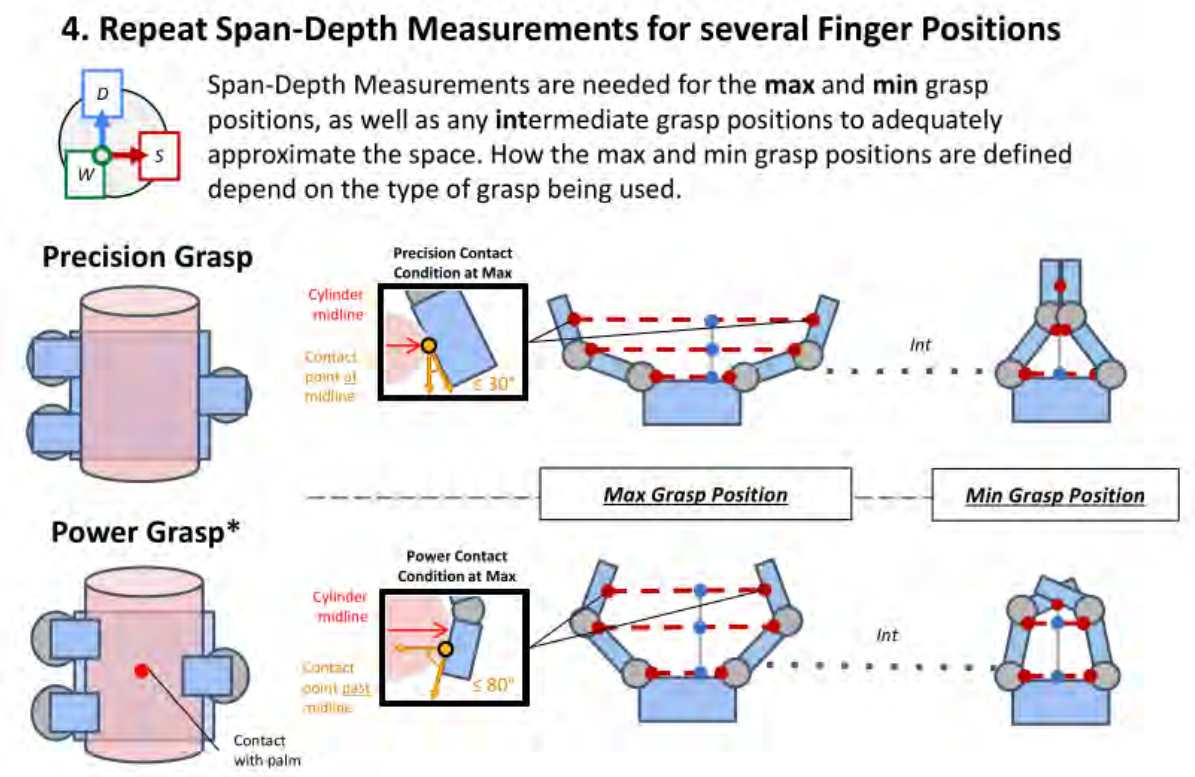

Figure A.2: Our measurement method, continued: 4) repeat step 3 along the hand's actuation profile. An actuation profile depends on the grasp being used, precision and power grasps are shown. One must make span-depth measurements at: i) the hand at the maximum open position to practically accomplish the type of grasp used and ii) the hand when the distal measurement is zero. Intermediate finger positions are used to better approximate the space, if needed.

straight up off the table. The width axis measures the height of objects that can be grasped by a hand. For most hands, the width measurements remain constant throughout actuation.

A.0.2 One-time Measurements

There are three measurements that are taken once and do not change with finger actuation. These are: the Maximum Open, and the Minimum and Maximum Width measurements. The Maximum Open measurement is used to record the span when the fingers are completely open. The Minimum Width measures the shortest object the hand could pick up off of the table. The Maximum Width represents the tallest object or width of the hand, depending on finger layout.

The Maximum Open measurement measures the distance between the ends of the distal links, without taking grasping into account. For this measurement, we open the hand as far as it will go. This is the finger configuration typically used in other work (127; 128).

It is important to consider the height an object has to be for the hand to have antipodal contact (see Fig. A.1). Minimum Width is the distance from the tabletop to the lowest contact point at which fingers on opposite sides would connect with the object.

Our definition for Maximum Width depends on the hand orientation. In general, Maximum Width represents the tallest object which could fit inside the hand (e.g. Fig. A.1, bottom-right, the tallest object that fits under the top finger of the hand labelled 'Spread Fingers'). For hands without an upper limit (also in Fig. A.1), the tallest object could (theoretically) be infinite. Instead, in these cases, we record the hand's palm width with a '+' after the measurement.

A.0.3 Span-Depth Measurements at a given Finger Position

When measuring a hand configuration we require at least two span-depth measurements (Base and Distal) in order to approximate the enclosed grasp shape (see left of Fig. A.1). The locations of these measurements are based on depth. Each measurement records the Depth and the Span, for a minimum of two measurement pairs.

The Base measurement is taken at the center of the proximal joints. If the proximal joints are flush with the palm, the base measurement is taken at a depth of zero (at the palm).

The Distal measurement occurs at the distal link. We provide two locations: at the tip or at the center of the distal link (on the fingerpad surface), depending on the finger configuration used to accomplish the grasp. The tip should be used only when the tip of the finger is in contact with the hypothetical cylinder (in this case the fingerpad surface is perpendicular to the contact).

The Mid measurement(s) (there can be more than one) are taken between the Base and Distal measurements. They are intended to capture how the enclosed space widens between the Base and Distal measurements. The measurer should choose the number and placement of these measurements to capture maxima (and possibly minima) of the changes in Span with respect to Depth in the hand's space. For the hands measured in this paper we chose one Mid measurement and placed it at the distal joint as an example.

A.0.4 Finger Positions to Measure

We approximate how the enclosed space changes as the hand is actuated using at least two finger positions. These finger positions correspond to the Maximum and Minimum *f*unctional grasps attainable according to the type of grasp being performed (see right of Fig. A.2). These functional configurations must represent grasps, and therefore are not necessarily the widest/narrowest figure position.

Using linear interpolation we can generate approximate Span-Depth measurements at any point in the actuation. Where this approximation differs too much from the actual measurements, an intermediate measurement should be added. For the hands measured in this paper we chose one intermediate measurement for each hand.

Intermediate finger positions represent any finger position between the Max and Min positions, but they are not required. The intent of the Intermediate positions is to approximate how the Span-Depth measurements change as the fingers are actuated. When determining intermediate finger positions, make sure that each finger is actuated the same amount, as if all fingers were actuated for the same amount of time.

A.0.5 Power Grasp Measurements

We define the power grasp functionality as a stable grasp with at least three contact points on an ovoid object. This is typically one contact point on the palm and the others at the fingers. The finger contact points should be *past* the centerline of the object and at an angle of at least 80° relative to the distal measurement line (see bottom row of Fig. A.2) as a guideline.

We define two power grasp variations: A spherical power grasp that fully encloses the object from three (or more) directions, and a cylindrical power grasp that encloses a (2D) circular area. Hands may be capable of none, one, or both grasps — which variations to measure is determined by the measurer.

The Span-Depth measurements are slightly different for the spherical power grasp because the contact points are no longer planar. Instead of a single pan length measurement we measure the area of a disk that fits at each depth, effectively merging span and width.

A.0.6 Precision Grasp Measurements

We define the precision grasp functionally as a stable grasp with finger contacts at the centerline of an ovoid shape held in the distal links. The distal link contact surfaces should be oriented at most 30° outward relative to the depth axes (see top row of Fig. A.2) as a functional guideline. The intent here is to eliminate grasps in which the fingers contact the object without sufficient frictional force to keep the object from "popping" out of the grasp.

A.0.7 Improving Measurement Transparency

We include here brief recommendations on what measurers can do to make the measurements as transparent as possible for end-users.

Measurements can be performed on a physical or simulated representation of the hand. For physical hands, it may be difficult in practice to hold the fingers in the desired configurations, particularly for underactuated hands performing power grasps. In this case we suggest using an actual object to keep the hand in position.

Regardless of the medium used to measure the hand, we recommend providing pictures of each measurement to maximize measurement transparency.

A.0.8 Software Tools

We provide additional software tools to 1) interpolate the measurements, 2) determine if an object will fit in the hand, and 3) determine qualitative (small, medium, large) object-hand region definitions. All of these are parameterized by the grasp type t.

Span s (optionally width w for spherical grasp types) is defined as a piece-wise linear function of the depth, d. Each hand configuration defines $n \geq 2$ sets of depth-span(width) measurements. These sets are, in turn, linearly interpolated based on the percentage actuation, a:

$$(s_a, d_a)_n = \text{ConfigInterp}(t, a) \tag{A.1}$$

$$s = \text{SpanInterp}(t, (s_a, d_a)_n, d) \tag{A.2}$$

Given an object's cross-sectional measurements (o_s, o_d) and optional height (o_w), and desired grasp type t, we define a simple search function that determines an ideal actuation percentage for enclosing the object. This function returns the size of the object with respect to each axes x as well as the best actuation percentage a and depth d to place the object's center at:

$$(tS/S/M/L/tL)_x, a, d = \text{Fit}(t, o_s, o_d, o_w) \tag{A.3}$$

The size measurements are calculated based on the maximum M_x and minimum m_x values for each axes x:

$$s_x = \frac{O_x - m_x}{M_x - m_x} \tag{A.4}$$

We define the size ranges as Too Small ($s_x < 0$), Small ($0 \leq s_x < 0.3$), Medium ($0.3 \leq s_x < 0.7$), Large ($0.7 < s_x \leq 1.0$), and Too Large ($s_x > 1$). The closer s_x is to 0 or 1, the less tolerance there is for error when grasping the object.

Inverting the mid-point of these ranges (eg, using $s_x = 0.15$ and calculating O_x) is a straightforward way to define a canonical "small" object size with respect to the hand.

Appendix B: Study Surveys

B.1 Tool Use and Actuation Survey

Please see next page.

Hand/Task Survey, Round 1

Subject _____ Hand _____ Trial 1
Experimenter will fill out the above entries before the survey is started.

Please answer the following questions to the best of your ability based on your experience so far in the study.

1. How successful were you at performing the task?

Not successful			Somewhat successful						Successful
1	2	3	4	5	6	7	8	9	10

2. If you were successful, how efficiently were you able to complete the task?

Not efficient			Somewhat efficient						Efficient
1	2	3	4	5	6	7	8	9	10

3. How intuitive was it to control the hand?

Not intuitive			Somewhat intuitive						Intuitive
1	2	3	4	5	6	7	8	9	10

4. How close did you come to performing the task the way you would have liked?

Not close			Somewhat close						Close
1	2	3	4	5	6	7	8	9	10

5. What improvements would you make to the hand and why?

Hand/Task Survey, Round 2

Subject _____ Hand _____ Trial 2
Experimenter will fill out the above entries before the survey is started.

Please answer the following questions to the best of your ability based on your experience so far in the study.

6. How successful were you at performing the task?

Not successful			Somewhat successful						Successful
1	2	3	4	5	6	7	8	9	10

7. If you were successful, how efficiently were you able to complete the task?

Not efficient			Somewhat efficient						Efficient
1	2	3	4	5	6	7	8	9	10

8. How intuitive was it to control the hand?

Not intuitive			Somewhat intuitive						Intuitive
1	2	3	4	5	6	7	8	9	10

9. How close did you come to performing the task the way you would have liked?

Not close			Somewhat close						Close
1	2	3	4	5	6	7	8	9	10

10. What improvements would you make to the hand and why?

11. If you could choose one joint to make fully posable for all fingers on a hand, which would you choose and why? Circle the joint on the diagram below. Why?

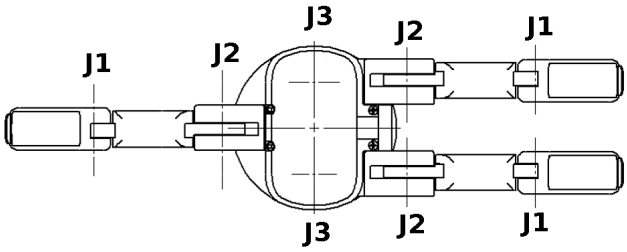

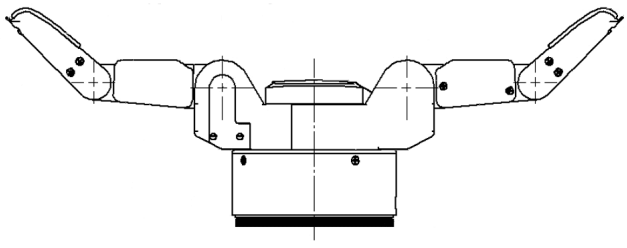

12. If you could choose one finger to make fully posable, which finger would you choose and why? Circle the finger on the diagram below. Why?

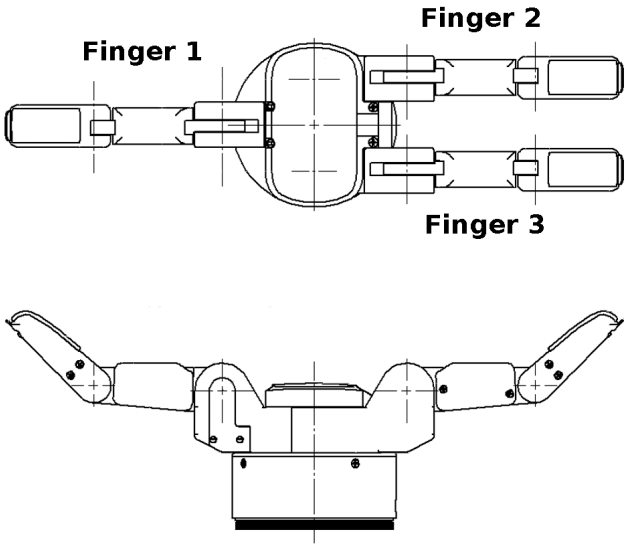

13. If you had to chose one hand from the study to perform this (and similar tasks), which hand would you use? Why?

B.2 Validation Study Survey

Please see next page.

Subject #: _____ **Hand**:_____
Experimenter will fill out the above.

1v1 Hand Survey

Please answer the following questions to the best of your ability based on your experience so far in the study.

Given your experience in this study with this hand, how much would you agree or disagree with each question, for each direction? Write one of the following answers in the box:

- '+' if you strongly agree
- '🅾️' if you strongly disagree
- Otherwise, nothing

E	W	
		It felt easy to go far in this direction.
		I was satisfied with the control I had over the hand for this direction.
		I was consistent between the trials for this direction.
		Sliding the fingers along the sides of the object was useful for this direction.
		During the trials for this direction, I was tempted to let go and regrasp the object.

Subject #: _____ **Hand**:_____

Experimenter will fill out the above.

Hand #1

Please answer the following questions to the best of your ability based on your experience so far in the study.

Given your experience in this study with this hand, how much would you agree or disagree with each question, for each direction? Write one of the following answers in the box:

- '+' if you strongly agree
- '🔴' if you strongly disagree
- Otherwise, nothing

N	NE	E	SE	S	SW	W	NW	CW	CCW	
										It felt easy to go far in this direction.
										I was satisfied with the control I had over the hand for this direction.
										I was consistent between the trials for this direction.
										Sliding the fingers along the sides of the object was useful for this direction.
										During the trials for this direction, I was tempted to let go and regrasp the object.

What did you especially like about this hand design? Why?

What did you **not** like about this hand design? Why?

Subject #: _____ **Hand**:_____

Experimenter will fill out the above.

Did you feel like the distal link was the right length? Would you have preferred if it was shorter or longer? Why?

Did you feel like the proximal link was the right length? Would you have preferred if it was shorter or larger? Why?

Did you feel like the palm was the right width? Would you have preferred if the fingers were closer or farther apart? Why?

Generally, when you had to rotate and translate the object, how well did the hand perform? Is there something we can change in the design to make it work better for these combined trials? Why?

Subject #: _____ **Hand**:_____

Experimenter will fill out the above.

Hand #2

N	NE	E	SE	S	SW	W	NW	CW	CCW	
										It felt easy to go far in this direction.
										I was satisfied with the control I had over the hand for this direction.
										I was consistent between the trials for this direction.
										Sliding the fingers along the sides of the object was useful for this direction.
										During the trials for this direction, I was tempted to let go and regrasp the object.

What did you especially like about this hand design? Why?

What did you **not** like about this hand design? Why?

Subject #: _____ **Hand**:_____

Experimenter will fill out the above.

Did you feel like the distal link was the right length? Would you have preferred if it was shorter or longer? Why?

Did you feel like the proximal link was the right length? Would you have preferred if it was shorter or larger? Why?

Did you feel like the palm was the right width? Would you have preferred if the fingers were closer or farther apart? Why?

Generally, when you had to rotate and translate the object, how well did the hand perform? Is there something we can change in the design to make it work better for these combined trials? Why?

Subject #: _____ **Hand**:_____

Experimenter will fill out the above.

Hand #3

N	NE	E	SE	S	SW	W	NW	CW	CCW	
										It felt easy to go far in this direction.
										I was satisfied with the control I had over the hand for this direction.
										I was consistent between the trials for this direction.
										Sliding the fingers along the sides of the object was useful for this direction.
										During the trials for this direction, I was tempted to let go and regrasp the object.

What did you especially like about this hand design? Why?

What did you **not** like about this hand design? Why?

Subject #: _____ **Hand**:_____

Experimenter will fill out the above.

Did you feel like the distal link was the right length? Would you have preferred if it was shorter or longer? Why?

Did you feel like the proximal link was the right length? Would you have preferred if it was shorter or larger? Why?

Did you feel like the palm was the right width? Would you have preferred if the fingers were closer or farther apart? Why?

Generally, when you had to rotate and translate the object, how well did the hand perform? Is there something we can change in the design to make it work better for these combined trials? Why?

Subject #: _____ **Hand**:_____

Experimenter will fill out the above.

After Completion

Which number hand was the hardest to use? Why?

Which number hand was the easiest to use? Why?

Which number hand do you think had the best all-around performance? Why?

Considering your entire experience in this study, are there answers that you would like to revise? For which hands? Why?

Appendix C: Best Trials for all Hands, all Rotation Conditions

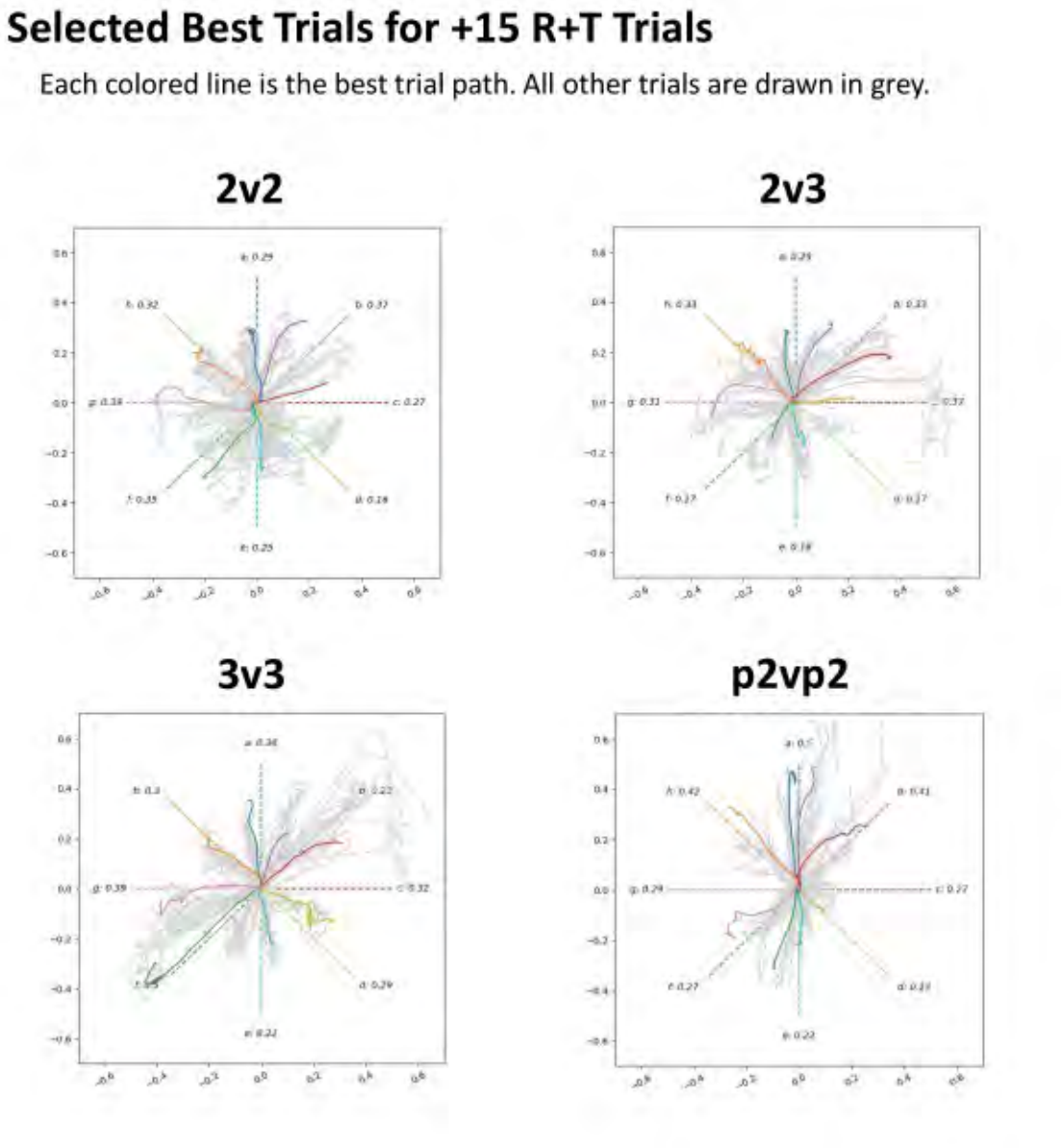

Figure C.1: Best trials for the +15 Rotation+Translation trials are shown as colored lines in each direction for the 2v2, 2v3, 3v3, and p2vp2 hands. The grey lines show other unselected trials for reference.

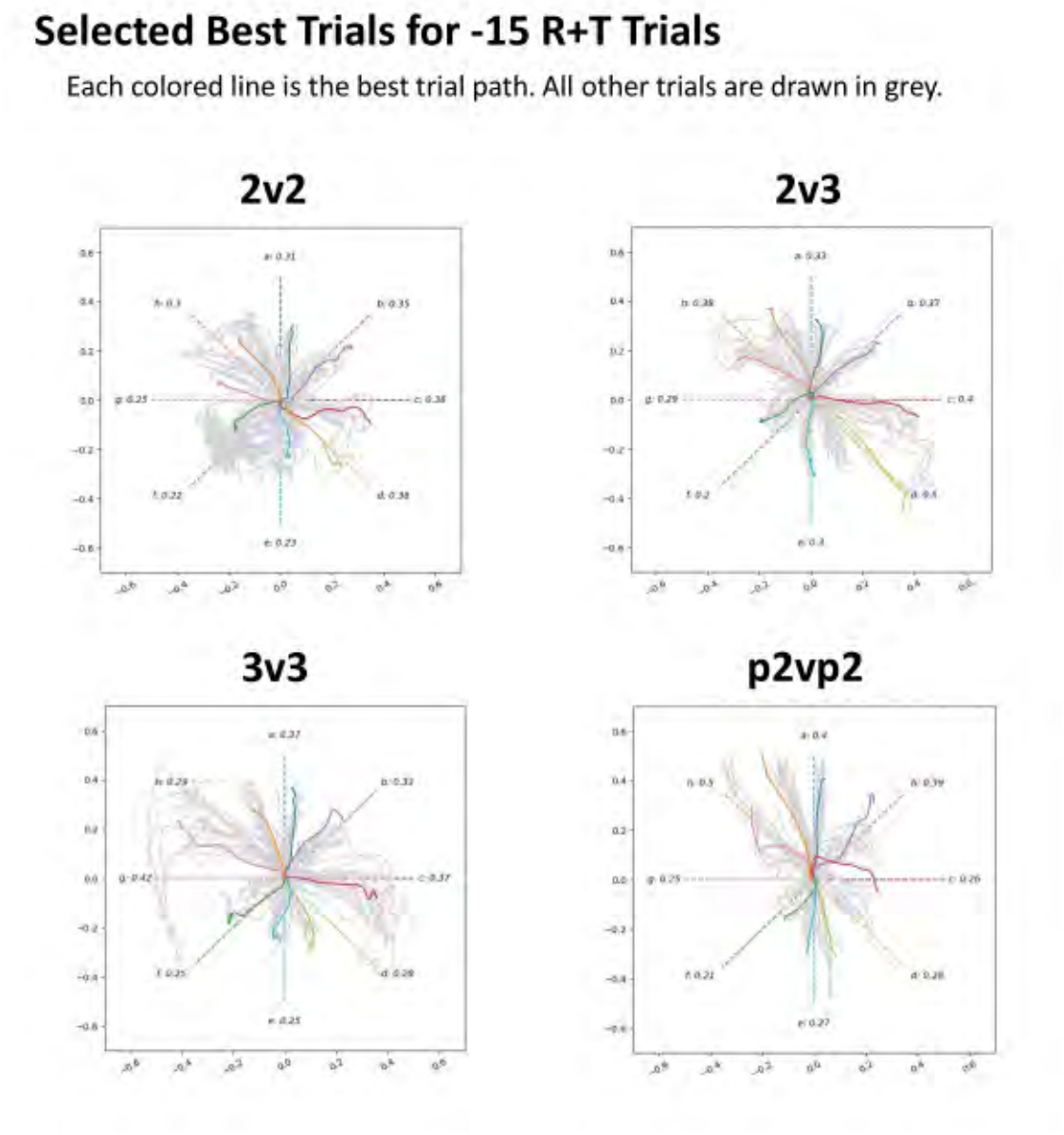

Figure C.2: Best trials for the -15 Rotation+Translation trials are shown as colored lines in each direction for the 2v2, 2v3, 3v3, and p2vp2 hands. The grey lines show other unselected trials for reference.

Appendix D: Full Asterisk Test Results

D.1 Averaged Trial Paths and Rotation Condition Analysis

See figures D.1 (2v2, page 87), D.2(2v3, page 88), D.3 (3v3, page 89), D.4 (p2vp2, page 90), and D.5 (2v1 & p1vp1, page 91) show the averaged asterisk paths in for both the validation (top) and exploration (middle) studies, and rotation-only results (bottom).

2v2 Hand Results

Max Span	Max Depth	Obj Size	Init Dist
170 mm	135 mm	43 mm	101 mm

2v2 hand setup in validation study

Validation Study Results

-15 R+T

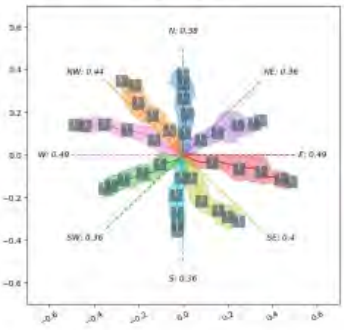

Translation-Only

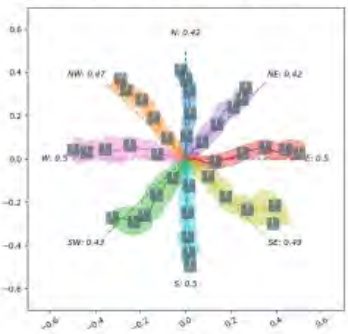

+15 R+T

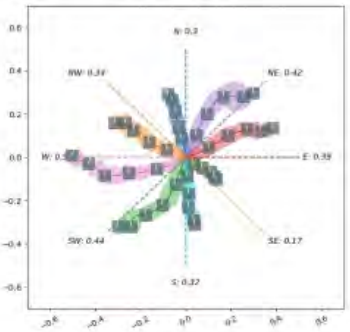

Exploration Study Results

-15 R+T

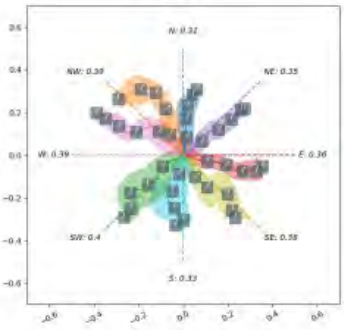

Translation-Only

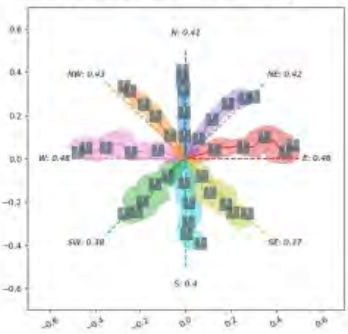

+15 R+T

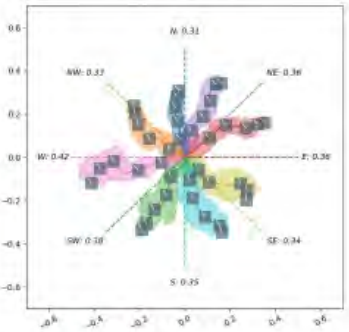

Rotation-Only Results

Exploration

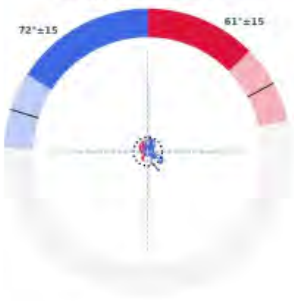

Validation

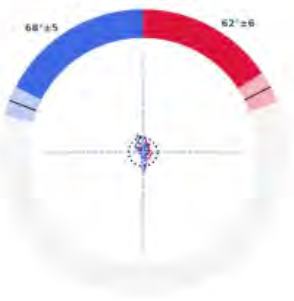

Figure D.1: Comprehensive Asterisk Test Results for the 2v2 hand, for both the Experimental and Validation studies.

2v3 Hand Results

Max Span	Max Depth	Obj Size	Init Dist
195 mm	140 mm	49 mm	105 mm

2v3 hand setup in validation study

Validation Study Results

-15 R+T

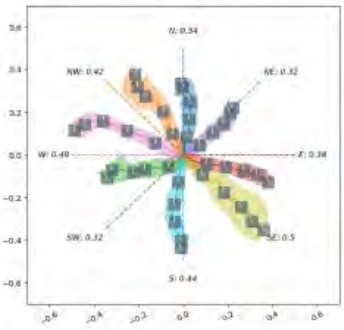

Translation-Only

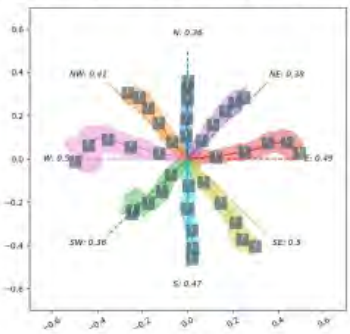

+15 R+T

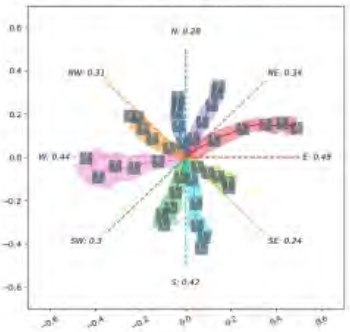

Exploration Study Results

-15 R+T

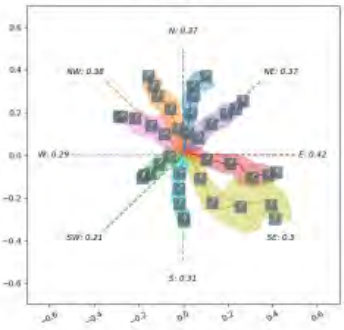

Translation-Only

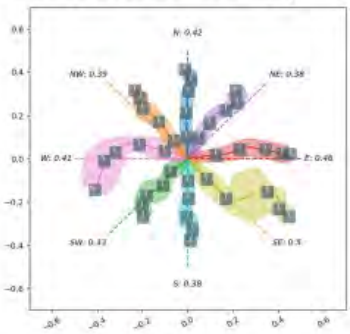

+15 R+T

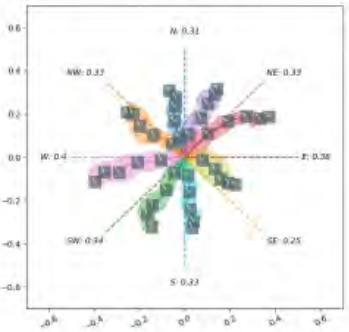

Rotation-Only Results

Exploration

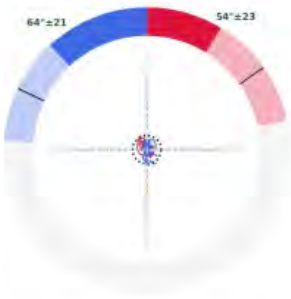

Validation

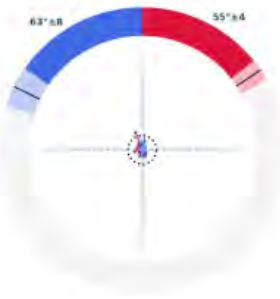

Figure D.2: Comprehensive Asterisk Test Results for the 2v3 hand, for both the Experimental and Validation studies.

3v3 Hand Results

Max Span	Max Depth	Obj Size	Init Dist
210 mm	140 mm	53 mm	105 mm

3v3 hand setup in validation study

Validation Study Results

-15 R+T

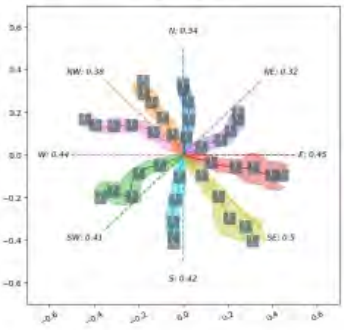

Translation-Only

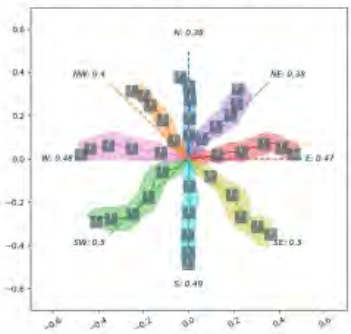

+15 R+T

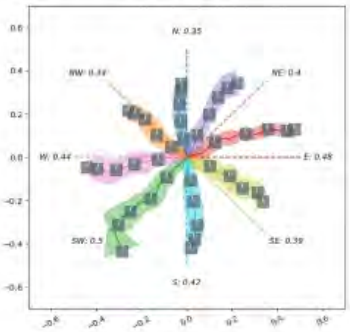

Exploration Study Results

-15 R+T

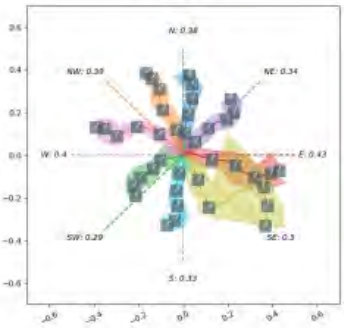

Translation-Only

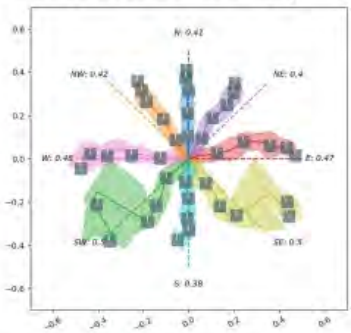

+15 R+T

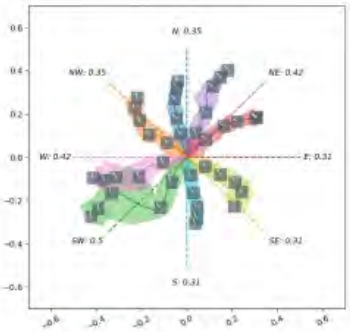

Rotation-Only Results

Exploration

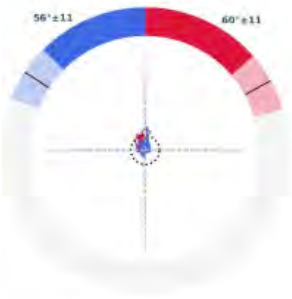

Validation

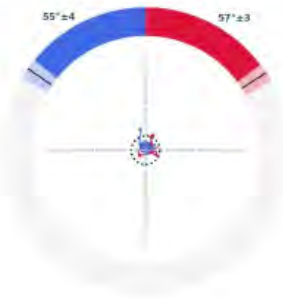

Figure D.3: Comprehensive Asterisk Test Results for the 3v3 hand, for both the Experimental and Validation studies.

p2vp2 Hand Results

Max Span	Max Depth	Obj Size	Init Dist
261 mm	115 mm	65 mm	86 mm

p2vp2 hand setup in validation study

Validation Study Results

-15 R+T

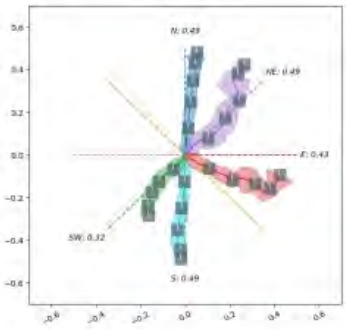

Translation-Only

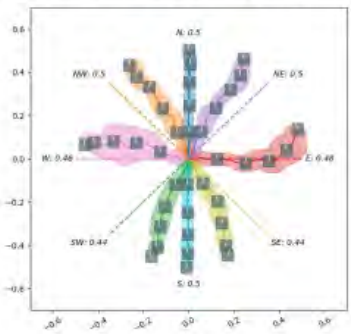

+15 R+T

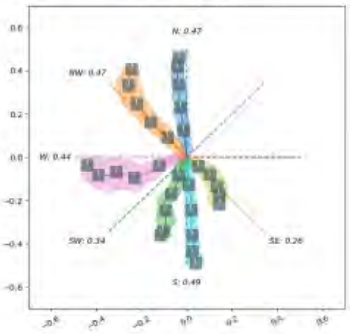

Exploration Study Results

-15 R+T

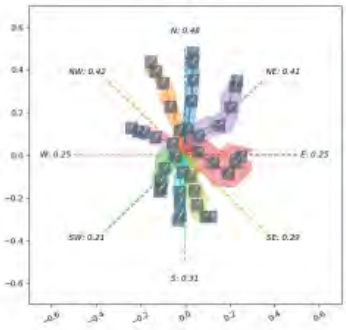

Translation-Only

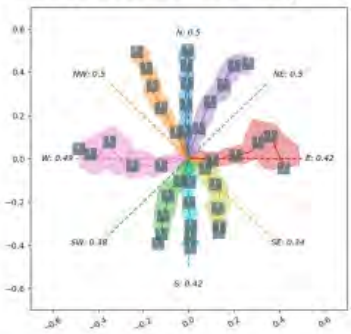

+15 R+T

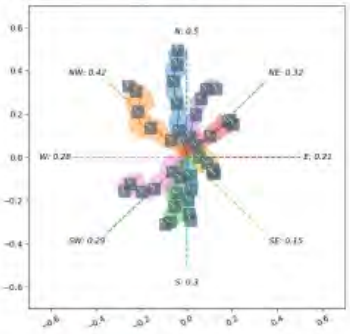

Rotation-Only Results

Exploration

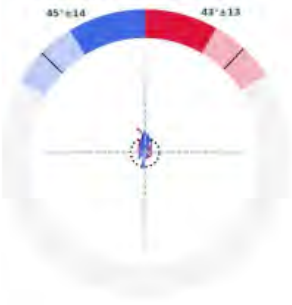

Validation

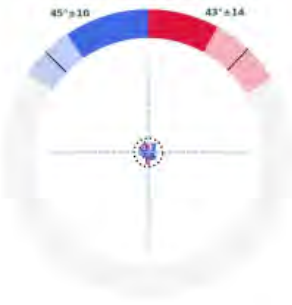

Figure D.4: Comprehensive Asterisk Test Results for the p2vp2 hand, for both the Experimental and Validation studies.

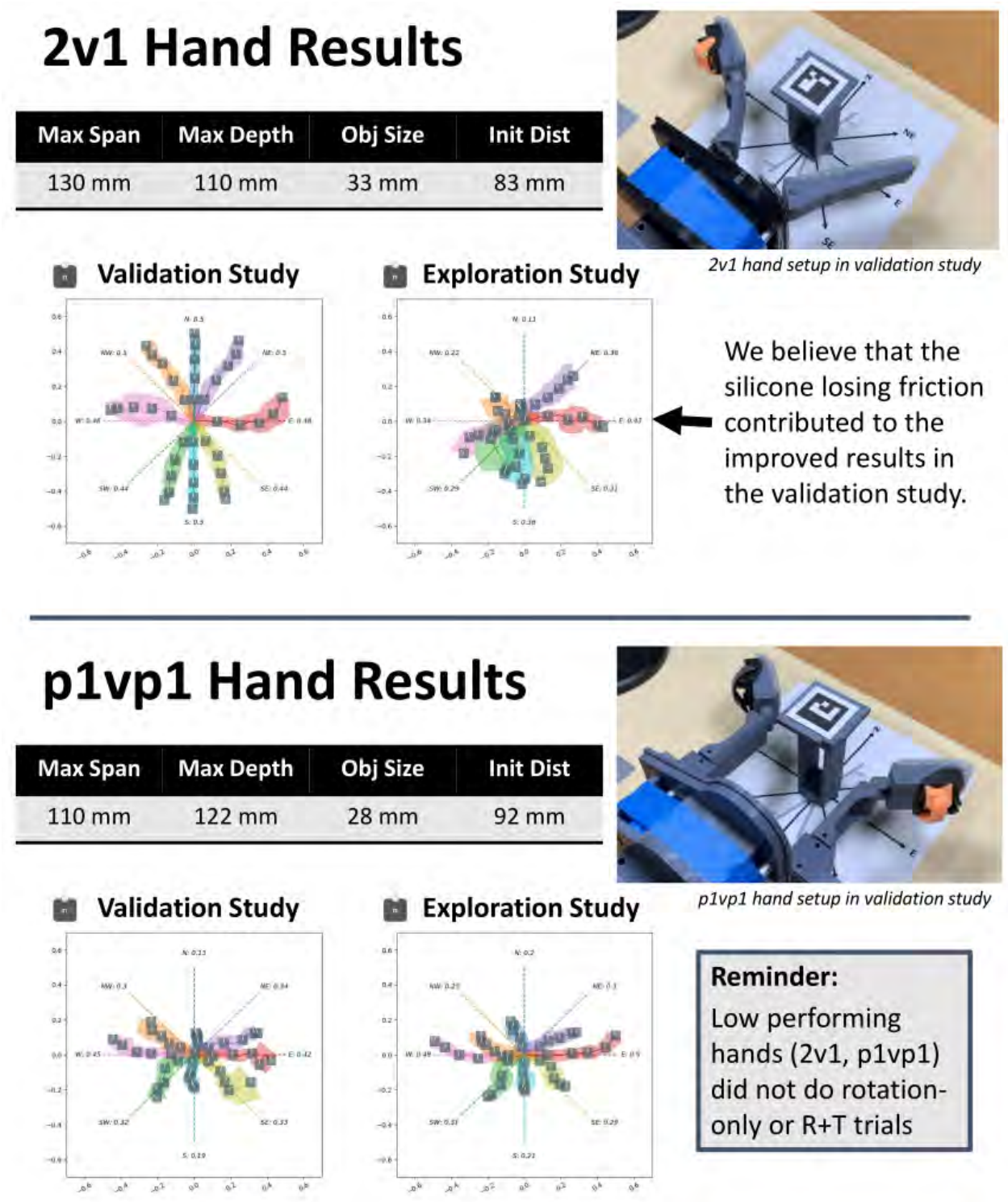

Figure D.5: Comprehensive Asterisk Test Results for the 2v1 and p1vp1 hands, for both the Experimental and Validation studies.

D.2 Rotation+Translation Trials Statistically Compared to Translation-Only Trials, Exploration vs Validation Statistical Comparisons

See figures D.6 (2v2, page 93), D.7(2v3, page 94), D.8 (3v3, page 95), D.9 (p2vp2, page 96), and D.10 (2v1 & p1vp1, page 97) show statistical comparisons: comparing the rotation+translation trials to the translation-only trials (top) and comparing the exploration and validation trials (bottom).

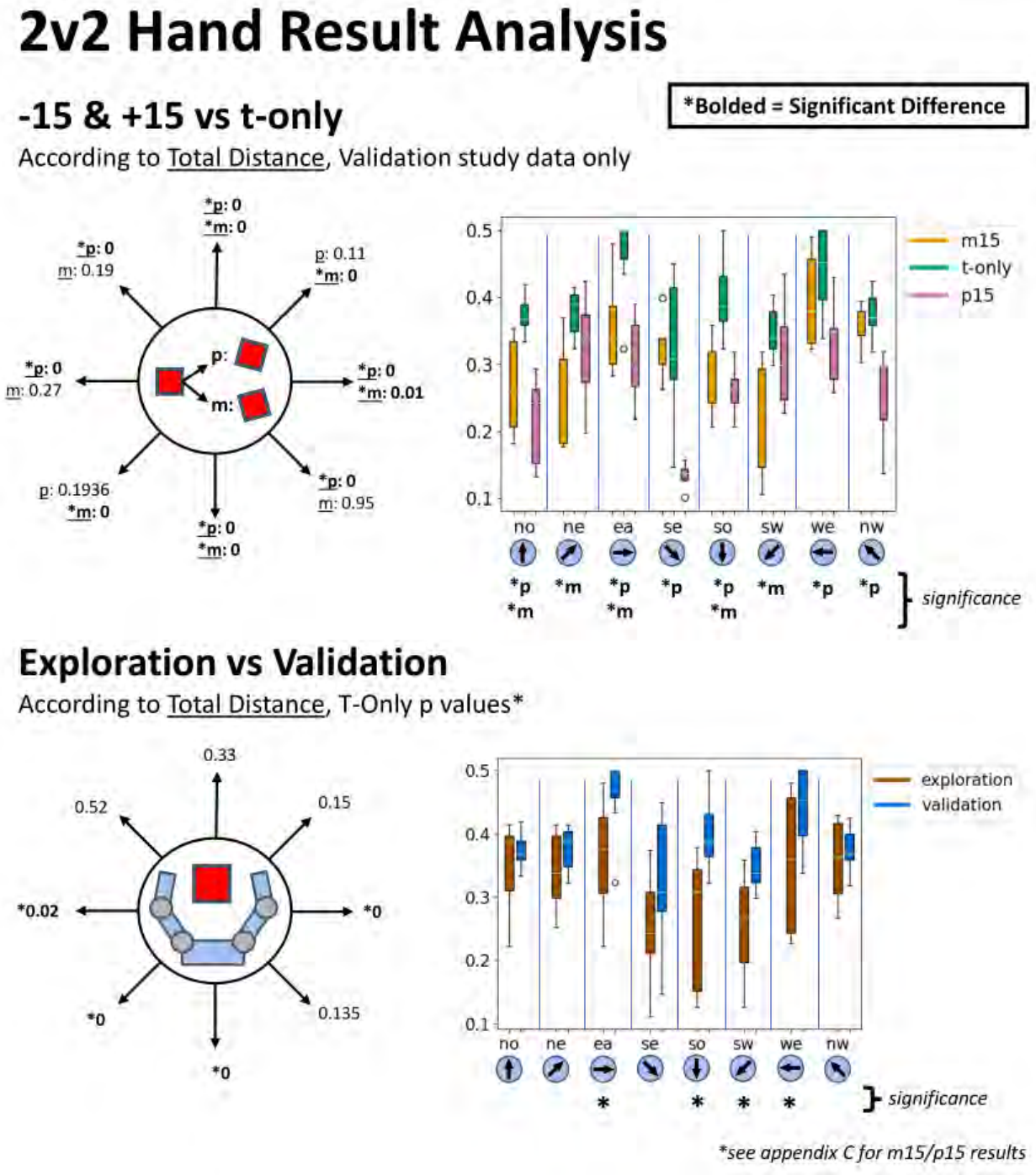

Figure D.6: Statistical Results for the 2v2 hand, (top) between t-only and +/-15 degrees and (bottom) between Experimental and Validation studies.

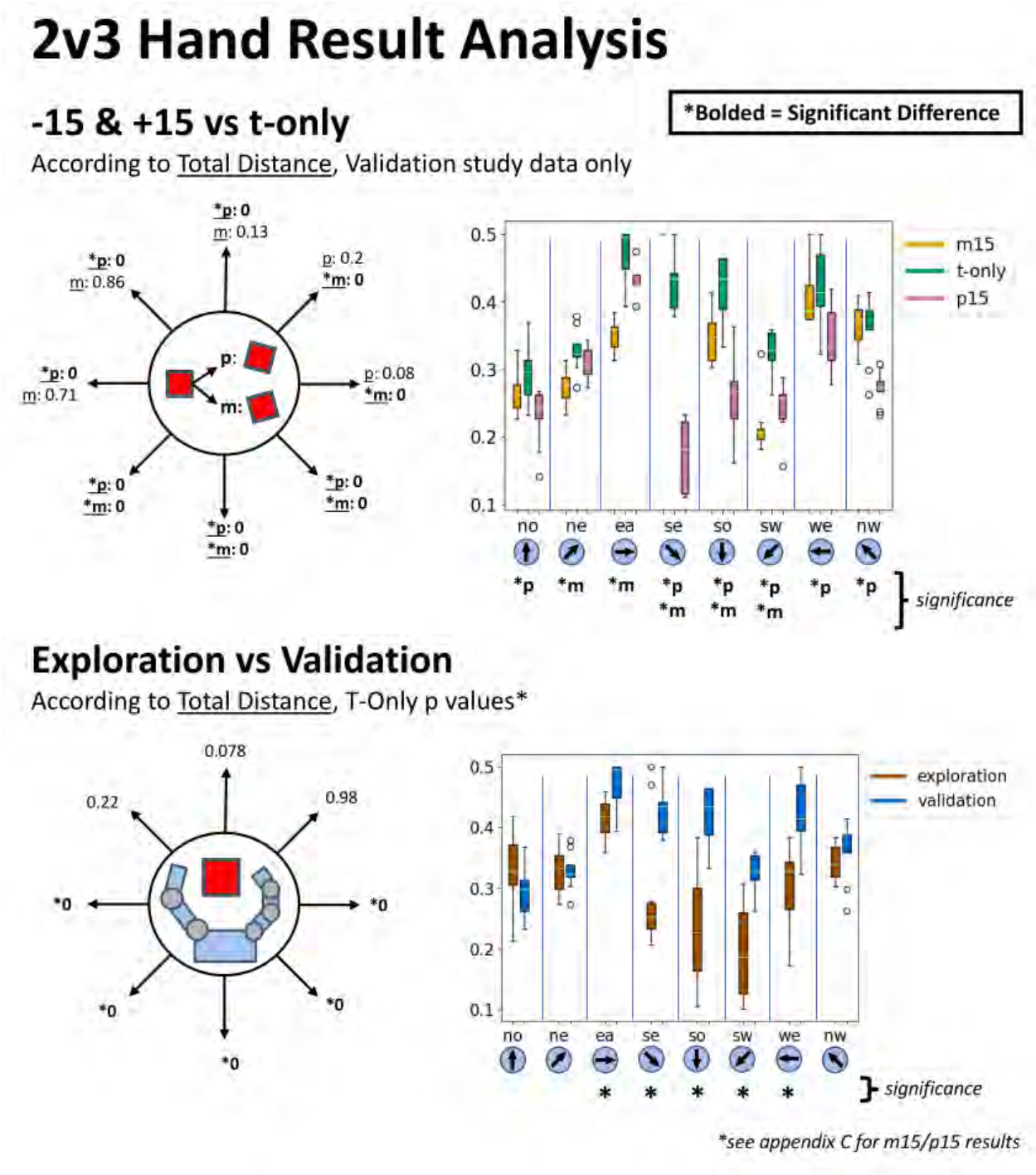

Figure D.7: Statistical Results for the 2v3 hand, (top) between t-only and +/-15 degrees and (bottom) between Experimental and Validation studies.

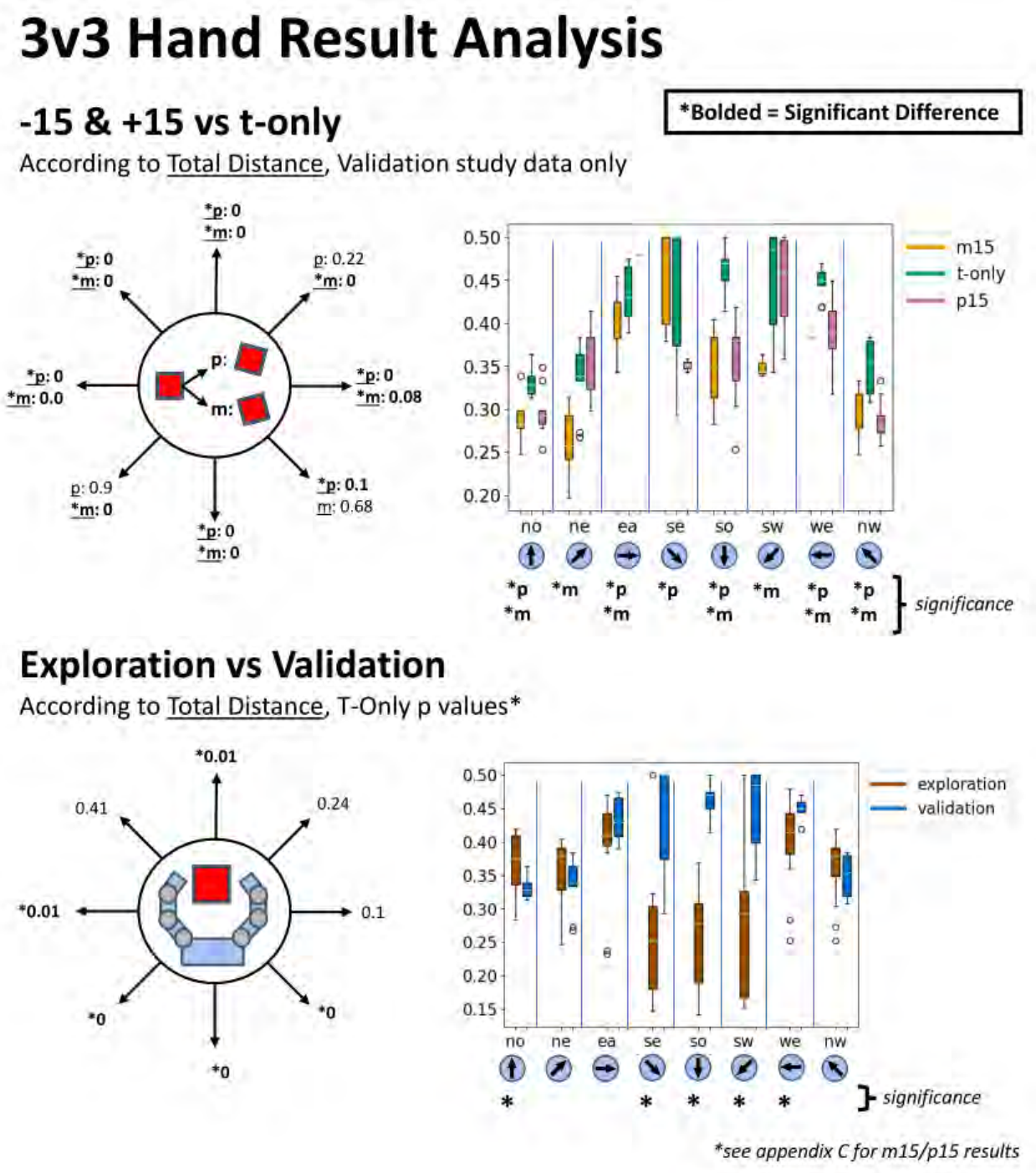

Figure D.8: Statistical Results for the 3v3 hand, (top) between t-only and +/-15 degrees and (bottom) between Experimental and Validation studies.

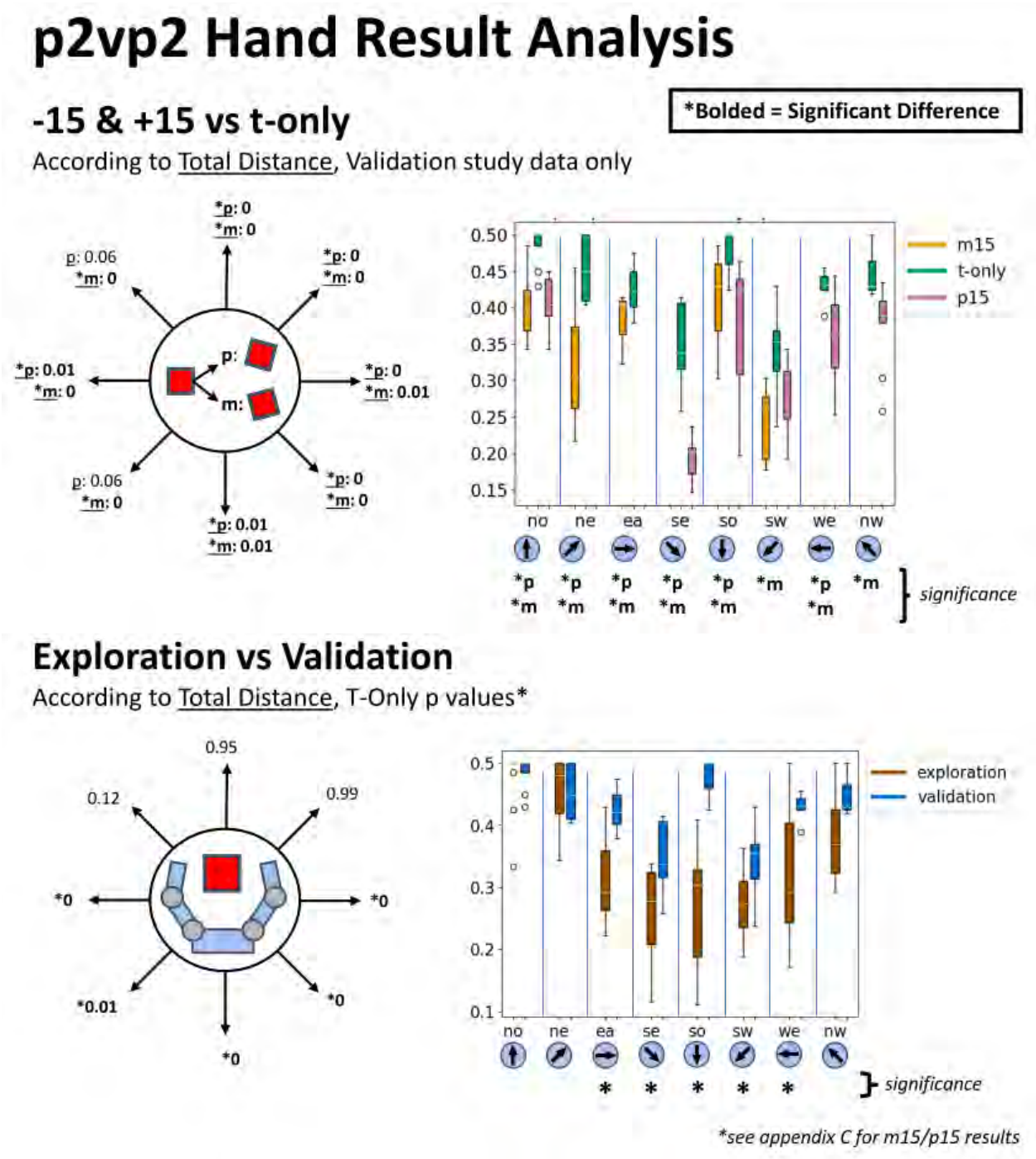

Figure D.9: Statistical Results for the p2vp2 hand, (top) between t-only and +/-15 degrees and (bottom) between Experimental and Validation studies.

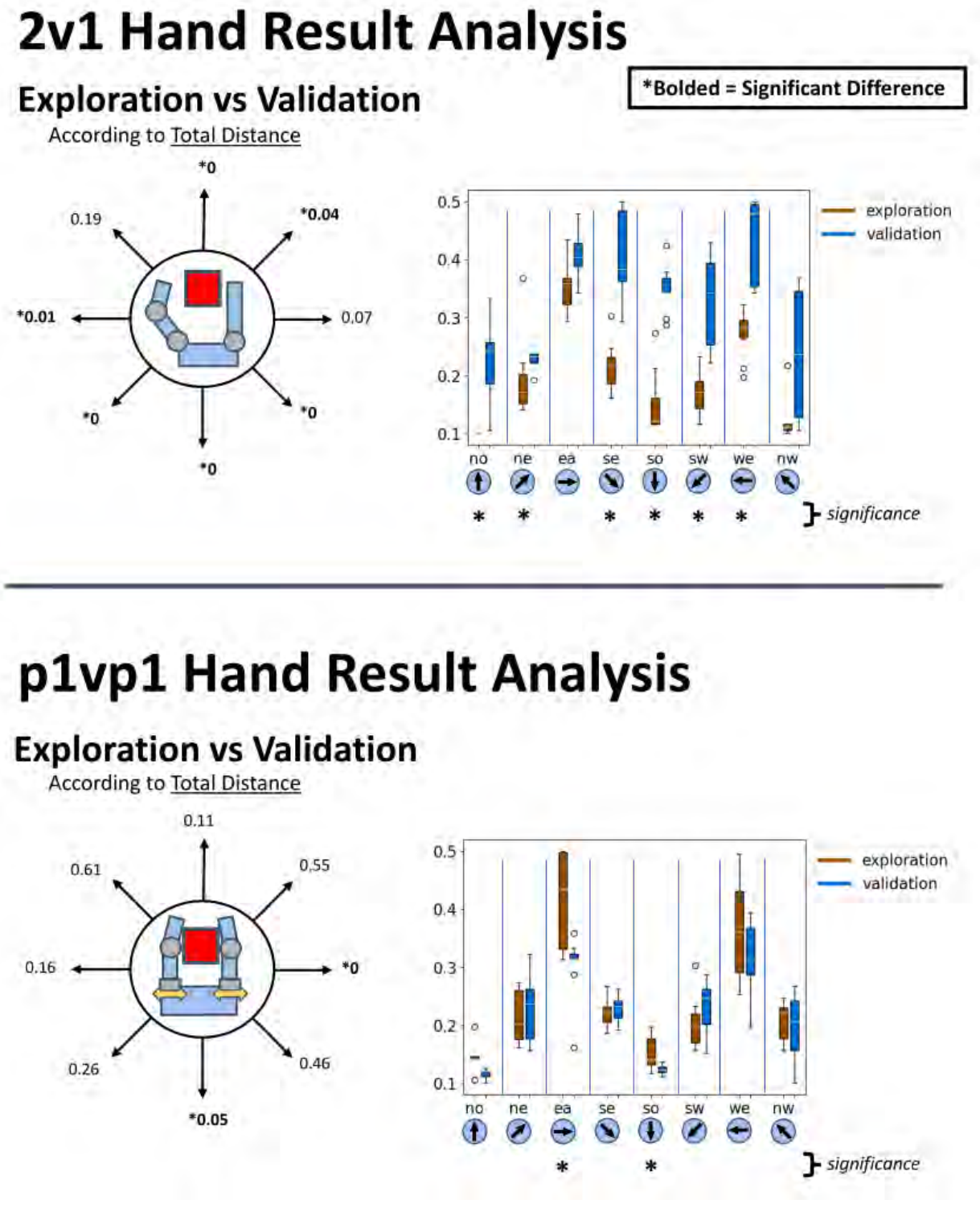

Figure D.10: Statistical Results for the 2v1 and p1vp1 hands, (top) between t-only and +/-15 degrees and (bottom) between Experimental and Validation studies.

D.3 2v2 Comparisons with Other Hands in Validation Study

Figures D.11, D.13, and D.12 show the significant differences between the hands for each direction, with respect to total distance.

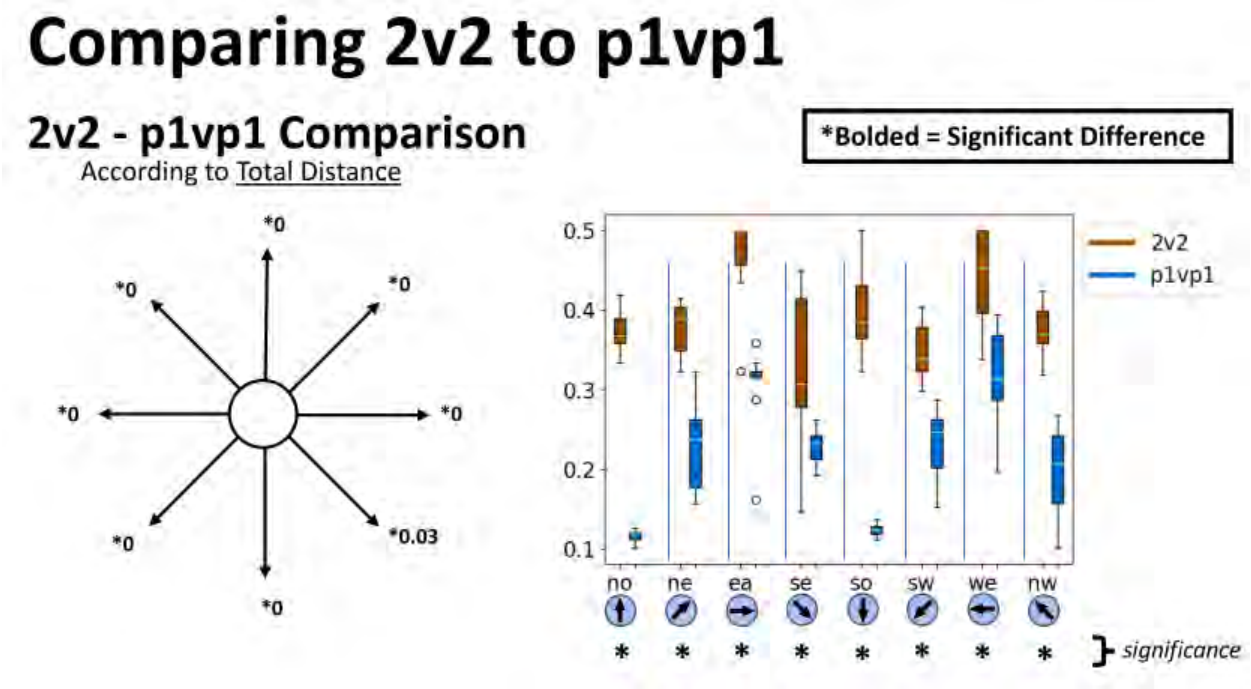

Figure D.11: Statistical Comparisons between the 2v2 and p1vp1 according to total distance values in each direction. As shown, 2v2 significantly outperforms the p1vp1 hand in every direction.

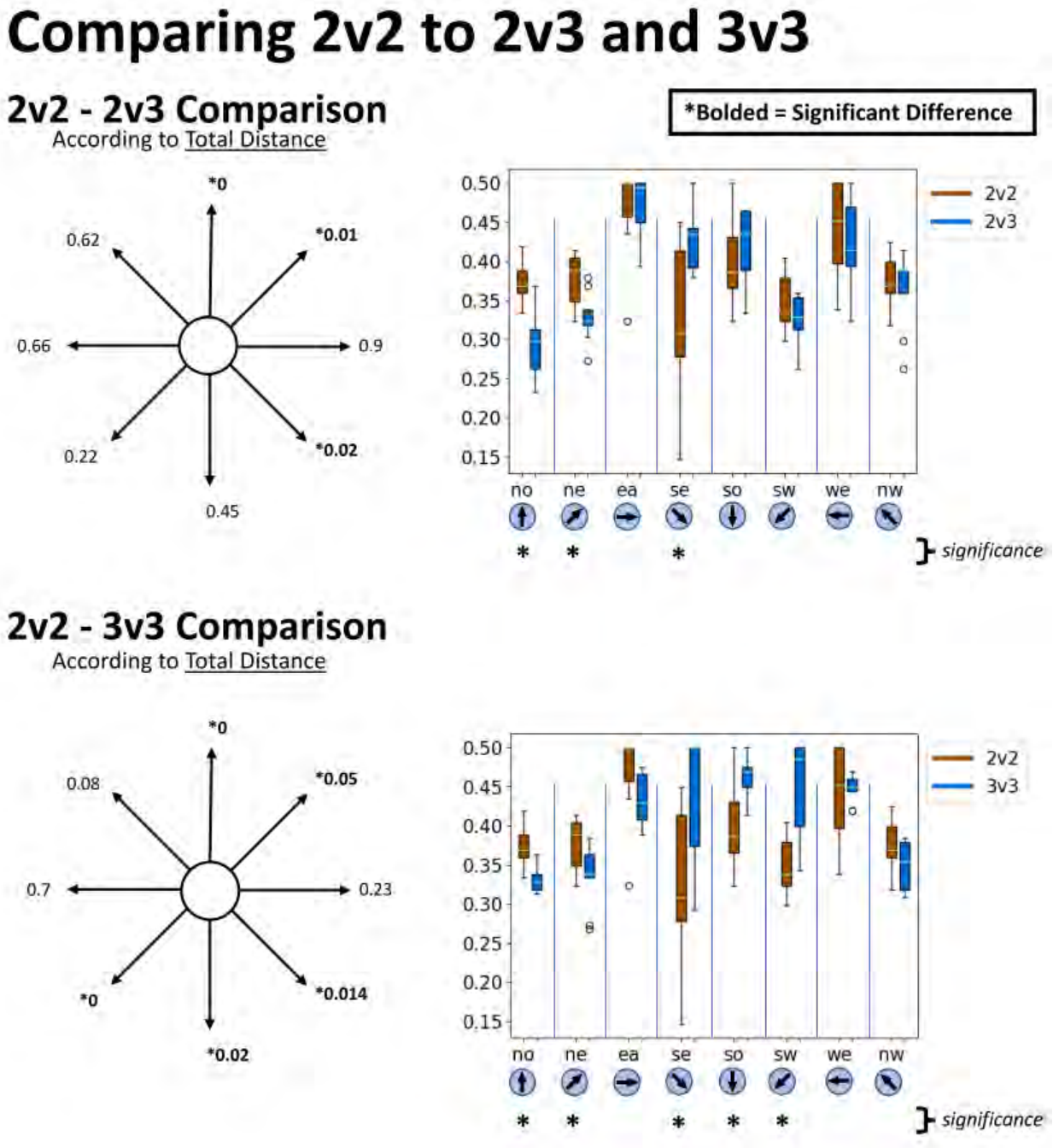

Figure D.12: Statistical Comparisons between the 2v2 and 2v3 (top), 3v3 (bottom) according to total distance values in each direction.

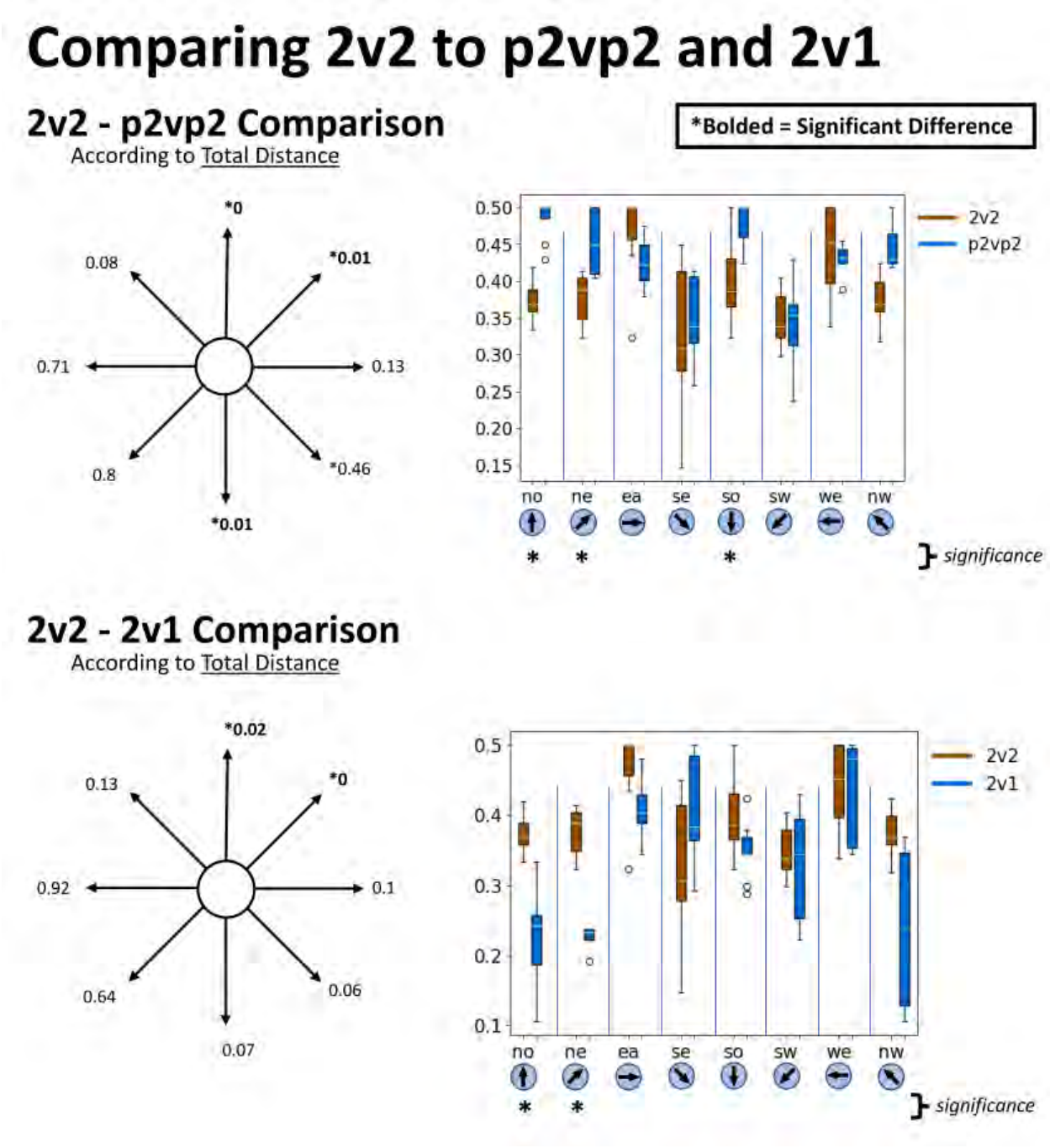

Figure D.13: Statistical Comparisons between the 2v2 and p2vp2 (top), 2v1 (bottom) according to total distance values in each direction.

D.4 Results from Extra Hands in Exploratory study not included in Validation study

The exploratory study included more hands that were not studied in the Validation study: the Barrett hand, 1v1, 2v0, f1v1 hands. In addition, a rotation+translation trials were collected for the exploratory study and are also provided. Applicable data is shown in Figure D.15 (translation-only, rotation+translation) and Figure D.16 (rotation-only). Please reference Figure D.14 for more.

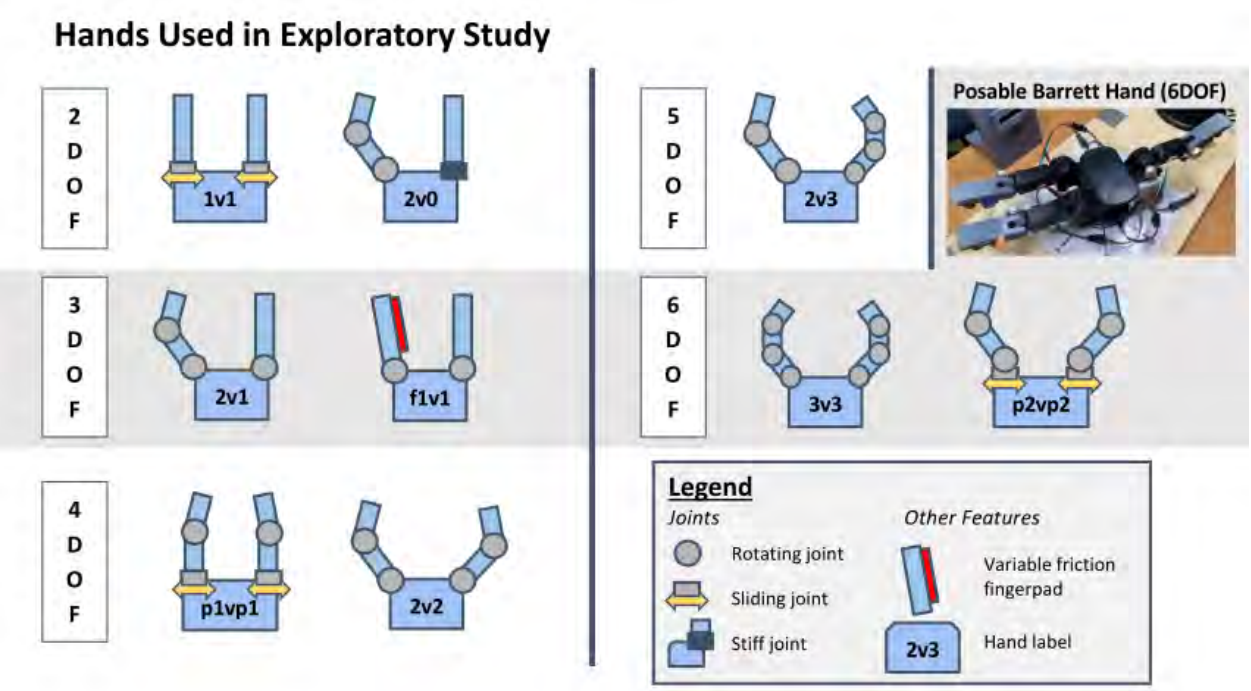

Figure D.14: The ten hands studied in the exploration study utilized rotary joints and planar joints at the palm to cover a variety of degrees of freedom.

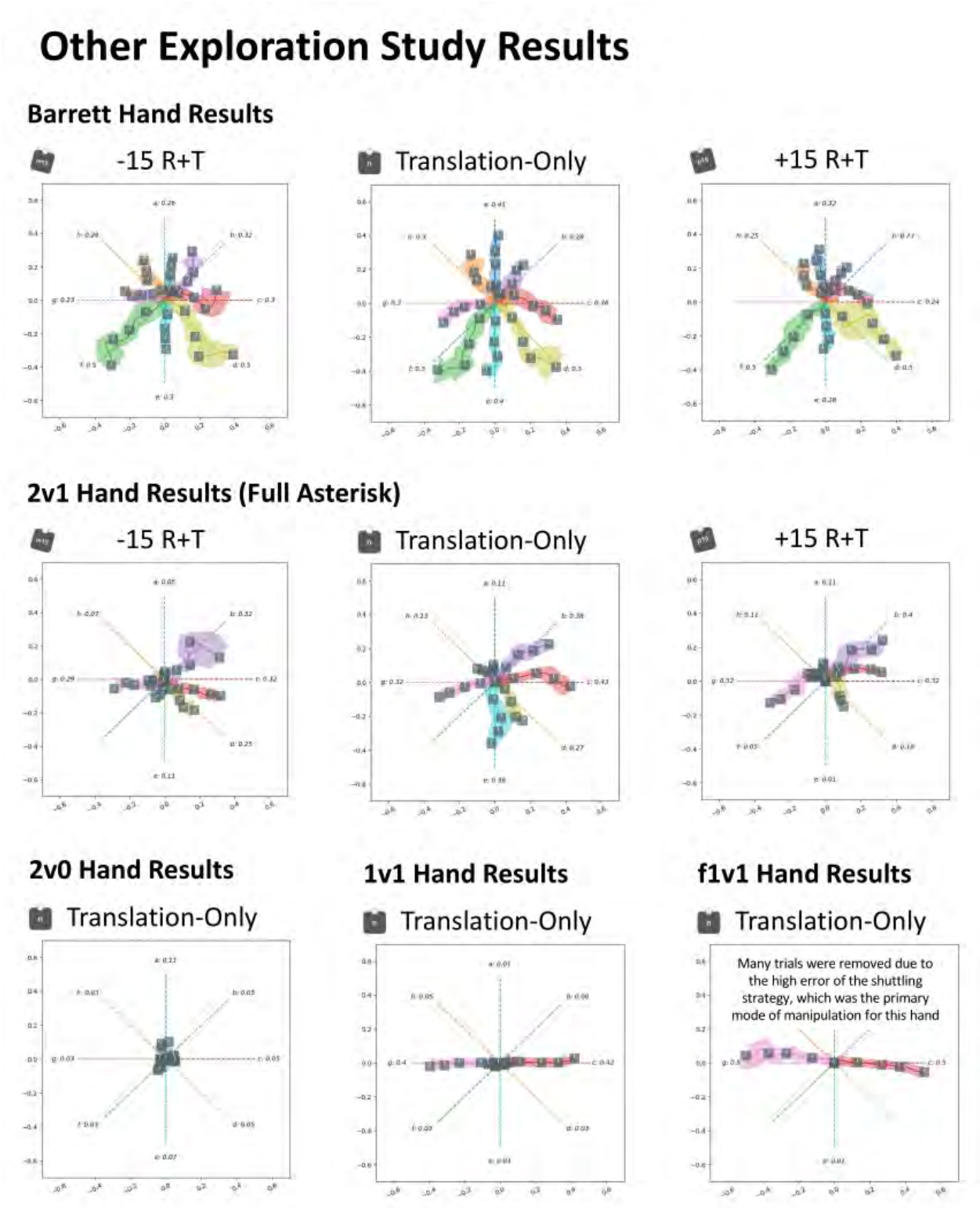

Figure D.15: Asterisk Test Results for the Barrett, 2v1, 2v0, 1v1, and f1v1 hands, for the exploration study. The 2v0, 1v1, and f1v1 hands were not capable of rotation.

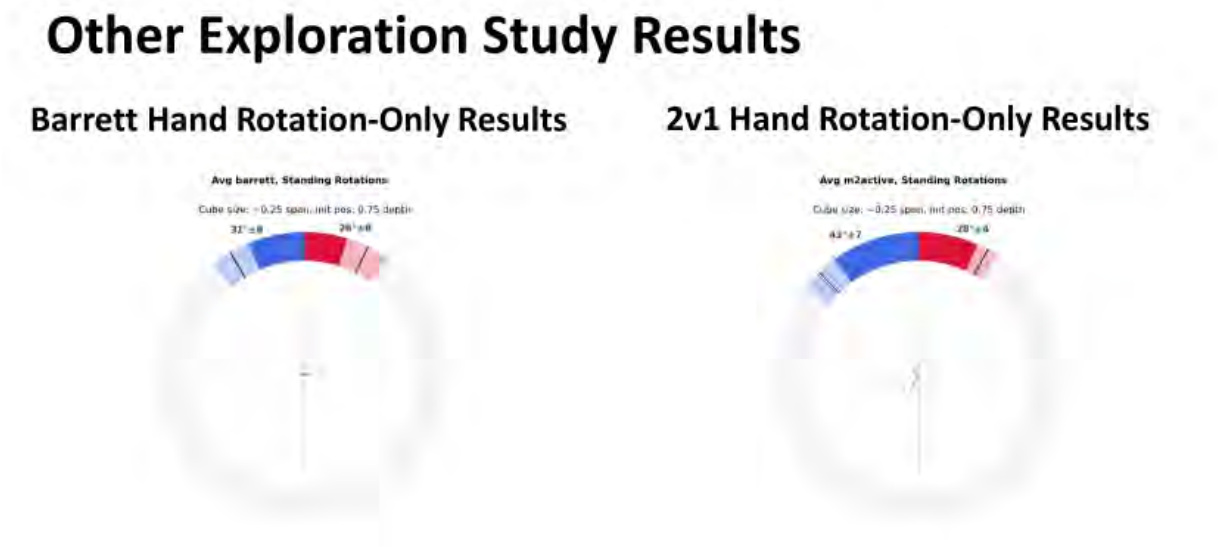

Figure D.16: Rotation-only Results for the Barrett and 2v1 hands, for both the Experimental and Validation studies. The 2v0, 1v1, and f1v1 hands were not capable of rotation.

Bibliography

[1] T. Feix, J. Romero, H.-B. Schmiedmayer, A. M. Dollar, and D. Kragic, "The grasp taxonomy of human grasp types," *IEEE Transactions on Human-Machine Systems*, vol. 46, no. 1, pp. 66–77, 2016.

[2] J. Fischer, N. W. Thompson, and J. W. Harrison, "The prehensile movements of the human hand," in *Classic Papers in Orthopaedics*. Springer, 2014, pp. 343–345.

[3] M. R. Cutkosky *et al.*, "On grasp choice, grasp models, and the design of hands for manufacturing tasks." *IEEE Transactions on robotics and automation*, vol. 5, no. 3, pp. 269–279, 1989.

[4] M. Controzzi, C. Cipriani, and M. C. Carrozza, "Design of artificial hands: A review," *The Human Hand as an Inspiration for Robot Hand Development*, pp. 219–246, 2014.

[5] J. Morrow, H.-S. Shin, C. Phillips-Grafflin, S.-H. Jang, J. Torrey, R. Larkins, S. Dang, Y.-L. Park, and D. Berenson, "Improving Soft Pneumatic Actuator fingers through integration of soft sensors, position and force control, and rigid fingernails," in *IEEE International Conference on Robotics and Automation (ICRA)*. IEEE, 2016, pp. 5024–5031.

[6] S. Jacobsen, E. Iversen, D. Knutti, R. Johnson, and K. Biggers, "Design of the Utah/MIT dextrous hand," in *IEEE International Conference on Robotics and Automation (ICRA)*, vol. 3. IEEE, 1986, pp. 1520–1532.

[7] C. Loucks, V. Johnson, P. Boissiere, G. Starr, and J. Steele, "Modeling and control of the stanford/jpl hand," in *Proceedings. 1987 IEEE International Conference on Robotics and Automation*, vol. 4. IEEE, 1987, pp. 573–578.

[8] G. Hirzinger, J. Butterfass, S. Knoch, and H. Liu, "Dlr's multisensory articulated hand," in *Experimental Robotics V*. Springer, 1998, pp. 47–55.

[9] L. U. Odhner, R. R. Ma, and A. M. Dollar, "Experiments in underactuated in-hand manipulation," in *Experimental Robotics*. Springer, 2013, pp. 27–40.

[10] B. Calli, A. Walsman, A. Singh, S. Srinivasa, P. Abbeel, and A. M. Dollar, "Benchmarking in manipulation research: Using the yale-cmu-berkeley object and model set," *IEEE Robotics & Automation Magazine*, vol. 22, no. 3, pp. 36–52, 2015.

[11] R. R. Ma, W. G. Bircher, and A. M. Dollar, "Toward robust, whole-hand caging manipulation with underactuated hands," in *2017 IEEE International Conference on Robotics and Automation (ICRA)*. IEEE, 2017, pp. 1336–1342.

[12] B. Calli and A. M. Dollar, "Vision-based model predictive control for within-hand precision manipulation with underactuated grippers," in *Proc. IEEE Int. Conf. Robot. Autom.* IEEE, 2017, pp. 2839–2845.

[13] ——, "Vision-based model predictive control for within-hand precision manipulation with underactuated grippers," in *2017 ICRA*. IEEE, 2017, pp. 2839–2845.

[14] L. U. Odhner, R. R. Ma, and A. M. Dollar, "Open-loop precision grasping with underactuated hands inspired by a human manipulation strategy," *IEEE Transactions on Automation Science and Engineering*, vol. 10, no. 3, pp. 625–633, 2013.

[15] L. U. Odhner, L. P. Jentoft, M. R. Claffee, N. Corson, Y. Tenzer, R. R. Ma, M. Buehler, R. Kohout, R. D. Howe, and A. M. Dollar, "A compliant, underactuated hand for robust manipulation," *The International Journal of Robotics Research*, vol. 33, no. 5, pp. 736–752, 2014.

[16] D. M. Aukes, B. Heyneman, J. Ulmen, H. Stuart, M. R. Cutkosky, S. Kim, P. Garcia, and A. Edsinger, "Design and testing of a selectively compliant underactuated hand," *The International Journal of Robotics Research*, vol. 33, no. 5, pp. 721–735, 2014. [Online]. Available: http://dx.doi.org/10.1177/0278364913518997

[17] Y. Yang, Y. Chen, Y. Li, M. Z. Chen, and Y. Wei, "Bioinspired Robotic Fingers Based on Pneumatic Actuator and 3d Printing of Smart Material," *Soft Robotics*, vol. 4, no. 2, pp. 147–162, 2017.

[18] V. Tincani, M. G. Catalano, E. Farnioli, M. Garabini, G. Grioli, G. Fantoni, and A. Bicchi, "Velvet fingers: A dexterous gripper with active surfaces," in *Intelligent robots and systems (IROS), 2012 IEEE/RSJ International conference on*. IEEE, 2012, pp. 1257–1263.

[19] V. Tincani, G. Grioli, M. G. Catalano, M. Garabini, S. Grechi, G. Fantoni, and A. Bicchi, "Implementation and control of the velvet fingers: a dexterous gripper with active surfaces," in *Robotics and Automation (ICRA), 2013 IEEE International Conference on*. IEEE, 2013, pp. 2744–2750.

[20] A. J. Spiers, B. Calli, and A. M. Dollar, "Variable-friction finger surfaces to enable within-hand manipulation via gripping and sliding," *IEEE Robotics and Automation Letters*, vol. 3, no. 4, pp. 4116–4123, 2018.

[21] R. R. Ma, A. Spiers, and A. M. Dollar, "M2 Gripper: Extending the Dexterity of a Simple, Underactuated Gripper," in *Advances in Reconfigurable Mechanisms and Robots II*, X. Ding, X. Kong, and J. S. Dai, Eds. Cham: Springer International Publishing, 2016, pp. 795–805. [Online]. Available: http://dx.doi.org/10.1007/978-3-319-23327-7_68

[22] C. McCann, V. Patel, and A. Dollar, "The stewart hand: A highly dexterous, six-degrees-of-freedom manipulator based on the stewart-gough platform," *IEEE Robotics & Automation Magazine*, vol. 28, no. 2, pp. 23–36, 2021.

[23] W. G. Bircher, A. M. Dollar, and N. Rojas, "A two-fingered robot gripper with large object reorientation range," in *Robotics and Automation (ICRA), 2017 IEEE International Conference on*. IEEE, 2017, pp. 3453–3460.

[24] R. R. Ma, N. Rojas, and A. M. Dollar, "Towards Predictable Precision Manipulation of Unknown Objects with Underactuated Fingers," in *Advances in Reconfigurable Mechanisms and Robots II*, X. Ding, X. Kong, and J. S. Dai, Eds. Cham: Springer International Publishing, 2016, pp. 927–937. [Online]. Available: http://dx.doi.org/10.1007/978-3-319-23327-7_79

[25] R. Balasubramanian and Y. Matsuoka, "The role of small redundant actuators in precise manipulation," in *2009 IEEE International Conference on Robotics and Automation*. IEEE, 2009, pp. 4409–4415.

[26] R. R. Ma and A. M. Dollar, "On dexterity and dexterous manipulation," in *2011 ICAR*. IEEE, 2011, pp. 1–7.

[27] B. Calli, A. Dollar, M. Roa, S. Srinivasa, and Y. Sun. (2020) Cfp: Benchmarking protocols for robotic manipulation. [Online]. Available: https://www.ieee-ras.org/publications/ra-l/special-issues/benchmarking-protocols-for-robotic-manipulation

[28] B. Calli, A. Dollar, S. Srinivasa, and M. Roa. (2017) Development of benchmarking protocols for robotic manipulation. [Online]. Available: http://ycbbenchmarks.com/IROS2017workshop.html

[29] B. Calli, A. Dollar, Y. Sun, and M. Roa. (2019) Benchmarks for robotic manipulation. [Online]. Available: http://www.ycbbenchmarks.com/ICRA2019_workshop

[30] J. Bimbo, D. Kanoulas, K. Harada, and G. Vezzani. (2020) Why robots fail to grasp? [Online]. Available: https://failtograsp.github.io/

[31] I. M. Bullock and A. M. Dollar, "Classifying human manipulation behavior," in *2011 ICORR*. IEEE, 2011, pp. 1–6.

[32] T. Feix, I. M. Bullock, and A. M. Dollar, "Analysis of human grasping behavior: Object characteristics and grasp type," *IEEE transactions on haptics*, vol. 7, no. 3, pp. 311–323, 2014.

[33] T. Feix, I. Bullock, and A. Dollar, "Analysis of human grasping behavior: Correlating tasks, objects and grasps," *IEEE transactions on haptics*, vol. 7, no. 4, pp. 430–441, 2014.

[34] S. Puhlmann, F. Heinemann, O. Brock, and M. Maertens, "A compact representation of human single-object grasping," in *Intelligent Robots and Systems (IROS), 2016 IEEE/RSJ International Conference on*. IEEE, 2016, pp. 1954–1959.

[35] I. M. Bullock, T. Feix, and A. M. Dollar, "Finding small, versatile sets of human grasps to span common objects," in *IEEE International Conference on Robotics and Automation (ICRA)*. IEEE, 2013, pp. 1068–1075.

[36] F. Heinemann, S. Puhlmann, C. Eppner, J. Élvarez Ruiz, M. Maertens, and O. Brock, "A taxonomy of human grasping behavior suitable for transfer to robotic hands," in *Robotics and Automation (ICRA), 2015 IEEE International Conference on*. IEEE, 2015, pp. 4286–4291.

[37] R. Balasubramanian, L. Xu, P. D. Brook, J. R. Smith, and Y. Matsuoka, "Physical human interactive guidance: Identifying grasping principles from human-planned grasps," *IEEE Transactions on Robotics*, vol. 28, no. 4, pp. 899–910, 2012.

[38] D.-A. Huang, M. Ma, W.-C. Ma, and K. M. Kitani, "How do we use our hands? discovering a diverse set of common grasps," in *Proceedings of the IEEE Conference on Computer Vision and Pattern Recognition*, 2015, pp. 666–675.

[39] C. Eppner, R. Deimel, J. Álvarez Ruiz, M. Maertens, and O. Brock, "Exploitation of environmental constraints in human and robotic grasping," *The International Journal of Robotics Research*, p. 0278364914559753, 2015.

[40] G. Juravle, H. Deubel, and C. Spence, "Attention and suppression affect tactile perception in reach-to-grasp movements," *Acta psychologica*, vol. 138, no. 2, pp. 302–310, 2011.

[41] S. K. Allani, B. John, J. Ruiz, S. Dixit, J. Carter, C. Grimm, and R. Balasubramanian, "Evaluating human gaze patterns during grasping tasks: robot versus human hand," in *Proceedings of the ACM Symposium on Applied Perception*. ACM, 2016, pp. 45–52.

[42] M. Unrath, Z. Zhang, A. Goins, R. Carpenter, W.-K. Wong, and R. Balasubramanian, "Using crowdsourcing to generate surrogate training data for robotic grasp prediction," in *Second AAAI Conference on Human Computation and Crowdsourcing*, 2014.

[43] B. John, J. Carter, J. Ruiz, S. K. Allani, S. Dixit, C. M. Grimm, and R. Balasubramanian, "Human-Planned Robotic Grasp Ranges: Capture and Validation," *arXiv preprint arXiv:1607.03366*, 2016.

[44] A. Kothari, J. Morrow, V. Thrasher, K. Engle, R. Balasubramanian, and C. Grimm, "Grasping objects big and small: Human heuristics relating grasp-type and object size," in *2018 ICRA*. IEEE, 2018.

[45] I. M. Bullock, R. R. Ma, and A. M. Dollar, "A hand-centric classification of human and robot dexterous manipulation," *IEEE transactions on Haptics*, vol. 6, no. 2, pp. 129–144, 2013.

[46] I. M. Bullock, T. Feix, and A. M. Dollar, "Dexterous workspace of human two-and three-fingered precision manipulation," in *Haptics Symposium (HAPTICS), 2014 IEEE*. IEEE, 2014, pp. 41–47.

[47] M. K. Burstedt, J. R. Flanagan, and R. S. Johansson, "Control of grasp stability in humans under different frictional conditions during multidigit manipulation," *Journal of neurophysiology*, vol. 82, no. 5, pp. 2393–2405, 1999.

[48] Y. Gloumakov, T. Feix, I. M. Bullock, and A. M. Dollar, "Object stability during human precision fingertip manipulation," in *Haptics Symposium (HAPTICS), 2016 IEEE*. IEEE, 2016, pp. 84–91.

[49] I. M. Bullock, T. Feix, and A. M. Dollar, "Human precision manipulation workspace: Effects of object size and number of fingers used," in *IEEE Annual International Conference on Engineering in Medicine and Biology Society (EMBC)*. IEEE, 2015, pp. 5768–5772.

[50] P.-L. Kuo, D. L. Lee, D. L. Jindrich, and J. T. Dennerlein, "Finger joint coordination during tapping," *Journal of biomechanics*, vol. 39, no. 16, pp. 2934–2942, 2006.

[51] D. Prattichizzo, M. Malvezzi, and A. Bicchi, "On motion and force control of grasping hands with postural synergies," 2010.

[52] G. Tessitore, C. Sinigaglia, and R. Prevete, "Hierarchical and multiple hand action representation using temporal postural synergies," *Experimental brain research*, vol. 225, no. 1, pp. 11–36, 2013.

[53] K. Wolf, A. Naumann, M. Rohs, and J. Müller, "A taxonomy of microinteractions: Defining microgestures based on ergonomic and scenario-dependent requirements," in *IFIP Conference on Human-Computer Interaction*. Springer, 2011, pp. 559–575.

[54] R. Balasubramanian, B. Dellon, S. Pradhan, S. Gibbs, and Y. Matsuoka, "Quantifying the Dimensions of Human Hand Dexterity Through a Survey of Daily Tasks," in *Workshop on Understanding the Human Hand for Advancing Robotic Manipulation at Robotics: Science and Systems*, 2009.

[55] I. KAPANDJI, "The Physiology of the Joints—Upper Limb, Vol. 1 (Edinburgh: Churchill-Livingstone)," 1982.

[56] J. Jahn, W. E. Janes, M. Saheb-Al-Zamani, C. M. Burbank, J. M. Brown, and J. R. Engsberg, "Identification of three movement phases of the hand during lateral and pulp pinches using video motion capture," *Hand*, vol. 8, no. 2, pp. 123–131, 2013.

[57] G. I. Bain, N. Polites, B. G. Higgs, R. J. Heptinstall, and A. M. McGrath, "The functional range of motion of the finger joints," *Journal of Hand Surgery (European Volume)*, vol. 40, no. 4, pp. 406–411, 2015.

[58] R. H. Cuijpers, J. B. Smeets, and E. Brenner, "On the relation between object shape and grasping kinematics," *Journal of Neurophysiology*, vol. 91, no. 6, pp. 2598–2606, 2004.

[59] K. Jordan, T. C. Pataky, and K. M. Newell, "Grip width and the organization of force output," *Journal of motor behavior*, vol. 37, no. 4, pp. 285–294, 2005.

[60] K.-S. Lee and M.-C. Jung, "Common patterns of voluntary grasp types according to object shape, size, and direction," *International Journal of Industrial Ergonomics*, vol. 44, no. 5, pp. 761–768, 2014.

[61] T. Watanabe, K. Owashi, Y. Kanauchi, N. Mura, M. Takahara, and T. Ogino, "The short-term reliability of grip strength measurement and the effects of posture and grip span," *The Journal of hand surgery*, vol. 30, no. 3, pp. 603–609, 2005.

[62] Y. Aldien, D. Welcome, S. Rakheja, R. Dong, and P.-E. Boileau, "Contact pressure distribution at hand–handle interface: role of hand forces and handle size," *International Journal of Industrial Ergonomics*, vol. 35, no. 3, pp. 267–286, 2005.

[63] I. M. Bullock, J. Z. Zheng, S. De La Rosa, C. Guertler, and A. M. Dollar, "Grasp frequency and usage in daily household and machine shop tasks," *IEEE transactions on haptics*, vol. 6, no. 3, pp. 296–308, 2013.

[64] K.-S. Lee and M.-C. Jung, "Investigation of hand postures in manufacturing industries according to hand and object properties," *International Journal of Industrial Ergonomics*, vol. 46, pp. 98–104, 2015.

[65] C. S. Edgren, R. G. Radwin, and C. B. Irwin, "Grip force vectors for varying handle diameters and hand sizes," *Human factors*, vol. 46, no. 2, pp. 244–251, 2004.

[66] P. L. Weir, C. L. MacKenzie, R. G. Marteniuk, S. L. Cargoe, and M. B. Frazer, "The effects of object weight on the kinematics of prehension," *Journal of Motor Behavior*, vol. 23, no. 3, pp. 192–204, 1991.

[67] M. H. Yun, "A hand posture measurement system for evaluating manual tool tasks," in *Proceedings of the Human Factors and Ergonomics Society Annual Meeting*, vol. 37. SAGE Publications Sage CA: Los Angeles, CA, 1993, pp. 754–758.

[68] N. Miyata, M. Kouchi, T. Kurihara, and M. Mochimaru, "Modeling of human hand link structure from optical motion capture data," in *IEEE/RSJ International Conference on Intelligent Robots and Systems (IROS)*, vol. 3. IEEE, 2004, pp. 2129–2135.

[69] N. Jarque-Bou, V. Gracia-Ibáñez, J.-L. Sancho-Bru, M. Vergara, A. Pérez-González, and F. J. Andrés, "Using kinematic reduction for studying grasping postures. An application to power and precision grasp of cylinders," *Applied ergonomics*, vol. 56, pp. 52–61, 2016.

[70] P. H. Thakur, A. J. Bastian, and S. S. Hsiao, "Multidigit movement synergies of the human hand in an unconstrained haptic exploration task," *Journal of Neuroscience*, vol. 28, no. 6, pp. 1271–1281, 2008.

[71] B. D. Argall, S. Chernova, M. Veloso, and B. Browning, "A survey of robot learning from demonstration," *Robotics and autonomous systems*, vol. 57, no. 5, pp. 469–483, 2009.

[72] N. Miyata, M. Kouchi, T. Kurihara, and M. Mochimaru, "Modeling of human hand link structure from optical motion capture data," in *IEEE/RSJ International Conference on Intelligent Robots and Systems (IROS)*, vol. 3. IEEE, 2004, pp. 2129–2135.

[73] M. V. Liarokapis, A. M. Dollar, and K. J. Kyriakopoulos, "Humanlike, task-specific reaching and grasping with redundant arms and low-complexity hands," in *International Conference on Advanced Robotics (ICAR)*. IEEE, 2015, pp. 490–497.

[74] S. Ekvall and D. Kragic, "Interactive grasp learning based on human demonstration," in *IEEE International Conference on Robotics and Automation (ICRA)*, vol. 4. IEEE, 2004, pp. 3519–3524.

[75] B. Huang, M. Li, R. L. De Souza, J. J. Bryson, and A. Billard, "A modular approach to learning manipulation strategies from human demonstration," *Autonomous Robots*, vol. 40, no. 5, pp. 903–927, 2016.

[76] S. B. Kang and K. Ikeuchi, "Toward automatic robot instruction from perception-mapping human grasps to manipulator grasps," *IEEE transactions on robotics and automation*, vol. 13, no. 1, pp. 81–95, 1997.

[77] M. Hueser, T. Baier, and J. Zhang, "Learning of demonstrated grasping skills by stereoscopic tracking of human head configuration," in *IEEE International Conference on Robotics and Automation (ICRA)*. IEEE, 2006, pp. 2795–2800.

[78] E. Oztop, L.-H. Lin, M. Kawato, and G. Cheng, "Dexterous skills transfer by extending human body schema to a robotic hand," in *IEEE-RAS International Conference on Humanoid Robots*. IEEE, 2006, pp. 82–87.

[79] C. Lee and Y. Xu, "Reduced-dimension representations of human performance data for human-to-robot skill transfer," in *IEEE/RSJ International Conference on Intelligent Robots and Systems (IROS)*, vol. 3. IEEE, 1998, pp. 1956–1961.

[80] C. Lee, "Learning reduced-dimension models of human actions," Ph.D. dissertation, Carnegie Mellon University, 2000.

[81] M. T. Ciocarlie and P. K. Allen, "Hand posture subspaces for dexterous robotic grasping," *The International Journal of Robotics Research*, vol. 28, no. 7, pp. 851–867, 2009.

[82] E. L. Sauser, B. D. Argall, G. Metta, and A. G. Billard, "Iterative learning of grasp adaptation through human corrections," *Robotics and Autonomous Systems*, vol. 60, no. 1, pp. 55–71, 2012.

[83] B. D. Argall, S. Chernova, M. Veloso, and B. Browning, "A survey of robot learning from demonstration," *Robotics and autonomous systems*, vol. 57, no. 5, pp. 469–483, 2009.

[84] A. E. Leeper, K. Hsiao, M. Ciocarlie, L. Takayama, and D. Gossow, "Strategies for human-in-the-loop robotic grasping," in *ACM/IEEE international conference on Human-Robot Interaction (HRI)*. ACM, 2012, pp. 1–8.

[85] D. Sakamoto, K. Honda, M. Inami, and T. Igarashi, "Sketch and run: a stroke-based interface for home robots," in *Proceedings of the SIGCHI Conference on Human Factors in Computing Systems*. ACM, 2009, pp. 197–200.

[86] D. Perzanowski, A. C. Schultz, W. Adams, E. Marsh, and M. Bugajska, "Building a multimodal human-robot interface," *IEEE intelligent systems*, vol. 16, no. 1, pp. 16–21, 2001.

[87] C. P. Quintero, R. T. Fomena, A. Shademan, N. Wolleb, T. Dick, and M. Jagersand, "Sepo: Selecting by pointing as an intuitive human-robot command interface," in *IEEE International Conference on Robotics and Automation (ICRA)*. IEEE, 2013, pp. 1166–1171.

[88] A. Fernández, L. Bergesio, A. M. Bernardos, J. A. Besada, and J. R. Casar, "A kinect-based system to enable interaction by pointing in smart spaces," in *IEEE Sensors Applications Symposium (SAS)*. IEEE, 2015, pp. 1–6.

[89] C. C. Kemp, C. D. Anderson, H. Nguyen, A. J. Trevor, and Z. Xu, "A point-and-click interface for the real world: laser designation of objects for mobile manipulation," in *ACM/IEEE International Conference on Human-Robot Interaction (HRI)*. IEEE, 2008, pp. 241–248.

[90] K. Ishii, S. Zhao, M. Inami, T. Igarashi, and M. Imai, "Designing laser gesture interface for robot control," in *IFIP Conference on Human-Computer Interaction*. Springer, 2009, pp. 479–492.

[91] A. Simorov, R. S. Otte, C. M. Kopietz, and D. Oleynikov, "Review of surgical robotics user interface: what is the best way to control robotic surgery?" *Surgical endoscopy*, vol. 26, no. 8, pp. 2117–2125, 2012.

[92] J. H. Palep *et al.*, "Robotic assisted minimally invasive surgery," *Journal of Minimal Access Surgery*, vol. 5, no. 1, p. 1, 2009.

[93] L.-W. Sun, F. Van Meer, J. Schmid, Y. Bailly, A. A. Thakre, and C. K. Yeung, "Advanced da vinci surgical system simulator for surgeon training and operation planning," *The International Journal of Medical Robotics and Computer Assisted Surgery*, vol. 3, no. 3, pp. 245–251, 2007.

[94] M. A. Diftler, J. Mehling, M. E. Abdallah, N. A. Radford, L. B. Bridgwater, A. M. Sanders, R. S. Askew, D. M. Linn, J. D. Yamokoski, F. Permenter *et al.*, "Robonaut 2-the first humanoid robot in space," in *IEEE International Conference on Robotics and Automation (ICRA)*. IEEE, 2011, pp. 2178–2183.

[95] R. Balasubramanian, L. Xu, P. D. Brook, J. R. Smith, and Y. Matsuoka, "Physical human interactive guidance: Identifying grasping principles from human-planned grasps," *IEEE Transactions on Robotics*, vol. 28, no. 4, pp. 899–910, 2012.

[96] C. Erdogan, A. Schröder, and O. Brock, "Coordination of intrinsic and extrinsic degrees of freedom in soft robotic grasping," in *2018 IEEE International Conference on Robotics and Automation (ICRA)*. IEEE, 2018, pp. 4251–4256.

[97] R. Deimel and O. Brock, "A novel type of compliant and underactuated robotic hand for dexterous grasping," *The International Journal of Robotics Research*, vol. 35, no. 1-3, pp. 161–185, 2016.

[98] J. Morrow, A. Kothari, Y. H. Ong, N. Harlan, R. Balasubramanian, and C. Grimm, "Using human studies to analyze capabilities of underactuated and compliant hands in manipulation tasks," in *2018 IEEE/RSJ International Conference on Intelligent Robots and Systems (IROS)*. IEEE, 2018, pp. 2949–2954.

[99] L. U. Odhner, R. R. Ma, and A. M. Dollar, "Open-loop precision grasping with underactuated hands inspired by a human manipulation strategy," *IEEE Transactions on Automation Science and Engineering*, vol. 10, no. 3, pp. 625–633, 2013.

[100] B. Yang, P. E. Lancaster, S. S. Srinivasa, and J. R. Smith, "Benchmarking robot manipulation with the rubik's cube," *IEEE Robotics and Automation Letters*, vol. 5, no. 2, pp. 2094–2099, 2020.

[101] J. Falco, D. Hemphill, K. Kimble, E. Messina, A. Norton, R. Ropelato, and H. Yanco, "Benchmarking protocols for evaluating grasp strength, grasp cycle time, finger strength, and finger repeatability of robot end-effectors," *IEEE robotics and automation letters*, vol. 5, no. 2, pp. 644–651, 2020.

[102] W. S. You, Y. H. Lee, G. Kang, H. S. Oh, J. K. Seo, and H. R. Choi, "Kinematic design optimization of anthropomorphic robot hand using a new performance index," in *2017 14th International Conference on Ubiquitous Robots and Ambient Intelligence (URAI)*. IEEE, 2017, pp. 20–25.

[103] Nist. Grasping performance metrics and test methods: In-hand manipulation preliminary benchmark. [Online]. Available: https://www.nist.gov/el/intelligent-systems-division-73500/robotic-grasping-and-manipulation-assembly/grasping

[104] C. Hazard, N. Pollard, and S. Coros, "Automated design of robotic hands for in-hand manipulation tasks," *International Journal of Humanoid Robotics*, vol. 17, no. 01, p. 1950029, 2020.

[105] F. L. Hammond, J. Weisz, A. Andrés, P. K. Allen, and R. D. Howe, "Towards a design optimization method for reducing the mechanical complexity of underactuated robotic hands," in *2012 IEEE International conference on robotics and automation*. IEEE, 2012, pp. 2843–2850.

[106] V. Ortenzi, M. Controzzi, F. Cini, J. Leitner, M. Bianchi, M. A. Roa, and P. Corke, "Robotic manipulation and the role of the task in the metric of success," *Nature Machine Intelligence*, vol. 1, no. 8, pp. 340–346, 2019.

[107] A. S. Morgan, K. Hang, W. G. Bircher, F. M. Alladkani, A. Gandhi, B. Calli, and A. M. Dollar, "Benchmarking cluttered robot pick-and-place manipulation with the box and blocks test," *IEEE Robotics and Automation Letters*, vol. 5, no. 2, pp. 454–461, 2019.

[108] K. Van Wyk, M. Culleton, J. Falco, and K. Kelly, "Comparative peg-in-hole testing of a force-based manipulation controlled robotic hand," *IEEE Transactions on Robotics*, vol. 34, no. 2, pp. 542–549, 2018.

[109] N. Rojas, R. R. Ma, and A. M. Dollar, "The gr2 gripper: An underactuated hand for open-loop in-hand planar manipulation," *IEEE Transactions on Robotics*, vol. 32, no. 3, pp. 763–770, 2016.

[110] R. R. Ma and A. M. Dollar, "An underactuated hand for efficient finger-gaiting-based dexterous manipulation," in *2014 IEEE International Conference on Robotics and Biomimetics (ROBIO 2014)*. IEEE, 2014, pp. 2214–2219.

[111] A. Morgan, K. Hang, B. Wen, K. E. Bekris, and A. Dollar, "Complex in-hand manipulation via compliance-enabled finger gaiting and multi-modal planning," *IEEE Robotics and Automation Letters*, 2022.

[112] W. G. Bircher, A. S. Morgan, and A. M. Dollar, "Complex manipulation with a simple robotic hand through contact breaking and caging," *Science Robotics*, vol. 6, no. 54, p. eabd2666, 2021.

[113] D. M. Aukes, B. Heyneman, J. Ulmen, H. Stuart, M. R. Cutkosky, S. Kim, P. Garcia, and A. Edsinger, "Design and testing of a selectively compliant underactuated hand," *The International Journal of Robotics Research*, vol. 33, no. 5, pp. 721–735, 2014.

[114] H. Stuart, S. Wang, O. Khatib, and M. R. Cutkosky, "The ocean one hands: An adaptive design for robust marine manipulation," *The International Journal of Robotics Research*, vol. 36, no. 2, pp. 150–166, 2017.

[115] T. Yoshikawa, "Manipulability of robotic mechanisms," *The international journal of Robotics Research*, vol. 4, no. 2, pp. 3–9, 1985.

[116] W. G. Bircher, A. S. Morgan, and A. M. Dollar, "Complex manipulation with a simple robotic hand through contact breaking and caging," *Science Robotics*, vol. 6, no. 54, 2021.

[117] I. M. Bullock, R. R. Ma, and A. M. Dollar, "A hand-centric classification of human and robot dexterous manipulation," *IEEE transactions on Haptics*, vol. 6, no. 2, pp. 129–144, 2012.

[118] S. Garrido-Jurado, R. Muñoz-Salinas, F. J. Madrid-Cuevas, and M. J. Marín-Jiménez, "Automatic generation and detection of highly reliable fiducial markers under occlusion," *Pattern Recognition*, vol. 47, no. 6, pp. 2280–2292, 2014.

[119] J. Morrow, N. Nishat, J. Campbell, R. Balasubramanian, and C. Grimm, "Grasping benchmarks: Normalizing for object size & approximating hand workspaces," June 2021, arXiv preprint: arXiv:2106.10402.

[120] C. F. Jekel, G. Venter, M. P. Venter, N. Stander, and R. T. Haftka, "Similarity measures for identifying material parameters from hysteresis loops using inverse analysis," *International Journal of Material Forming*, may 2019. [Online]. Available: https://doi.org/10.1007/s12289-018-1421-8

[121] T. Eiter and H. Mannila, "Computing discrete fréchet distance," Citeseer, Tech. Rep., 1994.

[122] B. Calli, A. Singh, A. Walsman, S. Srinivasa, P. Abbeel, and A. M. Dollar, "The ycb object and model set: Towards common benchmarks for manipulation research," in *2015 ICAR*. IEEE, 2015, pp. 510–517.

[123] Z. Xu and E. Todorov, "Design of a highly biomimetic anthropomorphic robotic hand towards artificial limb regeneration," in *2016 ICRA*. IEEE, 2016, pp. 3485–3492.

[124] E. Todorov and Z. Ghahramani, "Analysis of the synergies underlying complex hand manipulation," in *EMBS 2004*, vol. 2. IEEE, 2004, pp. 4637–4640.

[125] R. R. Ma, A. Spiers, and A. M. Dollar, "M2 gripper: Extending the dexterity of a simple, underactuated gripper," in *Advances in reconfigurable mechanisms and robots II*. Springer, 2016, pp. 795–805.

[126] "Applied hand dimensions," https://github.com/OSUrobotics/Applied-Hand-Dimensions, 2020.

[127] M. R. Dogar and S. S. Srinivasa, "Push-grasping with dexterous hands: Mechanics and a method," in *IEEE IROS*. IEEE, 2010, pp. 2123–2130.

[128] H. Stuart, S. Wang, O. Khatib, and M. R. Cutkosky, "The ocean one hands: An adaptive design for robust marine manipulation," *The International Journal of Robotics Research*, vol. 36, no. 2, pp. 150–166, 2017.